Fall 2019

Evaluating Measurement of Strain Hardening Method for Mechanical Assessment of Geomembrane Service Life in MSW Landfills

Alaa Alsharaballi

EVALUATING MEASUREMENT OF STRAIN HARDENING METHOD FOR MECHANICAL ASSESSMENT OF GEOMEMBRANE SERVICE LIFE IN MSW LANDFILLS

by

Alaa Alsharaballi

Bachelor of Science
University of Technology, 2002

Master of Science
University of Technology, 2006

Submitted in Partial Fulfillment of the Requirements

For the Degree of Doctor of Philosophy in

Civil Engineering

College of Engineering and Computing

University of South Carolina

2019

Accepted by:

Charles Pierce, Major Professor

Sarah Gassman, Committee Member

Addis Kidane Committee Member

Joseph Flora, Committee Member

Nicole Berge, Committee Member

Cheryl L. Addy, Vice Provost and Dean of the Graduate School

DEDICATION

To my parents, to my wife, to my kids with love.

ACKNOWLEDGEMENTS

This work would have not been achieved without the help, support, and motivation of many people who contributed or accompanied me during this work. It is to them that I owe my deepest gratitude.

I would like to express the deepest gratitude to my advisor, Dr. Charles Pierce who has always guided me during my study journey. His encouragement and kindness have a great impact on how to deals with research problems and move up in thinking and do my best.

I would like to thank my committee members, Dr. Sarah Gassman, Dr. Joseph Flora, Dr. Addis Kidane and Dr. Nicole Berge for their notes and suggestions that improve my skills in both research and presentation.

Special thanks to my colleagues and friends at the University of South Carolina, for their support and encouragement during my PhD study.

The financial support provided by the Iraqi government, NSF, and Geosynthetic Institute greatly acknowledged.

A deep appreciation to my wife Larah for her incredible support, blessing me with kids along study journey and putting extra hours with the babies so I can complete this milestone. Special thanks as well to my uncle Dr. Abdullah Abbas for encouraging me to come to the US and mentoring me during my study.

ABSTRACT

The increased household production result in more construction of municipal solid waste (MSW) landfills and lagoons. One major part of these engineering projects is high-density polyethylene (HDPE) geomembrane. Geomembrane is an impermeable layer that used along bottom and sides of landfills and lagoons to contain the leachate and to protect the groundwater. Although of their chemicals resistance and high strength, it can be aged under service conditions such as high temperature, ultraviolet (UV) light, and chemicals exposure. These conditions accelerate oxidation of geomembrane and lead to brittle behavior and stress cracking which reduce its service life.

Our objective in this work is to properly evaluate and characterize HDPE geomembranes. The conventional method for evaluating geomembrane service life is the stress crack resistance (SCR) test in accordance with ASTM D5397. This method has many disadvantages such as time-consuming, expensive apparatus, and low repeatability of results. Recently, a new method has been standardized to characterize crack resistance of pipe resins from the slope of the curve of the tensile test at strain hardening region at high temperature. Few researchers have investigated this method for HDPE geomembrane. However, no standard has been approved yet for the method for geomembrane resins.

Thus, in this research, a series of tensile test at specific displacement rates have been performed for high-density polyethylene (HDPE) geomembrane at room

temperature to study and standardize a method to measure strain hardening modulus. The proper displacement rate and measurement method have been specified based on data analysis. It is shown that low displacement rates are more acceptable to measure strain hardening modulus for geomembrane samples.

Research has been conducted on how to overcome the limitations encountered during strain measurement using existing conventional methods. These limitations are successfully resolved, and we managed to obtain dependable strain hardening modulus throughout the entire testing range

Finally, another set of experimentations are also proposed to be performed for oven aged samples. The aim of this experiment is to study and verify the method of strain hardening modulus for aged HDPE geomembrane. However, several strain measurement problems are encountered while testing the aged samples. Most of the tensile testing data could not be recorded and thus not being able to obtain proper data to finally achieve representative strain hardening curve. Samples are retrieved periodically and kept in the dark for future work.

TABLE OF CONTENTS

LIST OF TABLES

LIST OF FIGURES

CHAPTER 1

INTRODUCTION

1.1 Motivation

According to the United States Environmental Protection Agency, 250 million tons of household waste was disposed in landfills in 2011. The generation of municipal solid waste (MSW) continues to increase with the increase in population, requiring more landfills and/or increased landfill capacities. Leachate from MSW is a hazardous material that can have adverse effects on the environment and human health if released into the natural ground beneath the landfill. The Resource Conservation and Recovery Act (RCRA) requires the use of flexible, impermeable geomembranes along the bottom and sides of landfills to contain the leachate and to protect the groundwater. High-density polyethylene (HDPE) is used widely as a geomembrane in landfills, as well as at the bottom of leachate ponds where removed leachate is often stored. Although HDPE geomembranes have good chemical resistance and high strength, they can be aged under severe conditions such as high temperature (which can develop in MSW landfills), ultraviolet (UV) light (which can penetrate in leachate ponds), and chemical exposure. These conditions accelerate oxidation in landfill environment and lead to brittle behavior and stress cracking in geomembrane which reduce its service life. Many tests are used to evaluate serviceability of non aged and aged geomembrane.

Among these tests, environmental stress crack resistance (ESCR) is perhaps the most important. Although this method has been used for decades, it has many drawbacks:

1) It required a specific expensive complex equipment with accessories for preparing specimens and a detergent with good quality (not old or used many times) to incubate the sample in it, 2) Results varied a lot and depending on many factors such as laboratory agent experience and sample preparation, 3) long test times reach up to 5,000 hours for some current geomembrane, and 4) it is expensive to test and for a geomembrane that fails at 300-500 hours, it costs $375 and test is more expensive when testing high crack resistance geomembrane that breaks at up to 5000 hours.

Several researchers studied new alternative methods to replace conventional SCR test with a more simplified approach. A new method is introduced to simulate the fibrils condition developed in craze formation and predict resistance to slow crack propagation in HDPE products from a tensile measurement performed at 80 °C. It is shown that the slope of the stress-strain curve above its natural draw ratio -strain hardening modulus - correlates well with failure time determined by conventional SCR tests While this method has been standardized for HDPE pipe resins, it is not yet been approved for HDPE geomembrane. In addition, the method required using oven chamber that allow performing tensile tests at high temperature which is not always available in lab.

1.2 Research objectives

The specific objectives of this research are to:

1- Development test method of strain hardening for HDPE geomembrane resins using tensile test in simplified test condition (room temperature).

2- Evaluate how the test method and data analysis affect the magnitude and repeatability of values reported for the strain hardening modulus.

3- Study the effect of degradation on the stress-strain curve of accelerated aged HDPE geomembrane and adjust the measurement methods of strain hardening modulus accordingly.

4- Evaluate a new design of dot that replaces conventional dot types for tensile test and overcome the limitations in the technique used in this research and limitation of other techniques in the literature.

1.3 Thesis outline

The main body of this research comprises of seven chapters including five main chapters (Chapters 2-5) in addition to thesis introduction (Chapter 1) and conclusions (Chapter 7).

Chapter 2 presents a literature review and background of stress crack resistance of HDPE geomembrane and tests method that used to evaluate its service life and crack resistance. The limitation of these methods has been described, and alternative tests that expect to overcome these limitations have been presents.

The standards that followed to evaluate mechanical properties of geomembranes, including tensile properties, are presented in Chapter 3. A 1 mm HDPE geomembrane has been tested following common standard for the tensile test (ASTM D6693). This Chapter focuses on tensile test properties, validation of tensile test, and effect of the number of replicates and displacement rate on data repeatability. Based on this Chapter, a suggestion has been concluded regarding the number of replicates for tensile test.

The strain hardening modulus as an alternative test to stress crack resistance test has been described in Chapter 4. The strain hardening test has been performed at more

simplified conditions (room temperature) to make the test more accessible and able to perform at any laboratory. Modulus has been measured in multiple ways, and results have been discussed. Suggestions have been presented regard displacement rate and measurement method. This research task will be submitted as a paper to the ASTM Geotechnical Test Journal.

A problem has been faced while measuring the strain of the tensile test for HDPE geomembrane in Chapter 4. Paint marker dot that locate on tensile specimen fadeaway results in loosing data at some point during tensile test. Chapter 5 focus on developing new dot type that allows measuring the strain of very extensible material such as geomembrane. Limitation of conventional dot types has been studied according to literature. Tests results of conventional dots and newly developed dot has been compared. This research task will be submitted as a technical note to the ASTM Journal of Testing and evaluation.

Chapter 6 focuses on studying the strain hardening method for oven aged geomembrane samples. The effect of aging on the tensile test curve and results have been described. The strain hardening modulus measurement methods have been modified according to change in tensile test curve of aged samples. Suggestions have been presented to select the most representative measurement methods of strain hardening modulus based on their values and expectation. Extra unaged and aged samples have been retrieved and sent to a lab to measure stress crack resistance according to conventional standard (ASTM D5397). Results of stress crack and strain hardening tests have been compared to figure out the relation between them and to validate the use of

strain hardening test instead as an alternative to conventional crack resistance test methods. Multiple journals are considered for submitting the work in this research.

The conclusion of this work has been presented in Chapter 7. Also, recommendations for future work based on researches that have been performed in this work have been listed.

CHAPTER 2

BACKGROUND AND LITERATURE REVIEW

This chapter introduces stress cracking of high-density polyethylene and explain tests that used to evaluate material service life and crack resistance and an alternative test. A brief history of stress crack resistance has been given, including researchers attempts to improve the test. While the test has been used for a decade to assess the service life of HDPE geomembrane, it is no longer sustain the improved polyethylene resins. The strain hardening test represents an alternative test because it takes a very short time and easy to perform. It basically represents the slope of strain hardening region in draw ratio-true strain curve. However, there are several issues that have to be studied. First, while the strain hardening modulus test has been standardized for pipe HDPE resins, no test standard for HDPE geomembrane resin yet. Second, the test required an oven chamber which adds a limitation to the test. An oven chamber that fits with a tensile device that used to perform the tensile test is not necessarily available in materials laboratories.

2.1 Background on stress crack resistance (SCR)

Stress crack growth is associated with applied stresses lower than the material yield stress. The stress cracking involves brittle cracking of polymers from its adjacent failure surfaces. Environmental stress cracking is a type of crack growth where the material exposed to surfactant and high temperature. Microscopic imperfections result in

cracks and propagate through crystalline regions of polymers. The ability of plastic materials to resist cracking named environmental stress crack resistance (ESCR). Assessing the ESCR of polyethylene is important for various applications to estimate products service life before failure. Crack resistance test is used to measure the durability of materials and its service life.

Crack resistance test is performed by applying a constant load on a specimen. Constant tensile load test is started at 1960 [1]. The test developed later to ASTM D2552 at which unnotched specimen is used [2]. Because of sample nature of unnotched test, the test takes long time and results has random results. The limitations of this test were overcome later using notched constant tensile load test (NCTL) by applying a notch on the sample surface. The notch at this test generate plane strain condition which is similar to that exist in field condition. It also reduced test time and increased the reproducibility of results [3].

SCR test is performed under a constant load and an accelerated environmental condition. Sample incubated at an elevated temperature of 50 °C and a surfactant bath to accelerate the crack propagation [4]. A notch with 20 % of sample thickness is placed on one side of the sample. Samples immersed in a 10 % IGEPAL surfactant solution. A series of tests are performed at various percentage of the yield stress range from 20% to 60% of the yield stress of the materials that measured previously at room temperature at tensile test. Data experiment is presented by a curve of logarithm of percent yield stress against the logarithm of failure time in hours (Figure 2.1). Each curve represents a single geomembrane material. Two linear regions can be noticed at each curve: one at high percent of yield stress and the other at low yield stress. The high stress region represents

ductile break specimens that have a shallow slope. The other zone with low stress level shows much steeper slope line with brittle failure mode. Ductile and brittle zones are separated by the transition point (Figure 2-2).

Fracture morphology of sample fails in ductile mode is different than sample fails in brittle mode (Figure 2.3). In ductile mode, fracture surface revealing uniform elongating of the material within failure surfaces. However, in brittle failure mode, fracture surface shows short fibril microstructure.

The NCTL test required measuring a series of tests at percentages of yield stress to construct ductile-to-brittle curve and find the minimum time to reach the beginning of the brittle zone. This test takes a very long time and may extend to weeks or months to generate the entire curve (Hsuan 1993, Hsuan 1995) [4, 5]. An alternative has been proposed to reduce test time by applying stress value less than the transition value [4]. A single point (SP-NCTL) test is well suited for testing geomembrane for quality control and evaluating performance [5].

Slow crack growth, and thus stress cracking, can be accelerated by increasing temperature [6]. The higher the incubation temperature, the lower the test time [5]. Testing time can be minimized by using high temperature such as 50 C. Using 75 °C for crack resistance test result in decrease test time to reach 60 hours instead of 100 hours using 50 °C (Figure 2.4). However, it is not recommended to increase temperature greater than 85 °C to avoid changes in intrinsic HDPE properties. On the other hand, low crack resistance HDPE samples required using lower temperature (such as 50 C°) to get greater statistical reliability [5].

Similar to temperature, the incubation solution has an acceleration effect on SCR. Wetting solution is prepared by 10% IGEPAL solution (CO-630) and 90% tap water [5]. It is indicated that the wetting solution cause plasticization in polymer crack tip region results in accelerating the test [7].

2.2 Material resins and test types

Crack resistance tests are used to rank the performance of different polyethylene resins such as pipe resins, bimodal HDPE pipe PE80 and PE100, unimodal resin, polytetrafluorethylene, LDPE and HDPE, aged pipe resin PE80 and PE100, geomembrane resins, aged HDPE pond liner, and aged geomembrane liners.

There are several methods used to investigate SCR of various polyethylene products [8]. Table 2.1 shows the most used tests for polyethylene materials. These test methods can be classified into constant stress and constant strain methods. These methods are designed to accelerate stress cracking compare to field conditions. Factors that accelerate the test are temperature, detergent, and notching. Among these methods, NCTL test according to ASTM D5397 is used to rank crack resistance of HDPE geomembrane.

2.3 Notched constant tensile load (NCTL) test according to ASTM D5397

Notched Constant Tensile Load test is standardized as an ASTM D5397 in 1999 [9]. This standard is used to develop a test data to evaluate the susceptibility of geomembrane sheet to stress cracking under a constant tensile load condition and an accelerated environmental condition. The yield stress of the sample is calculated

previously according to ASTM D638 at room temperature. Series of tests at a range of load levels are performed. The crack resistance sample punched using die according to ASTM D1822 type L (Figure 2.5). The length of the narrow section of the specimen is 13 mm and the width is 3.2 mm. The sample notch in the narrow section to 20 % of its thickness and left ligament thickness of 80 %.

Dumbbell-shaped NCTL specimens are loaded at several stress levels of 20 to 65 % of yield stress at a maximum increment of 5 %. The test is performed in the presence of a surface-active agent at an elevated temperature of 50 C. A uniform concentration throughout the bath can be achieved by using agitator. Typical apparatus can hold 20 specimens (Figure 2.6).

Thirty individual tests will be required to develop the entire curve with ten increments and three specimens at each increment. The time at which the specimen fails is recorded. The results of a series of such tests performed at different stress levels are presented by plotting stress level against failure time for each stress level on log-log axis (Figure 2.7). The test required to challenge the weakest direction which is usually the cross machine direction. For cross machine direction samples, notch aligned in the machine direction.

2.3.1 Calculation of NCTL

The arithmetic mean of three replicates failure time for each of the applied stress levels is calculated. The coefficient of variation is calculated according to the equation:

$$COV = \frac{SD}{Mean} * 100. \quad \text{(2.1)}$$

While COV is the coefficient of variation, and SD is a standard deviation.

2.3.2 Single point NCTL test

At the end of ASTM D5397, an appendix has been shown to describe the procedure of Single Point Notched Constant Tensile Load (SP-NCTL) Test. Five test specimen required for the test all in the same direction. This procedure is recommended for sheets with thicknesses ranging from 1.0 to 2.5 mm. All specimens are to be loaded to an equal stress level. Only one stress level applied to test specimens which is 30% of room temperature yield stress. Specimens of both Tensile and SCR tests should be bunched from the same material in the same direction. The duration of the test should be either a predetermined time period or taken to failure. At predetermined time period, tests are terminated immediately after the predetermined length of time. While test is continuing until all five specimens fail for non-predetermined time period test and the arithmetic mean of the five failure times is calculated along with the coefficient of variation (ASTM D5397) [9].

2.4 Environmental stress crack resistance (ESCR) and strain hardening modulus

A new method is introduced to simulate the fibrils condition developed in craze formation and predict resistance to slow crack propagation in HDPE products from a tensile measurement performed at 80 °C [10] (Figure 2.8). The materials that used in this research are a range of HDPEs, unimodal, molecularly broad Philips catalyst based (CrHDPE) as well as bimodal Ziegler-Natta HDPEs (biHDPEs). A standard environmental stress crack resistance test (ESCR) was performed at 75 C under constant tensile stress of 3 MPa in a detergent solution on sample that notched in the middle parallel with the short direction. Specimen dimensions for ESCR test are 63.5 X 12.7 X 1

mm^3. The standard of ESCR test has not been mentioned in this research. The materials for tensile test prepared by press at 160 °C to a sheet of 0.3 mm thickness. The preparation includes heating the material under a specific load, cooling down to room temperature, and annealing for 1 hour at 120 C followed by another cooling to room temperature. Test specimen (ISO37 type 3) are punched later from pressed sheets to use for tests. The tensile specimen is extended at a constant speed (10 mm/min) until it reaches 1200% of strain. This limit is selected based on the length limit of the temperature chamber. Both load and elongation are measured throughout the test. Optical extensometer is used to track two reflecting and self-adhesive dots to determine the elongation. Gauge length (distance between dots) is measured after preloading the specimen before each test. The test specimen is kept for about 30 minutes in the temperature chamber to allow thermal equilibrium prior to the test. Data of tensile test presented as a draw ratio in the horizontal axis and true stress in the vertical axis. The draw ratio is the ratio of the distance between gauge marks at a time to the original distance. The draw ratio is calculated on the basis of gauge length according to the equation [10]:

$$\lambda = \frac{\Delta L}{L} + 1 \quad \text{(2.2)}$$

Where λ is the draw ratio expressed as a dimensionless ratio, L_o is the initial distance between the gauge dots in millimeters and ΔL is the increase in the specimen length between the gauge dots marks in millimeters. Based on the definition of draw ratio, it is only a shift of engineering strain one unit to the right. True stress is calculated assuming conservative volume between marks on sample:

$$\sigma_t = \frac{\lambda . F}{A} \quad \text{(2.3)}$$

Where σ_t is the true stress in MPa, F is the measured force in Newtons; A is the initial cross-sectional area of the narrow section of the specimen in square millimeters.

The strain hardening modulus (Gp) is calculated as the average difference quotient of data at homogeneous part of the curve which lays between draw ratio of 9 and 12.

The ESCR data correlate well with Gp measured at 80 □ (Figure 2.9). The study suggested that strain hardening is sensitive to the molecular differences that governed slow crack resistance. It also assumed that the molecular and structural parameters governing creep of materials are the same as those determining Gp at elevated temperature. The elevated temperature enhanced chain mobility within the crystal, facilitating solid-state chain diffusion through the crystalline phase and subsequent crystal shear. Three replicates of strain hardening and ESCR tests have been performed to test reproducibility. The strain hardening test showed a clear lower deviation compared to that of ESCR (Table 2.2) [10].

2.4.1 Effects of temperature on measured Gp

Two Philips catalyst-based HDPE resins named as CrHDPE1 and CrHDPE2 have been tested in tensile at a displacement rate of 10 mm/min at room temperature. The ESCR of resins are 58 hours and 103 hours respectively. The term "true strain" has been used in this research although other researchers use the term draw ratio (λ). It is found that the stress-strain response does not differ significantly and no significant variation in tensile response at room temperature (Figure 2.10). However, when those materials are tested at the same displacement rate but at 80 °C, an obvious difference between the two curves is noticed (Figure 2.11) Kurelec 2005 [10].

It has been mentioned that at some circumstances such as at low displacement rate like 0.2 mm/min, the same ranking of materials based of strain hardening modulus could be observed at room temperature [10].

The Strain Hardening Method was further studied by many researchers to evaluate the crack resistance of different polyethylene resins such as pipe resins, bimodal HDPE pipe PE80 and PE100, unimodal resin, polytetrafluorethylene, LDPE and HDPE, aged pipe resin PE80 and PE100, geomembrane resins, aged HDPE pond liner, and aged geomembrane liner.

2.4.2 Standardized strain hardening method for HDPE pipe resins

The prediction of SCR of PE pipe resins using the strain hardening modulus method was published as an international standard in 2015 [12]. The test is performed using a universal testing machine equipped with optical extensometer at a crosshead speed of 20 mm/min and at 80 °C chamber temperature.

2.4.3 The use of G_p method for ranking geomembrane

There is an attempt to use the strain hardening method to rank HDPE geomembrane reins [11,13]. A 12 HDPE ,different geomembranes resins, have been selected from three manufacturers and tested in both SP-NCLT and strain hardening modulus tests. The strain hardening test was performed at 80 °C with a displacement rate of 10 mm/min. Gp has been measured between draw ratio of 8-12 (Figure 2.12). It is found that measured Gp correlates well with data obtained from SP-NCTL according to ASTM D5397 (Figure 2.13) [11].

The SP-NCTL of 1.5- and 2.0-mm HDPE geomembranes from three sites after two years of exposure from a lagoon, a water reservoir, and a landfill have been

measured [13]. The results compared to the strain hardening modulus (Gp) measured at 80 °C and 10 mm/min. A good correlation has been found between SP-NCTL failure times and the measured modulus (Figure 2.14). It is also found that the strain hardening modulus of HDPE geomembrane decreased by aging the material in lab at 80 °C and 50 bar oxygen pressure (Figure 2.15). It is suggested that the reduction in the mechanical properties starts after the depletion of the entire antioxidant content.

2.4.4 Strain hardening stiffness of HDPE resins at room temperature

The practical approach has been adopted to relate the tensile test to crack resistance of various types of HDPE products such as blow mold, injection mold, and HDPE pipe resins [14]. The test follows ASTM D 638 using the dogbone sample with 41 mm narrow section and 1.8 mm thickness. The specimen exposed to an extension of 7 and 0.5 mm/min displacement rates at room temperature. Hardening stiffness was measured from load displacement curve after the onset of hardening. It has been shown that hardening stiffness detected differences in NCTL of PE resins at a rate of 0.5 and 7 mm/min (Figure 2.16). It is found that the difference between PE resins was more pronounced at higher displacement rate (7 mm/min) compared to the low displacement rate (0.5 mm/min) (Figure 2.17). However, this research neglects the thickness of specimen, and the slope of total strain hardening region after onset has been used rather than a specific range of strain [5].

2.5 Improvement of geomembrane performance and requirement

It should be noticed that with new, improved geomembranes resins, crack resistance increase, and current resins reach 2500 to 5000 hours. The minimum

acceptable stress crack resistance of HDPE geomembrane was initially set at 200 hours. However, this value increased by standard specification [4] (GRI-GM13-2016) to 300 hours. And it is expected to further increase with the need for longer life and more crack resistance liners. This longtime test duration results in more cost and excessive time consumption to finally obtain the results. Also, several other factors such as the notching process, temperature control, and the detergent age used for the incubation step, all present additional sources of error upon crack resistance test results. These factors collectively observed and reported as being the main source for high data scattering of the SCR results [11]. Researchers pointed out the need to develop new laboratory tests to assess crack resistance of current high HDPE geomembrane [16]. It is hypothesized that strain hardening modulus measured at room temperature can be used as alternative to NCTL test for HDPE geomembrane.

Table 2.1 Conventional test methods used to determine the stress cracking resistance of PE grades and products [8].

Test methods	Standard	Applied load
Full notch creep test (FNCT)	ISO 16770	Constant stress
Double notch creep test (2NCT)	Analogous to ISO 16770	Constant stress
Accelerated creep test (ACT)	Analogous to ISO 16770	Constant stress
Notched constant tensile load (NCTL) test	ASTM D 5397	Constant stress
Pennsylvania edge notch tensile (PENT) test	ISO 16241	Constant stress
Notched pipe test (NPT)	ISO 13479	Constant stress
Point load test (PLT)	PAS 1075	Constant stress
Bent strip method	ISO 22088-3	Constant strain
Bell test	ASTM D 1693	Constant strain
Ball or pin impression method	ISO 22088-4	Constant strain
Cone test method	ISO 13480	Constant strain

Table 2.2 Replicates of strain hardening and ESCR tests (Kurelec 2005) [10]

Grades	ESCR (h)	SD	COV	Gp	SD	COV
Cr HDPE9	144	12	0.083	23.2	0.8	0.034
Cr HDPE9	89	7	0.079	22.9	0.4	0.017
Cr HDPE9	123	11	0.089	23.1	0.3	0.013

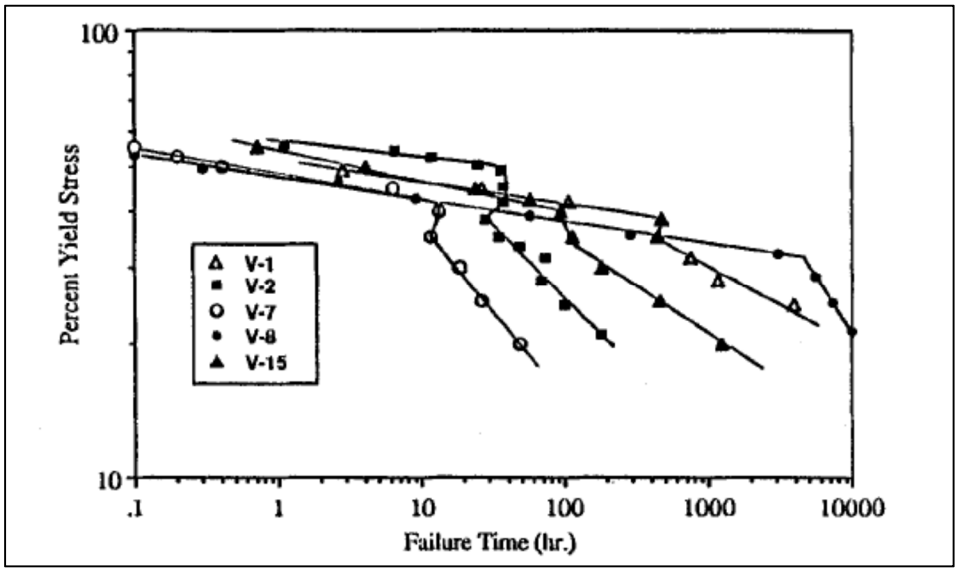

Figure 2.1 Stress versus Failure Time Curves for Five Virgin Geomembranes [3]

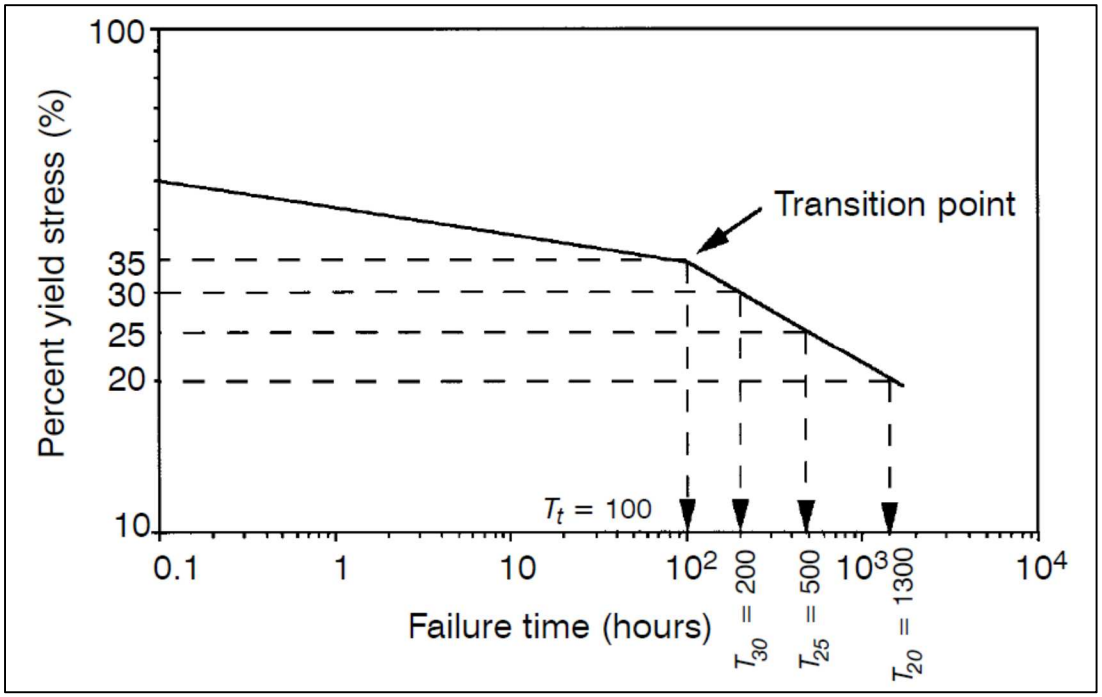

Figure 2.1 SP-NCTL test using the NCTL test response as a control curve [5]

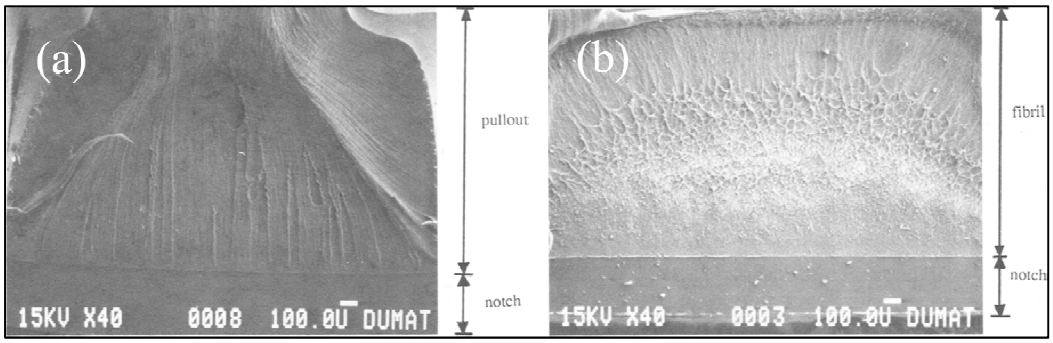

Figure 2.3 Failure surface morphology in a) Ductile mode b) brittle mode (Modified from [3]

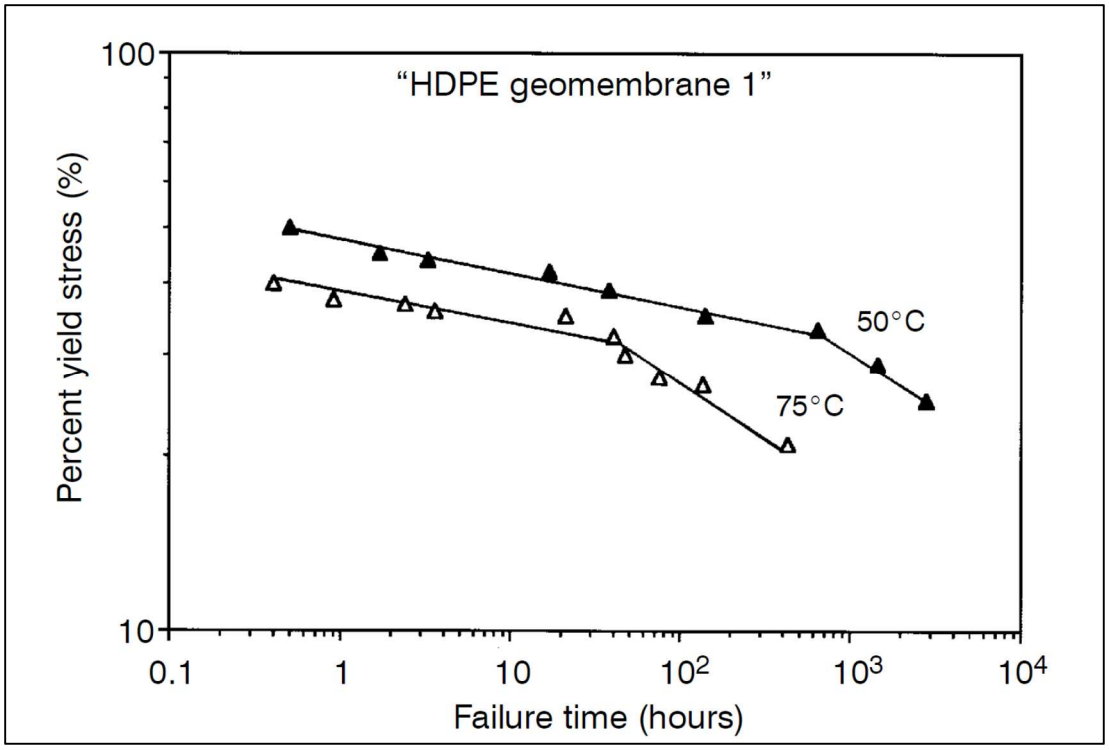

Figure 2.4 Effect of increasing test temperature on the failure times of NCTL tests [5]

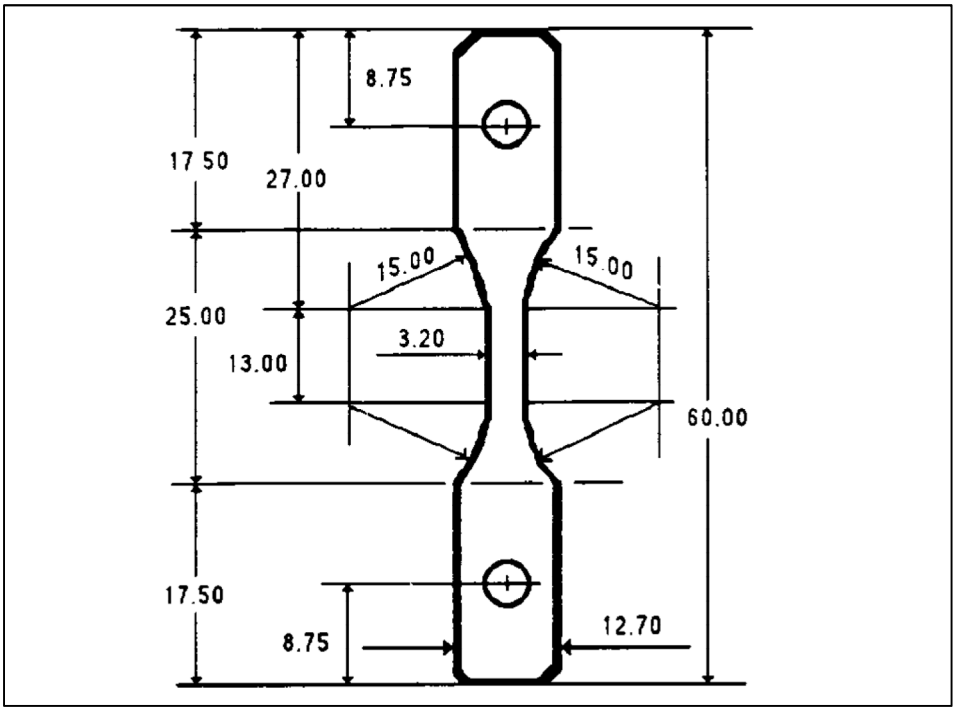

Figure 2.5 Dimensions (mm) of NCTL specimen test method D1822 type "L" (ASTM D5397) [9]

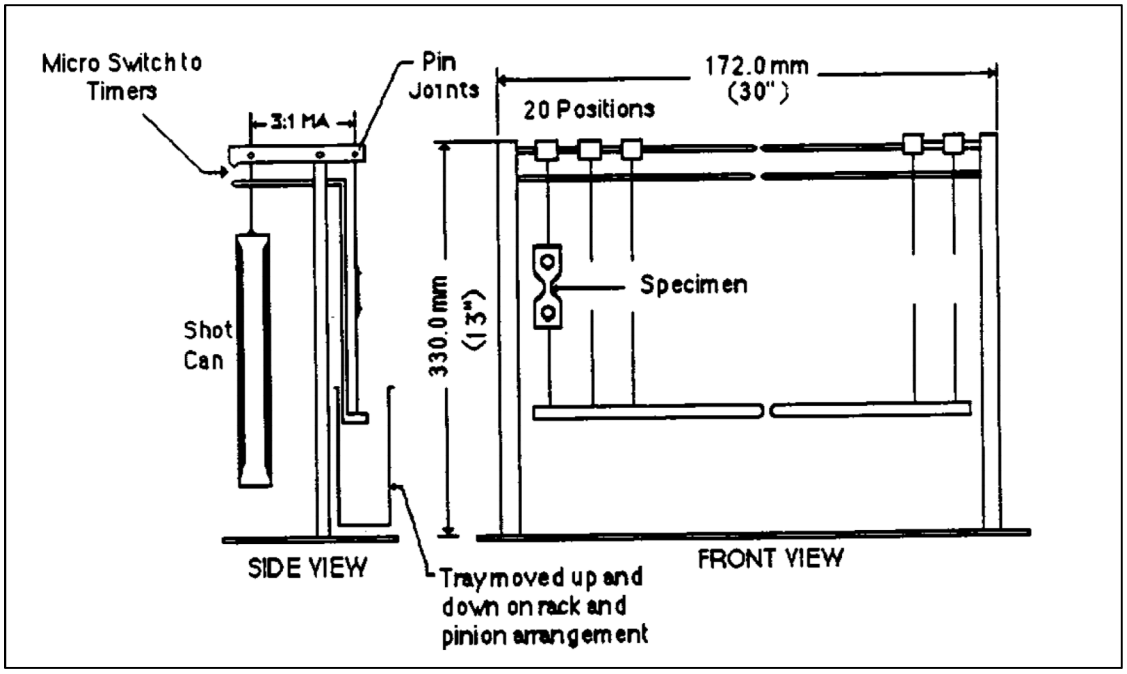

Figure 2.6 Constant stress loading apparatus consisting of twenty specimen test positions (ASTM D5397) [9]

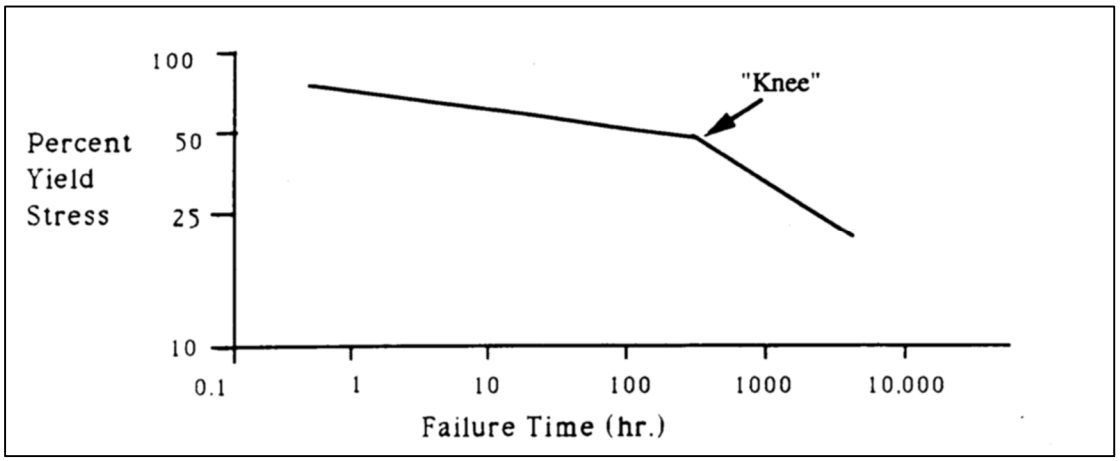

Figure 2.7 Possible response of curve resulting from a complete notched constant tensile load (NCTL) test [9]

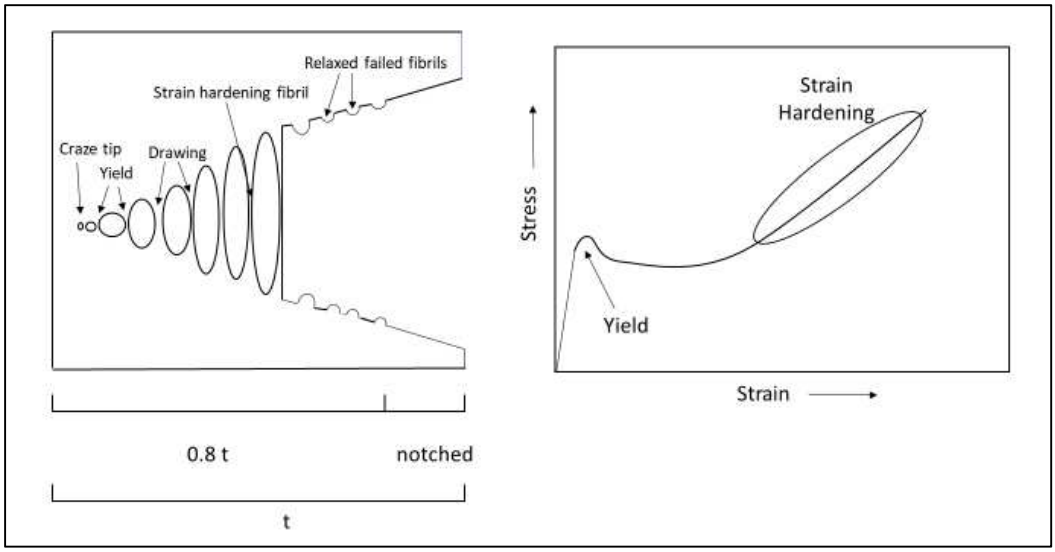

Figure 2.8 Schematic presentation of fibril strain hardening in a craze and its relation to uniaxial tensile Drawing (Modified from Engelsing et al. 2012) [11]

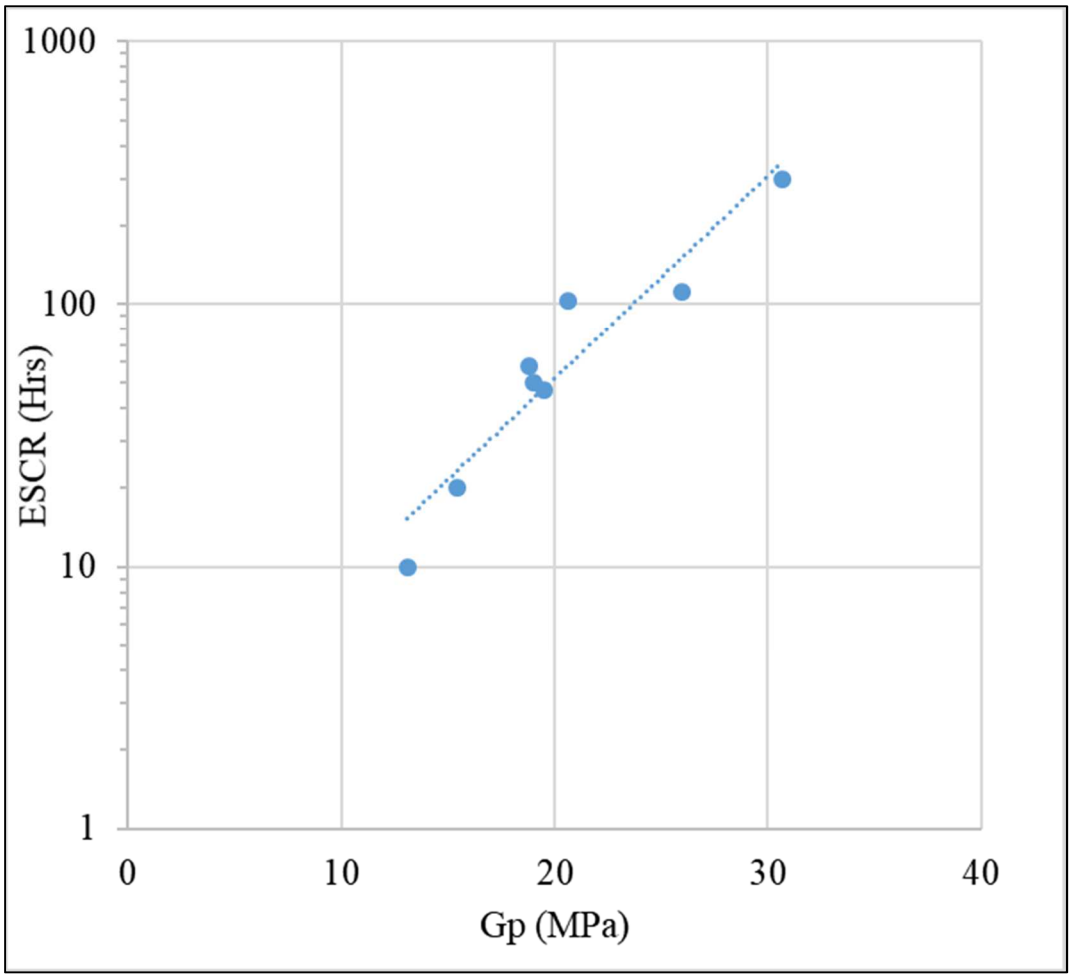

Figure 2.9 Strain hardening performed at 80 □ at 10 mm/min vs ESCR ((Modify Kurelec 2005) [10]

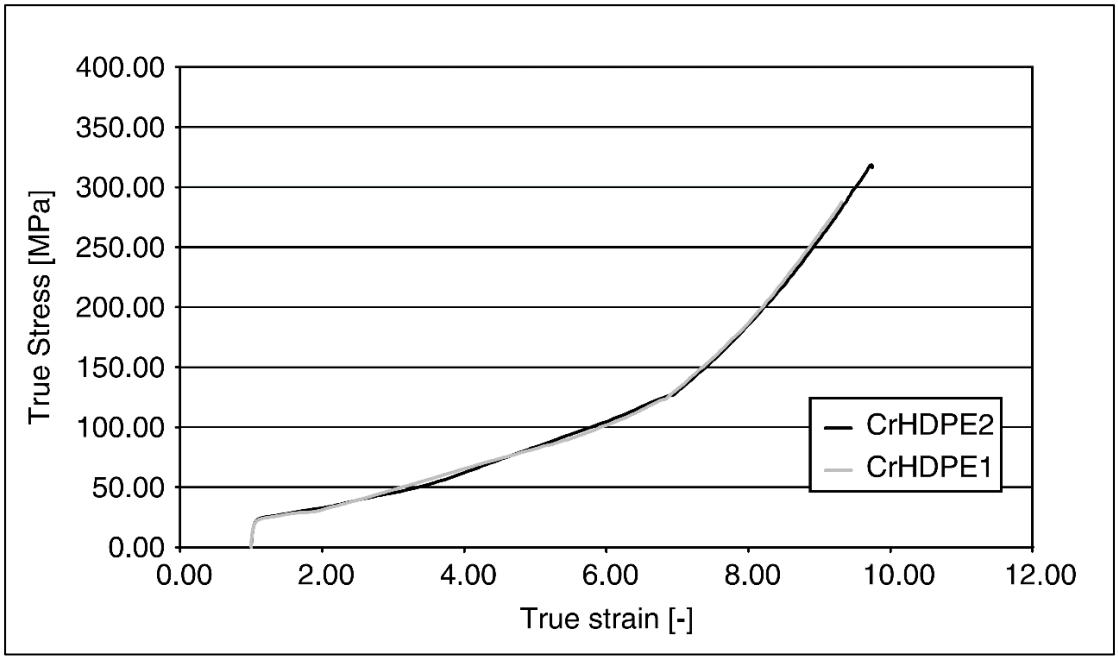

Figure 2.10 Stress–strain curves expressed as true stress–true strain performed at room temperature at 10 mm/min [10]

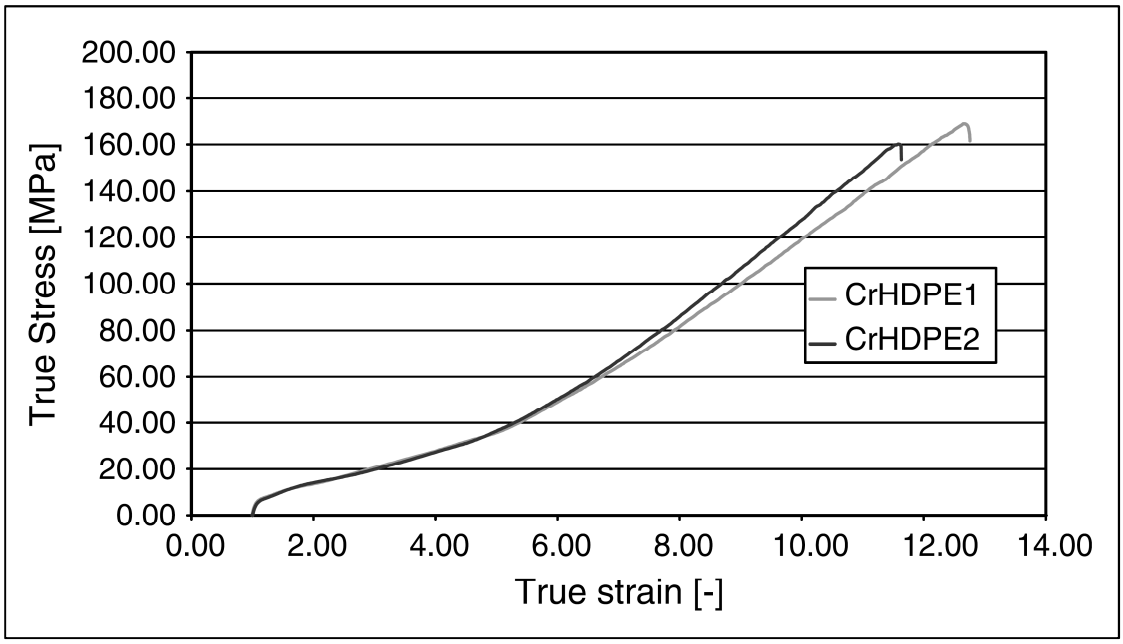

Figure 2.11 Stress–strain curves expressed as true stress performed at 80 °C at 10 mm/min [10]

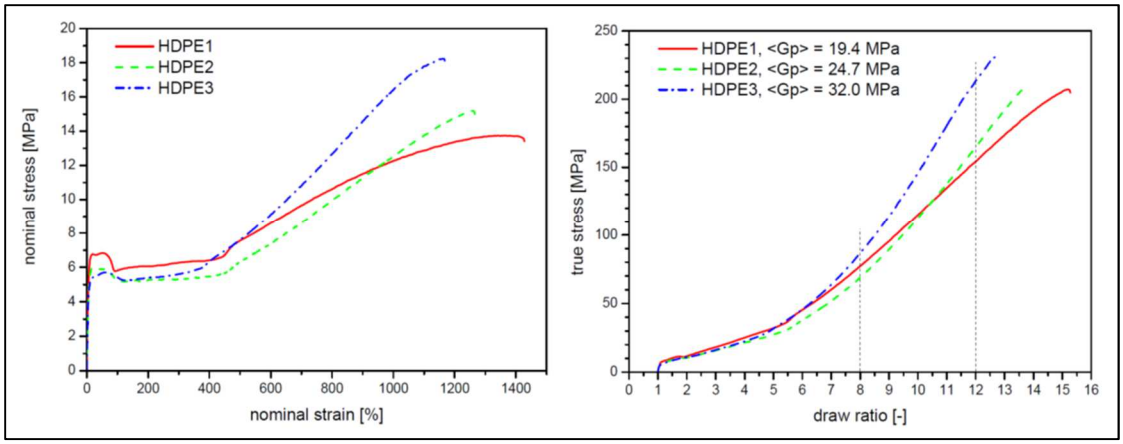

Figure 2.12 Nominal stress vs. nominal strain (left) and true stress vs. draw ratio (right) with indicated range for calculation of the strain hardening modulus <Gp> [11]

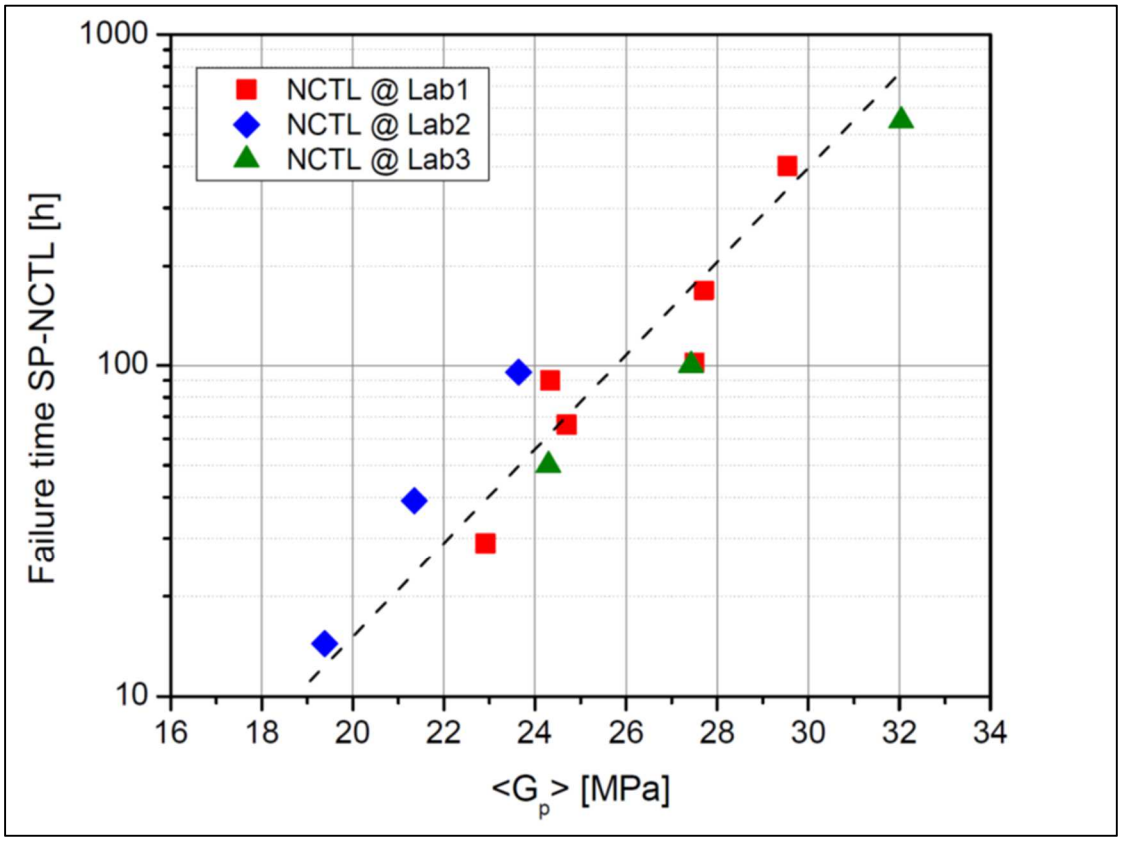

Figure 2.13 Strain hardening modulus <Gp> versus SP-NCTL failure times for different HDPE geomembranes [11]

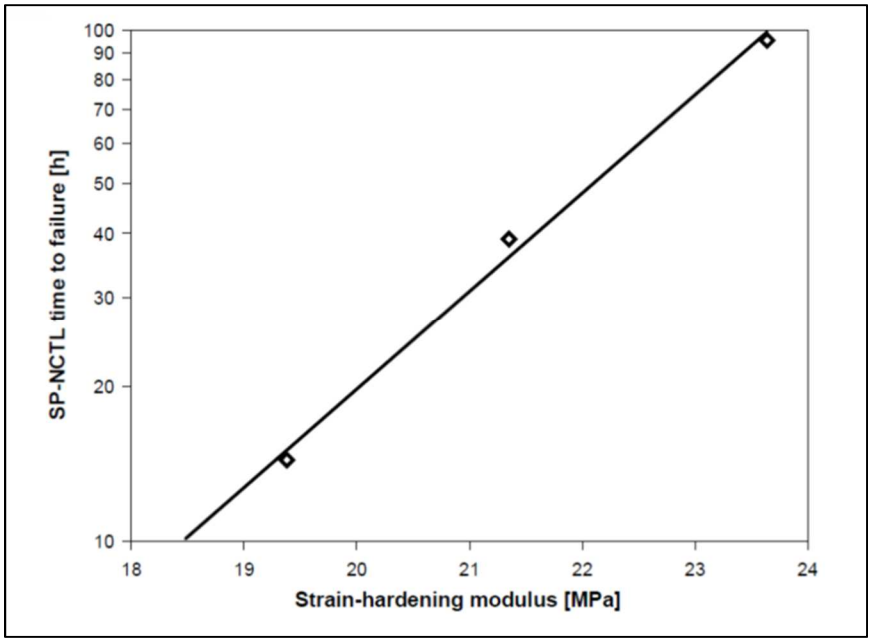

Figure 2.14 Strain hardening modulus <Gp> versus SP-NCTL failure times for three HDPE GMBs from three sites [13]

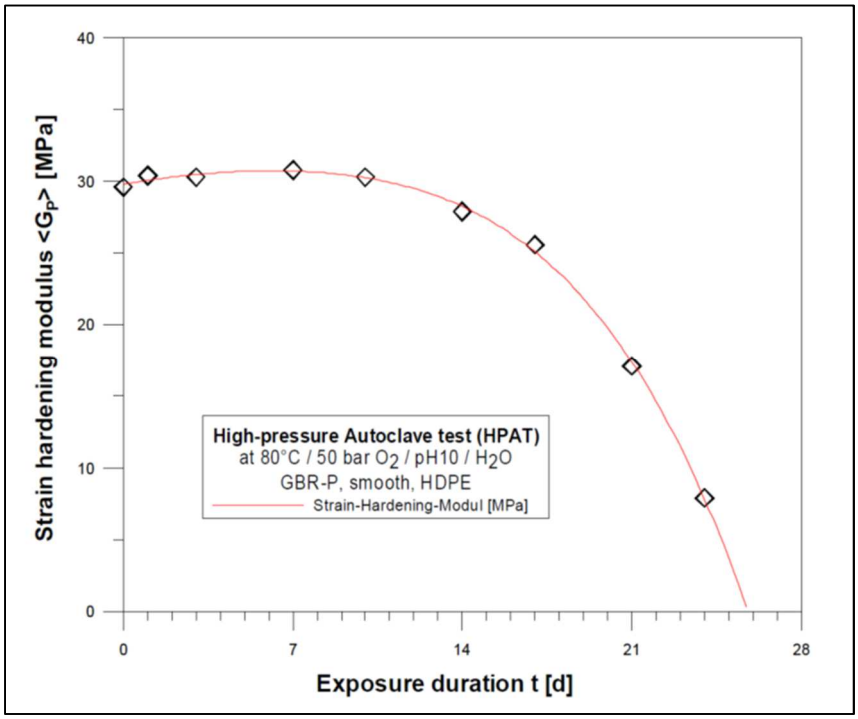

Figure 2.15 Example of the change of strain hardening modulus during the immersion in High-pressure Autoclave test (HPAT) at 80 °C and 50 bar oxygen pressure (material: HDPE geomembrane) [13]

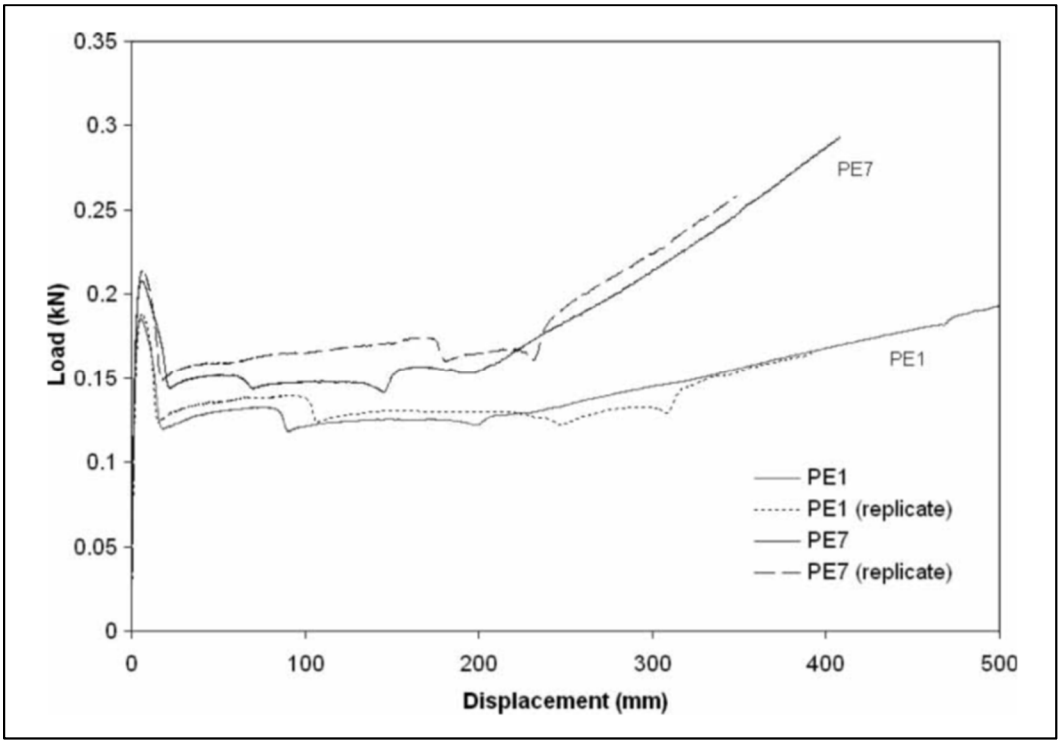

Figure 2.16 Tensile elongation at constant strain rate of 0.5 mm/min [14]

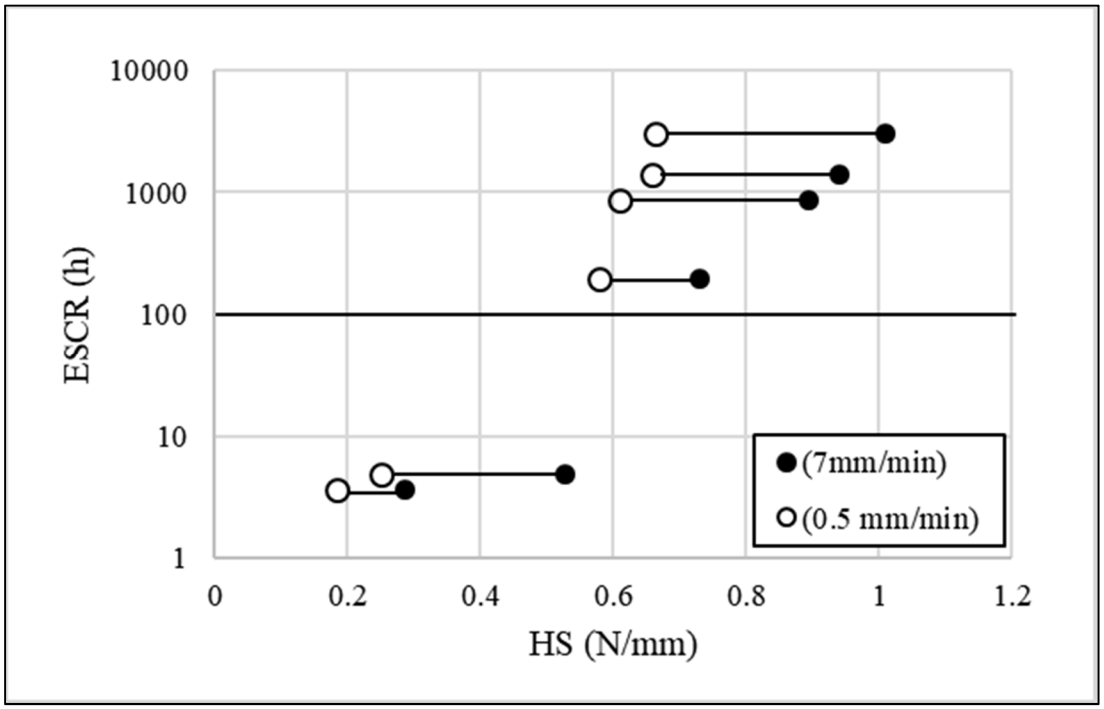

Figure 2.17 ESCR vs. hardening stiffness at different strain rates [modified from 14]

REFERENCES

[1] Lander, L. L. (1960). "Environmental stress rupture of polyethylene." *SPE J.,* VI, 1329-1332.

[2] Test method for environmental stress rupture of type III polyethylenes under constant tensile load." (1988). *ASTM D 2552,* Vol. 08.02, ASTM, Philadelphia, Pa.

[3] Hsuan, Y. G., Koerner, R. M., and Lord, A. E. (1992). "Notched constant tensile load (NCTL) test for high density polyethylene geomembranes." *ASTM Geotech. Testing J.,* submitted.

[4] Hsuan et al.1993 STRESS-CRACKING RESISTANCE OF HIGH-DENSITY POLYETHYLENE GEOMEMBRANES By Y. G. Hsuan, ~ R. M. Koerner, 2 Honorary Member, ASCE, and A. E. Lord Jr. 3

[5] Hsuan, Y. G., & Koerner, R. M. (1995). The Single Point-Notched Constant Load Test:A Quality Control Test for Assessing Stress Crack Resistance. *Geosynthetics International*, *2*(5), 831-843.

[6] Bragaw, C.G., 1980, "Prediction of Service Life of Polyethylene Gas Piping System" *Proceedings of the Seventh Plastic Fuel Gas Pipe Symposium*, November 1980, pp.20-24.

[7] Tonyali, K., Rogers, E.C. and Brown, H.R., 1987, "Stress-Cracking of Polyethylene in Organic Liquids", *Polymer*, Vol. 28, No. 9, pp. 1472-1477.

[8] Gerets, B., Wenzel, M., Engelsing, K., & Bastian, M. (2017). Slow Crack Growth of Polyethylene—Accelerated and Alternative Test Methods. In *Deformation and Fracture Behaviour of Polymer Materials* (pp. 177-187). Springer, Cham.

[9] ASTM D 5397, "*Evaluation of Stress Crack Resistance of Polyolefin Geomembranes Using Notched Constant Tensile Load Test*", American Society for Testing andMaterials, Philadelphia, PA, USA.

[10] Kurelec, L., Teeuwen, M., Schoffeleers, H., & Deblieck, R. (2005). Strain hardening modulus as a measure of environmental stress crack resistance of high density polyethylene. *Polymer*, *46*(17), 6369-6379.

[11] Engelsing, K. and Zanzinger, H. (2012). A new accelerated test method for stress

crack resistance of HDPE geomembranes. Segundo Congreso Panamericano de Géosintéticos, GEOAMERICAS 2012, 01-04 de Mayo, 2012, Lima, Peru, 8p.

[12] SHT test_ISO 18488: Polyethylene (PE)materials for piping systems _ Determination of Strain hardening Modulus in relation to slowcrack growth_Test method.

[13] Zanzinger, Helmut & Peggs, Ian. (2013). Stress cracking resistance of HDPE geomembranes with very high densities.

[14] Cheng, J. J., Polak, M. A., & Penlidis, A. (2008). A tensile strain hardening test indicator of environmental stress cracking resistance. *Journal of Macromolecular Science®, Part A: Pure and Applied Chemistry*, *45*(8), 599-611.

[15] GRI Test Method GM13 (2016). Standard Specification for "Test Methods, Test Properties and Testing Frequency for High Density Polyethylene (HDPE) Smooth and Textured Geomembranes (Revision 10), *GSI Geosynthetic Institute, Folsom, PA, USA.*

[16] D. Peggs, Ian. (2016). HDPE Geomembrane Stress Cracking: From There to Here to Where?. 216-225. 10.1061/9780784480182.019.

CHAPTER 3

TENSILE TESTS OF HIGH DENSITY POLYETHYLENE GEOMEMBRANE

3.1 Introduction

This chapter is concerned with tensile test standards for high density polyethylene (HDPE) geomembrane and related mechanical properties. A detailed explanation of standards is given to provide a general description including similarities and differences among tensile test standards, measurements, and reporting methods. The mechanical performance of 1 mm HDPE geomembrane was evaluated using a tensile test. Four tensile properties were monitored in this investigation: yield stress, yield strain, break strength, and break strain. Measured mechanical properties are validated by comparing them to manufacturer results GRI-GM13 [1], GSE [2], and Rowe and Ewais [3] in terms of variation. Therefore, two different replicates number have been selected based on standard test methods and the availability of the material. The effect of the number of replicates on data variability has been studied. Several sets of tests at low displacement rates have been performed for the same material. The effect of displacement rate on tensile properties and variation has also been studied.

3.2 Standard tensile tests for HDPE geomembranes

There are several tests that are used to measure mechanical properties of HDPE geomembrane. These tests are following standards published at the American Society for

Testing and Materials (ASTM). Mechanical tests for geomembrane may be used to evaluate the material in field and/or material in laboratory studies. Below are the standards that are used to evaluate geomembrane mechanical properties:

- ASTM D638- 14 Standard Test Method for Tensile Properties of Plastics [4]
- ASTM D6693/D6693M-04(2015) Standard Test Method for Determining Tensile Properties of Nonreinforced Polyethylene and Nonreinforced Flexible Polypropylene Geomembranes [5]
- ASTM D4833-07 Standard Test Method for Index Puncture Resistance of Geomembranes and Related Products [6]
- ASTM D8172-18 Standard Test Method for Shear and Peel Strength of Solvent-Welded Seams with Nonreinforced Geomembranes [7]
- ASTM D1004-13 Standard Test Method for Tear Resistance (Graves Tear) of Plastic Film and Sheeting [8]
- ASTM D5397-19 Standard Test Method for Evaluation of Stress Crack Resistance of Polyolefin Geomembranes Using Notched Constant Tensile Load Test [9]
- ASTM D1693-15 Standard Test Method for Environmental Stress-Cracking of Ethylene Plastics [10]

The first two standards (ASTM D638 and ASTM D6693) are used in researchers and by manufacturers to give initial index properties of HDPE geomembrane.

3.2.1 ASTM D638 –14 Standard test method for tensile properties of plastics

ASTM D638 is designed to produce data on tensile properties of plastic materials for their control and specification. It can be used for plastic specimens with a material

thickness of less than 14 mm. There are 5 different specimen types, each one with its own unique set of dimensions. Specimen types III and IV are used for testing nonrigid plastics such as HDPE geomembranes. Specimens with a thickness of 4 mm or less shall be tested using type IV while specimens with thickness between 7 mm and 14 mm shall be tested using type III.

There are several properties that are reported from this standard. These properties include: tensile strength at yield, tensile strength at break, percent elongation at yield, percent elongation at break, nominal strain at yield, nominal strain at break, modulus of elasticity or secant modulus, and Poisson's ratio.

Tensile strength at yield is calculated by dividing the yield load at yield point by average original cross-sectional area. Tensile strength at break is calculated by dividing the maximum load by the average original cross-sectional area. The results of strength are reported to three significant figures. Percent elongation at yield is calculated as the change in gage length at yield point divided by original gage length and multiply by 100. Percent elongation at break is calculated as the change in gage length at break point divided by original gage length. A suitable extensometer is used to measure the distance between two designated points within the gage length of the tested specimen as the specimen is stretched.

The standard includes the option of determining modulus and Poisson's ratio at room temperature. However, these properties are difficult to measure therefore required a specific type of extensometer to measure strain value at the beginning of the tensile test. The ASTM Committee D35 on Geosynthetics adopted ASTM D6693 instead of D638

[1]. Current researchers that deal with tensile mechanical properties follow the ASTM D6693 [3, 11, 12, 13].

3.2.2 ASTM D6693-15 Standard test method for determining tensile properties of nonreinforced polyethylene and nonreinforced flexible polypropylene geomembranes

The ASTM D6693 is another standard for tensile test. This standard covers the determination of the tensile properties of nonreinforced geomembranes. It is suitable for a material thickness of 0.25 - 6.3 mm. The data are appropriate for use in engineering design with consideration of test conditions as compared with in-service conditions. The specimen geometry in this standard has been adopted as type IV from Test Method D638. For polyethylene geomembranes, the standard specified displacement rate is 50 mm/min.

Yield and break stress are measured at yield point and break point respectively, similar to ASTM D638. However, they are measured by dividing the corresponding load by the original minimum width of the specimen and reported in unit load per unit length. Percent elongation at yield and percent elongation at break are calculated similarly to the ASTM D638 method. However, yield elongation is reported to the nearest 1% while break elongation is reported to the nearest 10%. Both standards required five specimens for isotropic material. For anisotropic materials, five normal to and five normal with the principal axis are tested. The gage mark was located to give a 25 mm gage length.

The mechanical properties that were reported following this standard are: tensile yield strength, tensile break strength, percent yield elongation, and percent break elongation.

3.3 Materials and methods

In this research, HDPE geomembrane will be tested in tensile instrument following the ASTM D6693. The following subsection will describe material that has been used, test methods, and measured properties.

3.3.1 HDPE geomembrane

HDPE geomembrane with 1 mm thickness is used for this study as received from the manufacturer. A limited area of this geomembrane is available as a roll at the University of South Carolina Civil and Environmental Engineering Department and stored in the dark at room temperature for several years. These conditions are necessary to prevent or reduce degradation of the geomembrane. No product data sheet for this geomembrane is available. Tensile test has been performed to provide data for mechanical properties of the material. Since the focus of this study is mechanical properties, no chemical properties are required to be measured.

3.3.2 Specimen shape and dimensions

A dogbone die produced by Pioneer Co, part number 16655, is used to cut specimens from geomembrane sheets. The die is used to produce specimen type IV which is applicable for both ASTM D638 type IV and ASTM D6693. Negative effects from imperfections on the edge of the geomembrane specimen can severely impact the results of the test [5]. Thus, a Teflon sheet is located under the geomembrane sheet to cut a smooth-edged specimen (Figure 3.1). Specimen type IV is used per ASTM D6693. The width of a specimen narrow section is 6 mm while the narrow section length is 33 mm (Figure 3.2). The thickness of each specimen is measured at three locations along the narrow section using a digital caliper with an accuracy of 0.02 mm and the average is

determined for later calculation. The width of narrow section of the specimen is 6 mm and is constant since the same die is used. Thus, only the thickness of specimens is measured for each specimen.

Geomembrane is considered as an anisotropic material. It is expected that each direction gives different mechanical properties results. Since the material that was used in this research is limited, the specimen has been cut and tested in only one direction, which is cross machine direction. In our experiment, all tensile specimens are cut in CMD and mechanical properties are measured in this direction.

3.3.3 Specimen gage length

Marks are applied using paint marker type edding 571, that come with calibration tools in the box of the extensometer. Paint marking allows the measuring of strain throughout the test. On the top and bottom of a rectangular piece of tape, rectangular holes were punched using a paper punch. Punched tape is stuck on the specimen and white marker is applied in the holes to give smooth edges to the marks (Figure 3.3). Marks are located to give a gage length of about 25 mm as recommended by ASTM D6693. Gage length between marks is measured using a digital caliber to assure reaching the required length center to center or edge to edge. This gage length between marks has been remeasured before the start of tensile test from the software window of the program. It is found that measured gage length is 25±1 mm. The two marks should be located within the 33 mm narrow section of the specimen. A specimen is subjected to preload of 3 N that found enough to get straight vertical alignment. Preload of tensile specimen is a common practice for tests that are performed to measure elastic modulus and strain hardening modulus, which will be measured and discussed in the next chapter [14, 15].

The gage length between the painted marks is also measured after applying preload using the video extensometer and read from screen on the computer through Bluehell 2 software prior to conducting the test (Figure 3.4). The instruction in the manual of the video extensometer recommends a rectangular mark that covers the total width (6 mm) of the specimen.

3.3.4 Tensile test equipment

The tensile test is performed using an Instron 5566 tensile device. A load cell with a capacity of 5 kN and serial number 64833, manufactured by Instron Co., is used to measure load during the test. The tensile device has a noncontact optical video extensometer type AVE that allows the measuring of strain within the field of view of 350 mm (Figure 3.5). Test parameters including displacement rate and sampling per second, are assigned as input to Bluehell 2 software. At 50 mm/min, sampling is conducted at 0.1 per second while sampling frequency decreases for lower displacement rate.

3.4 Test matrix

3.4.1 Displacement rates and sampling frequencies

Series of tests are performed on 1 mm GMB at displacement rates of 50 to 10 mm/min. Tensile tests at a displacement rate of 50 mm/min follow the ASTM D6693 that specified five replicates. Data of this rate and other lower displacement rates will be used later to measure another property, named strain hardening modulus, that related to the slope of strain hardening region. The sets of tests other than 50 mm/min were not following the standard and tested in only three replicates. Table 3.1 shows the testing

matrix for the current study indicating specimen designation, displacement rate, sampling frequency, and number of data point per 1 mm displacement rate for each displacement rate. Sampling frequency for a test performed at 50 mm/min displacement rate is selected to be 0.10 sec. This frequency is chosen to provide a reasonable data point and give acceptable load measurements that meet the requirement of load measuring according to the ASTM D6693 standard. The number of data point corresponding to the test that was performed at 50 mm/min is 13 points. The frequency has been factored according to the displacement rate to give the same data point per a unit displacement when testing at lower displacement rate.

3.4.2 Reporting of tensile properties

While tests in this research following ASTM D6693, some measured properties have been justified according to the aim of the research. The tensile device provides data of tensile test during the entire test time. These data include several measurements which are load, strain, time, and displacement. The engineering stress (σ) is calculated according to ASTM D6693. Stress is equal to the load divided by the initial cross-sectional area according to the following equation:

$$\sigma = \frac{P}{A_\circ} \quad \text{.....3.1}$$

While σ is normal stress, P is the applied load, and $A_\circ$ is original cross-sectional area of the specimen.

Elongation is measured as the change in length between gage marks divided by initial gage length and expressed as a percentage. Elongation is measured according to the following equation:

$$\text{Elongation} = \frac{\Delta l}{l_\circ} * 100 \quad \text{.....3.2}$$

While Δl is change in length between gage marks, $l_\circ$ is the initial gage length.

Instead of elongation, engineering strain (ε) will be measured through entire tests. Engineering strain is the change in length between gage marks to the initial length. Engineering strain is measured according to the following equation:

$$\varepsilon = \frac{\Delta l}{l_\circ} \quad \text{.....3.3}$$

Engineering strain will be used to calculate another term called draw ratio that will be used next chapter. Engineering stress and engineering strain could also be named stress and strain, respectively. Tensile properties including yield stress, yield strain, break stress, and break strain are measured from the stress-strain curve at each test. The yield point is the peak on a tensile curve with zero slope after the elastic region while the break point is the point of the maximum load before specimen rupture (Figure 3.6).

In order to study the variation of tensile properties and evaluate the results, the standard deviation and coefficient of variation have been measured. The standard deviation is measured based on a sample of data and is given by the equation:

$$\mathrm{SD} = \sqrt{\frac{\sum(\mathrm{X}-\mathrm{Mean})^2}{\mathrm{n}-1}} \quad \text{.....3.4}$$

While SD is standard deviation, X is each value in the data set, Mean is the mean of all values in the data set, and n is number of values in the data set.

While the coefficient of variation (COV) is measured according to the equation:

$$\mathrm{COV} = \frac{SD}{Mean} * 100 \quad \text{.....3.5}$$

3.5 Tensile test results and discussion

Tensile tests have been performed following the test matrix with displacement rates and replicates. Because of its high extensibility, HDPE geomembrane specimen elongates a lot before reaching break point. Figure 3.7 shows the tensile specimen before the test and after the break. The narrow section of the specimen extended several times its original length. As test progress, the paint marker dots become narrow following the changed width of the specimen narrow section. Paint markers dots also extended away that result in fading. The video extensometer detects white dots in contrast to the black color of geomembrane specimen. The extensometer, because of dot fading, lose tracking dots at some point during the progress of many tests. Figure 3.8 shows three selected replicates of tensile test curve performed at 50 mm/min. The video extensometer failed to measure engineering strain up to the break point at two replicates (U1-50 and U3-50). At these two specimens, the engineering stress is continuously measured while engineering strain stopped at some values.

3.5.1 Validation of mechanical properties of the geomembrane in this study that tested at 50 mm/min

Mechanical properties from tensile test of the selected geomembrane in this study have been compared with those with similar 1.0 mm thickness geomembrane from different resources. Five specimens have been tested in tensile at displacement rate of 50 mm/min. Table 3.2 shows individual results of mechanical properties of tensile test for the 1 mm HDPE geomembrane in this research. Yield stress and yield strain are presented in columns two and three in table 3.2. Yield properties show a consistence values with yield stress and yield strain around 21 MPa and around 0.1 mm/mm

respectively. While break stress is measured as the maximum stress before break, break strain cannot be measured at all replicates. The strain has been stopped for all test except replicate U2-50 before reaching break point. The problem is that video extensometer failed to track paint marker dots at these tests. However, break stress shows high variation with a different of 11.9 MPa between maximum and minimum measured values. One expected reason behind this high variation is the manufacturer imperfection of geomembrane material.

Table 3.3 shows tensile properties from Geosynthetic Research Institute (GRI-GM13), geomembrane product sheet from a known manufacturer geosynthetic company (GSE), Rowe and Ewais, and test results of studied geomembrane. GRI-GM13 specify the minimum material properties such as physical, chemical, and mechanicals properties that must be exceeded or met by manufactured geomembrane. The GSE product sheet shows a product mechanical properties of a 1.0 mm geomembrane. The mechanical properties of the geomembrane that has been used in our research are compared with all advance properties' values. The mean of yield stress and the mean of break stress of our sample exceeded all values that given in table 3.3. This gives a good indication that our geomembrane sample was still in good condition despite its manufacturing a long time ago. However, the mean value of yield strain of our sample is lower than all yield strain values in table 3.3 and is 10% lower than minimum value given by GRI-GM13. Specimens in this study is subjected to preload of 3 N. Preload gives a straight vertical aligned specimen. However, the elastic zone of HDPE is very small and could be affected by applied preload. Thus, applying preload results in specimen stretching, locating two dots in new positions after alignment, and then measuring yield strain at lower

displacement value and all that give lower yield strain.

Figures 3.9-3.11 compare tensile test results with comparative properties. Yield stress results showed that GRI-GM13, GSE, Rowe and Ewais, and test results are equal to 15, 15, 20.7, and 20.12 MPa respectively. The results showed that minimum average values for GRI- and GSE are same, while Rowe and Ewais and test results are higher than minimum, 15 MPa (Figure 3.9). The difference between Rowe and Ewais and test results is equal to 1.9 %. Yield stress of test results shows lower deviation compared to Rowe and Ewais results.

For figure 3.10, the results of break strength show similar trend of figure 3.9. For instance, minimum average value of GRI-GM13 and GSE are smaller than both Rowe and Ewais and test results by 20% approximately. Break strength of Rowe and Ewais and test results have same values, 35 MPa, roughly. However, test results showed higher variation compared to Rowe and Ewais results. Although missing data of break strain because of limitation of strain measurement, it is reasonable to expect comparative variation of break strain since break properties occurs at same failure point.

Minimum value of yield strain given by GRI-GM13 is close to GSE value, while Rowe and Ewais yield strain is higher than test results by 50%. However, the mean of yield strain from test results is lower than specified yield strain from GRI-GM13 by only 15 % (Figure 3.11). The proposed reason for such difference in yield strain is because specimens at test results are subjected to a preload prior to test initiation. Preload result in straight narrow section of specimen and stretch it within elastic zone. While specimen stretching before testing is necessary to measure gage length and strain, it may result in reaching yield strain earlier than non-preloaded specimen.

3.5.2 Variation of mechanical properties of five replicates tested at 50 mm/min

The mean and coefficient of variation of tensile properties for test results has been measured and compared with same thickness HDPE geomembrane tensile properties. Table 3.3 shows tensile properties from Geosynthetic Research Institute (GRI-GM13), geomembrane product sheet from a known manufacturer geosynthetic company (GSE), Rowe and Ewais, and test results of studied geomembrane. The variation of data from Both the GRI-GM13 and GSE were not available. The COV of yield properties of our geomembrane (σ_y and ε_y) are very close or lower than variation of Rowe and Ewais. However, COV of σ_b is more than 6 folds that of Rowe and Ewais. The test U5-50 of our sample show very low σ_b (26.2 MPa) compare to other four replicates of the sample. This specimen shows no abnormality during the test and after break. The early break of this specimen result in this high variation in break strength property. It is accepted that some specimen has premature break because of imperfection at some points on produced geomembrane. Because of limitation of strain measurement up to the end of test, the mean of break strain couldn't be measured. The ASTM D6693 presented precision information of tensile test of four different geomembrane types. The calculated value of COV of break strength of smooth HDPE was 10.7. The COV of test result of five replicates (16 %) is higher than COV values given in standard. The effect of replicates on variation will be studied in the next section.

3.5.3 Effect of replicates on tensile test properties at displacement rate of 50 mm/min

Mechanical properties have been measured for five replicates of tests that performed at displacement rate of 50 mm/min. In order to study the effect of replicates on

tensile properties, three replicates out of 5 replicates are selected to get 6 groups. Table 3.4 shows mean and variation of tensile properties of these groups. Yield stress shows the lower variation with a COV range 0.6-1.9% while yield strain shows a variation 2.6-8.6%. The variation range of yield stress from all groups (1-6) are lower than the variation given by Rowe and Ewais (COV=4.8%), while the maximum variation of yield strain of 6 groups is close or slightly greater than that given by Rowe and Ewais (COV=6.3%). On the other hand, groups show greater coefficient of variation of break strength (2.5-21.2%). Three groups that include results of test U5-50 shows the higher variation with values of around 20%. The COV of break strength of these groups are higher than COV in ASTM D6693 (10.5%). However, COV of groups 1-3 without test U5-50 shows acceptable COV with values of 2.5-7.5%. Test U5-50 has a valuable effect on variation of break strength. However, three replicates groups that exclude test U5-50 show acceptable variation of mechanical properties (groups 1-3 table 3.4). This suggest that three replicates test can be accepted to evaluate mechanical properties. Because of limitation of material, only three replicates will be used to study mechanical properties of the material at different displacement rates.

3.5.4 Effect of displacement rate on tensile properties

Tensile properties have been measured for displacement rates in the test matrix in table 3.1. Figure 3.12 shows yield stress of replicates at each displacement rate. The scattering of data is approximately similar among all rates. There is a slight lower scattering at test performed at 20 mm/min. Tests performed at 10 mm/min shows lower values of yield stress compared with other rates. On the other hand, yield strain data shows no relation with displacement rate with values around 0.1 mm/mm (Figure 3.13).

Figure 3.14 shows break strength of each replicate in the data sets. There is no relation between break stress and displacement rate. Break strength of test U5-50 is far not only from replicates at same displacement rate (50mm/min) but also from all replicates at other lower displacement rates.

Because of the limitation of paint marker dot and fading problem, most of the break strains have not been measured. Thus, the maximum strain that measured on a tensile curve is collected and denoted by ε_{max} in column 6 of table 3.5. The maximum measured strain ε_{max} that does not represent break strain because of the fading problem marked with stars. Other ε_{max} that has no mark represents break strain that has no measurement problem. Only 30% of tests has a continuous measured strain up to break point. Most values of measured ε_{max} exceed 7 mm/mm strain values. Column 5 in table 3.5 represents corresponding stresses measured at strain value ε_{max} on stress-strain curves. No trend has been noticed for each of ε_{max} or σ_{max} with displacement rates. Fading problem does not relate to displacement rate or testing time such as long test time at low displacement rates.

3.5.5 Variation of tensile properties with displacement rate

Mean and variation of each tensile property at displacement rates that given in test matrix have been calculated and shown in table 3.6. The average value of maximum measured strain of tensile test were exceed 7.0 mm/mm for all displacement rates. This give data of tensile test on strain hardening region at range of strain of 5.0-7.0 mm/mm. COV of yield stress are lower than COV calculated from ASTM D6693 (5.8%) at all displacement rates. Similar to yield stress, the coefficient of variation of yield strain are lower than that calculated from ASTM D6693 (35%). The repeatability of yield

properties suggested a good measurement of video extensometer and load cell at low value of strain and load. On the other hand, the COV of break strength measured at 50 mm/min was higher than COV calculated from ASTM D6693 (10.7). However, the COV of all other displacement rates lower than 50 mm/min are lower than the COV of break that calculated from ASTM D6693. The high COV of break strength at 50 mm/min is measured for five replicates and it has been shown that test U5-50 with lower value of break strength result in increased the variation. The low COV of break strength at displacement rates lower than 50 mm/min suggest a high repeatability of break property even with only three replicates test.

3.6 Conclusion

The mechanical properties of 1 mm HDPE geomembrane have been studied in this research. The following conclusions were reached.

1) The selected test parameters such as sampling frequency at each displacement rate result in acceptable measurement of load and strain and meet the required accuracy of tensile standard.
2) Tensile test properties at yield and break shows that the material is within the acceptable limits and meet the requirement given by GRI-GM13.
3) The onset of strain hardening region start at strain of 5.0 mm/mm. While the maximum measured strain at all displacement rates are greater than 7.0 mm/mm.
4) It is found that three replicates provide acceptable results repeatability compared with standards and literature variation.
5) The displacement rate has no effect on tensile properties or variation.

Table 3.1 Text matrix of tensile test experiment at selected rates

Specimen designation	Displacement rate (mm/min)	Sampling frequency (sec)	Number of data points /1 mm displacement
U1-50	50	0.10	13/mm
U2-50			
U3-50			
U4-50			
U5-50			
U1-30	30	0.16	13/mm
U2-30			
U3-30			
U1-25	25	0.20	13/mm
U2-25			
U3-25			
U1-20	20	0.25	13/mm
U2-20			
U3-20			
U1-10	10	0.50	13/mm
U2-10			
U3-10			

Table 3.2 Mechanical properties of 1 mm HDPE geomembrane in this research

Specimen designation	σ_y (MPa)	ε_y (mm/mm)	σ_b (MPa)	σ_{max} (MPa)	$\varepsilon_{max.}$ (mm/mm)
U1-50	20.7	0.107	39.8	35.9	8.08*
U2-50	21.4	0.096	38.1	38.1	8.04
U3-50	21.0	0.094	34.4	29.4	6.98*
U4-50	21.2	0.099	39.8	27.3	6.75*
U5-50	21.3	0.111	26.2	26.2	6.81*

Table 3.3 Tensile properties from GRI, GSE, Rowe and Ewais, and material in this study (all are 1.0 mm thickness)

Property	GRI-GM13			GSE product			Rowe and Ewais [20]			Test results		
	Mean	SD	COV%	Mean	SD	COV%	Mean	SD	COV%	Mean	SD	COV%
σ_y (MPa)	15.0	-	-	15.0	-	-	20.7	1.00	4.8	21.2	0.298	1.4
ε_y (mm/mm)	0.12	-	-	0.13	-	-	0.19	0.012	6.3	0.101	0.007	7.2
σ_b (MPa)	27	-	-	28	-	-	35.3	0.9	2.5	35.7	5.706	16.0
ε_b (mm/mm)	7.00	-	-	7.00	-	-	8.52	0.37	4.3	-	-	-

Table 3.4 Tensile properties of three replicates out of five for test perform at 50 mm/min

Group No.	Replicates	Property	Mean	SD	COV %
Data without test U5					
1	U1,U2,U3	σ_y (MPa)	21.09	0.390	1.8
		ε_y (mm/mm)	0.099	0.007	7.1
		σ_b (MPa)	37.4	2.762	7.4
2	U1,U2,U4	σ_y (MPa)	21.13	0.397	1.9
		ε_y (mm/mm)	0.101	0.006	5.6
		σ_b (MPa)	39.3	0.997	2.5
3	U2,U3,U4	σ_y (MPa)	21.26	0.199	0.9
		ε_y (mm/mm)	0.096	0.003	2.6
		σ_b (MPa)	37.5	2.792	7.5
Data with test U5					
4	U1,U2,U5	σ_y (MPa)	21.17	0.416	2.0
		ε_y (mm/mm)	0.105	0.008	7.4
		σ_b (MPa)	34.7	7.361	21.2
5	U2,U4,U5	σ_y (MPa)	21.35	0.130	0.6
		ε_y (mm/mm)	0.102	0.008	7.8
		σ_b (MPa)	34.8	7.385	21.2
6	U3,U4,U5	σ_y (MPa)	21.22	0.125	0.6
		ε_y (mm/mm)	0.101	0.009	8.6
		σ_b (MPa)	33.5	6.833	20.4

Table 3.5 Tensile properties from engineering stress-engineering strain curves of tests performed at displacement rate of 50, 30, 25, 20, and 10 mm/min

Specimen designation	σ_y (MPa)	ε_y (mm/mm)	σ_b (MPa)	σ_{max} (MPa)	$\varepsilon_{max.}$ (mm/mm)
U1-50	20.7	0.107	39.8	35.9	8.08*
U2-50	21.4	0.096	38.1	38.1	8.04
U3-50	21.0	0.094	34.4	29.4	6.98*
U4-50	21.2	0.099	39.8	27.3	6.75*
U5-50	21.3	0.111	26.2	26.2	6.81*
U1-30	21.2	0.103	32.7	32.0	7.38*
U2-30	20.3	0.101	37.8	37.8	8.18
U3-30	20.7	0.104	37.5	37.5	8.17
U1-25	21.0	0.107	40.0	28.4	7.02*
U2-25	20.7	0.102	36.1	36.1	8.02
U3-25	20.1	0.096	36.7	36.0	7.85*
U1-20	20.3	0.105	40.8	40.8	8.72
U2-20	20.1	0.099	38.8	36.5	8.14*
U3-20	20.0	0.110	39.2	38.6	8.49*
U1-10	19.5	0.107	38.3	33.9	7.95*
U2-10	19.1	0.108	35.9	26.1	6.90*
U3-10	19.8	0.100	37.1	26.3	6.82*

ε_{max} with star represent maximum strain detected by extensometer

Table 3.6 Mean of tensile properties, standard deviation, and coefficient of variation measured for samples at displacement rates of 50, 30, 25, 20, and 10 mm/min.

Rate (mm/min)	Property	Mean	SD	COV %
50	σ_y (MPa)	21.2	0.298	1.4
	ε_y (mm/mm)	0.101	0.007	7.2
	σ_b (MPa)	35.7	5.706	16.0
	σ_{max} (MPa)	31.4	5.241	16.7
	ε_{max*} (mm/mm)	7.35	0.670	9.1
30	σ_y (Mpa)	20.8	0.440	2.1
	ε_y (mm/mm)	0.103	0.002	1.5
	σ_b (MPa)	36.0	2.864	7.9
	σ_{max} (MPa)	35.8	3.280	9.2
	ε_{max*} (mm/mm)	7.92	0.459	5.8
25	σ_y (MPa)	20.6	0.456	2.3
	ε_y (mm/mm)	0.102	0.006	5.4
	σ_b (MPa)	37.7	2.096	5.6
	σ_{max} (MPa)	33.5	4.425	13.2
	ε_{max*} (mm/mm)	7.63	0.535	7.0
20	σ_y (MPa)	20.2	0.165	0.8
	ε_y (mm/mm)	0.105	0.006	5.3
	σ_b (MPa)	39.7	1.070	2.7
	σ_{max} (MPa)	38.7	2.152	5.6
	ε_{max*} (mm/mm)	8.45	0.292	3.5
10	σ_y (MPa)	19.5	0.368	1.9
	ε_y (mm/mm)	0.105	0.004	4.2
	σ_b (MPa)	37.1	1.205	3.2
	σ_{max} (MPa)	28.8	4.416	15.4
	ε_{max*} (mm/mm)	7.23	0.631	8.8

Five replicates for test at 50 mm/min, three replicates for other displacement rates lower than 50 mm/min.

Figure 3.1 Teflon sheet and Pioneer die mold that used to cut dogbone geomembrane specimen

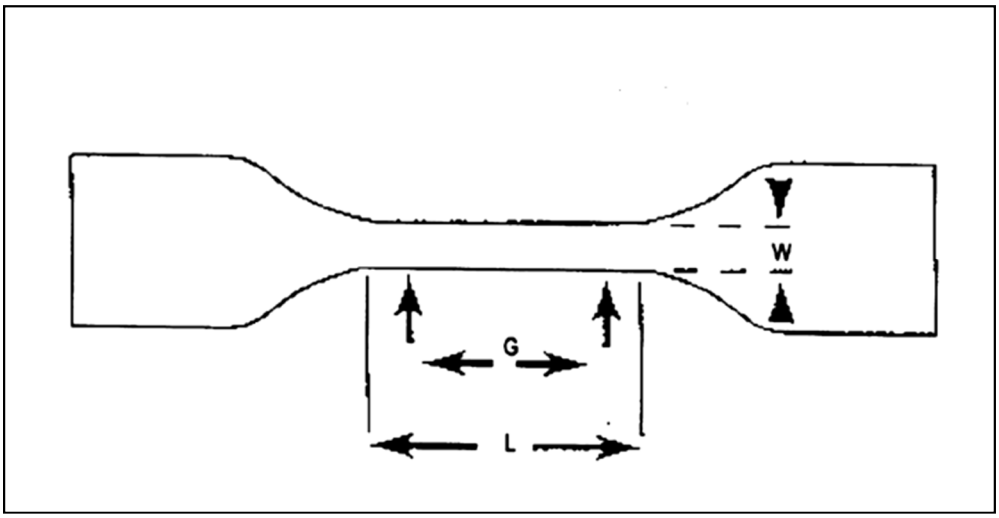

Figure 3.2 Specimen used for tensile test, G is gage length, w is width of narrow section, L is length of narrow section (Modified from [1])

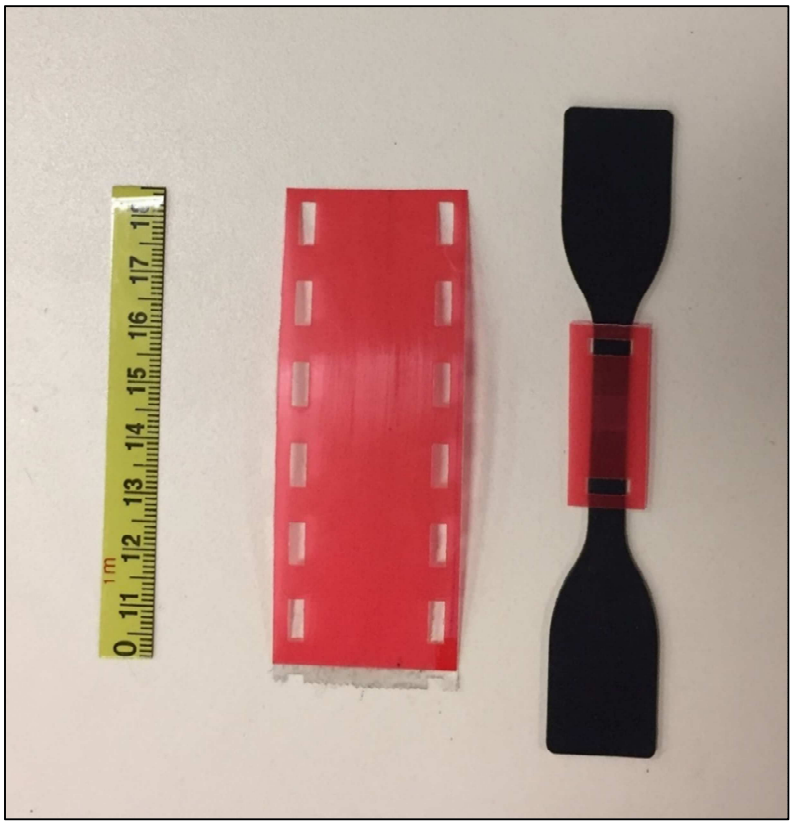

Figure 3.3 Preparing stick tape with a rectangular punched hole to locate gage marks

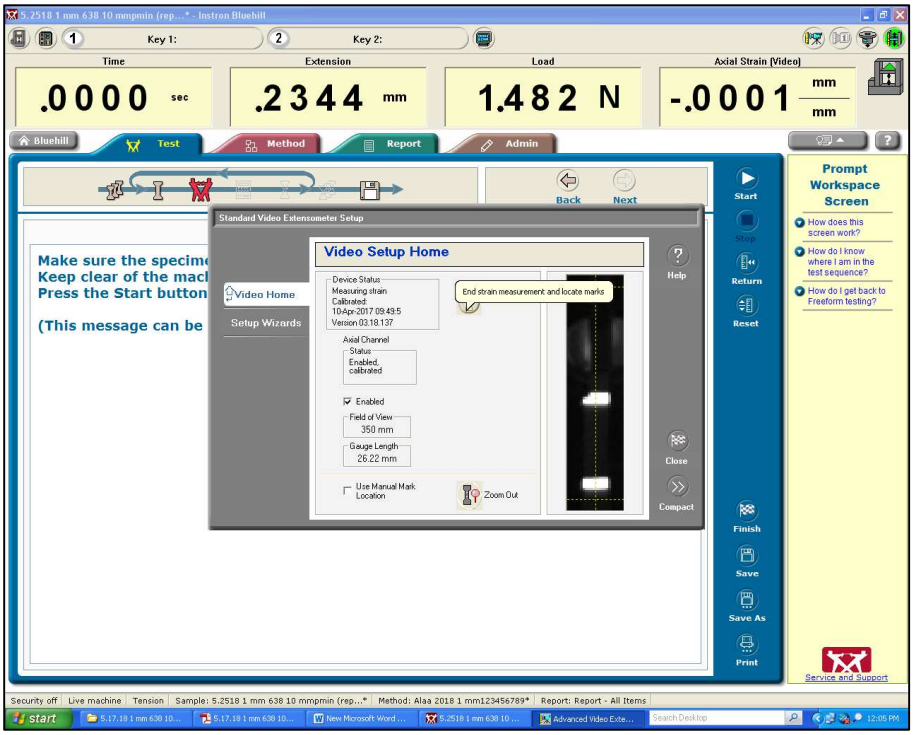

Figure 3.4 Screen shot of Bluhill 2 software shows measurement of gage length between gage markers

Figure 3.5 Experimental setup using an Instron 5566 and an Instron AVE video extensometer

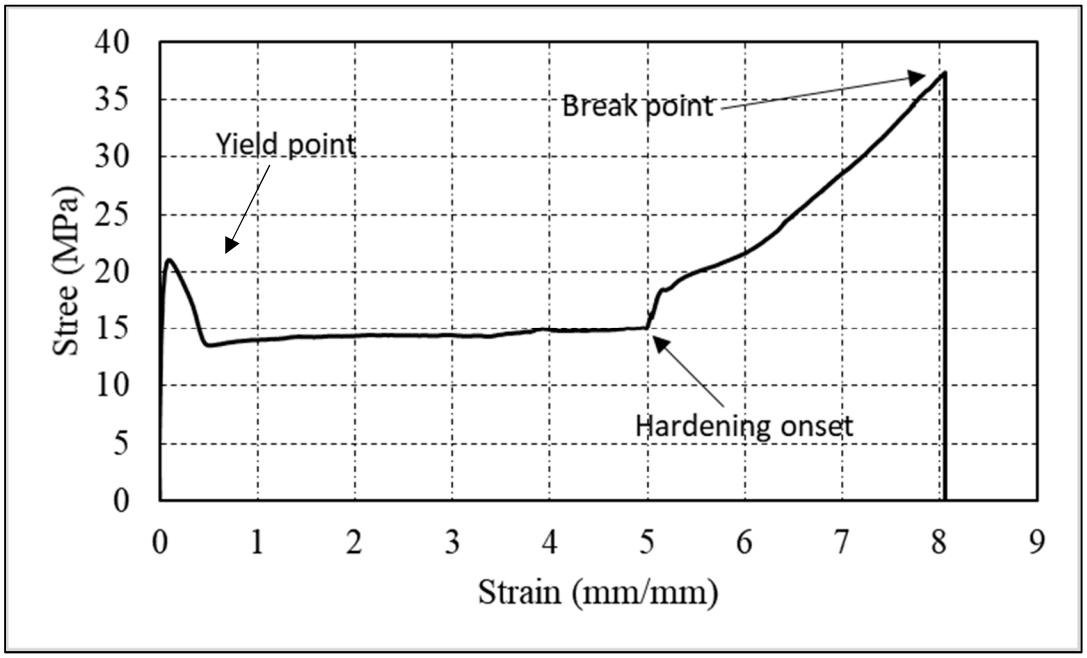

Figure 3.6 Typical stress-strain curve of HDPE geomembrane tensile test shows important features

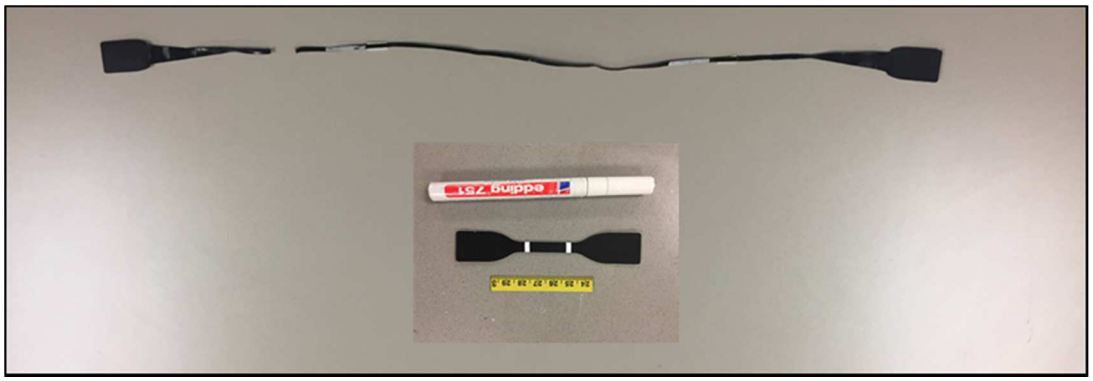

Figure 3.7 Dogbone tensile specimen before (below) and after (above) test shows high extensibility of HDPE geomembrane.

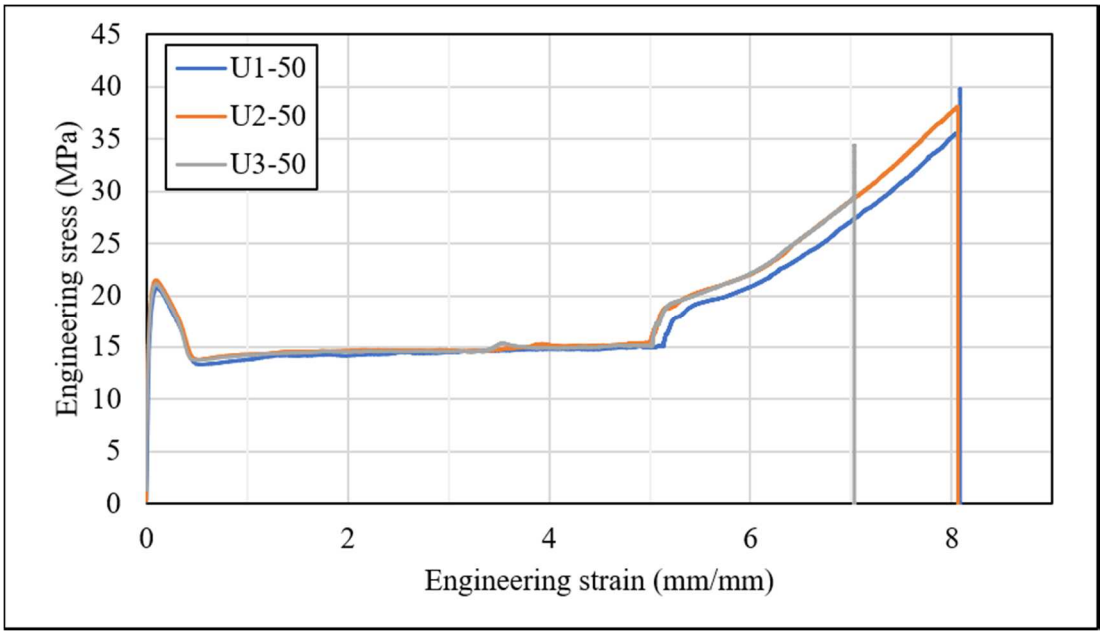

Figure 3.8 Engineering stress-engineering strain curves for three replicates at 50 mm/min

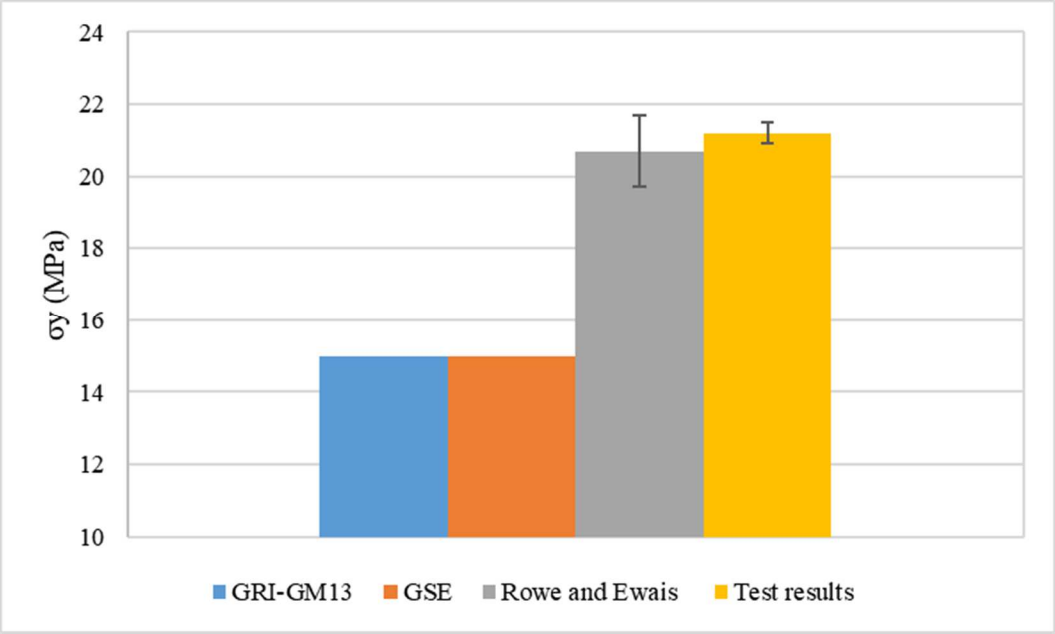

Figure 3.9 Compare yield stress results of HDPE geomembrane from several resources

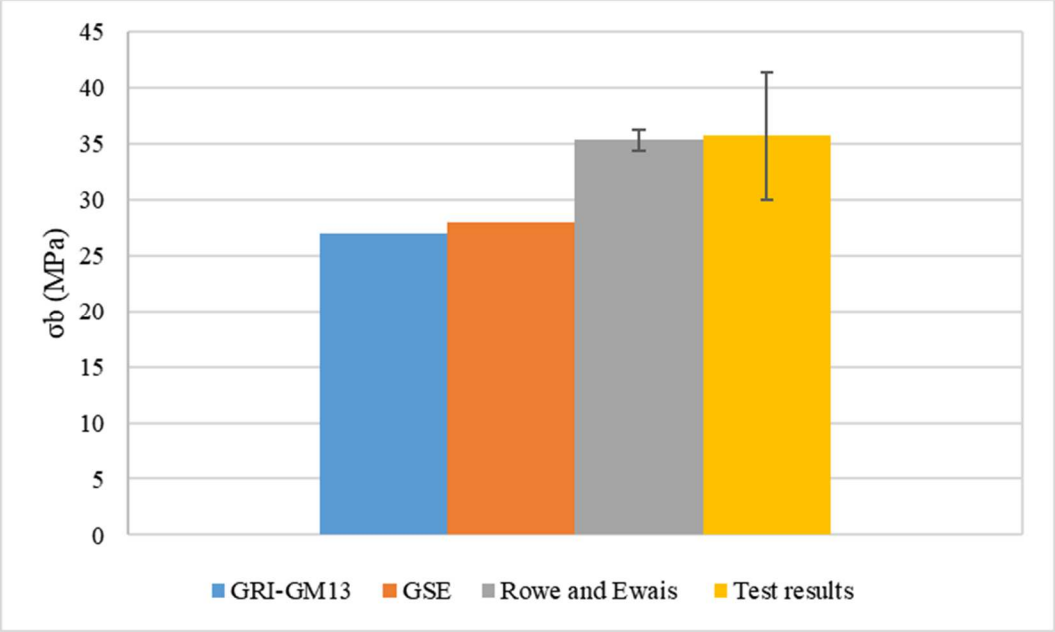

Figure 3.10 Compare break strength results of HDPE geomembrane from several resources

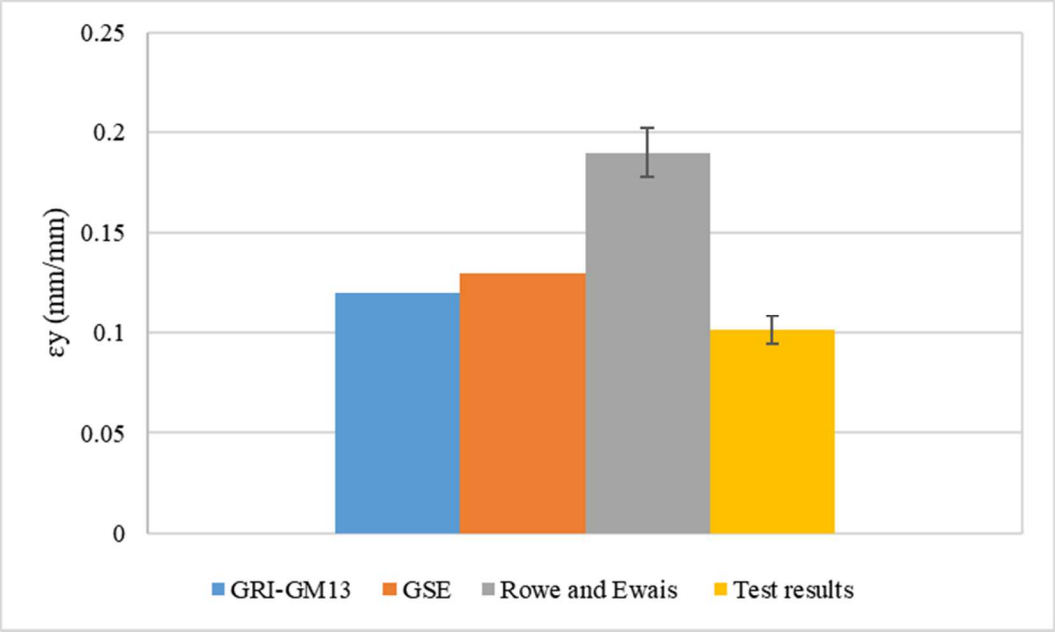

Figure 3.11 Compare yield stress results of HDPE geomembrane from several resources

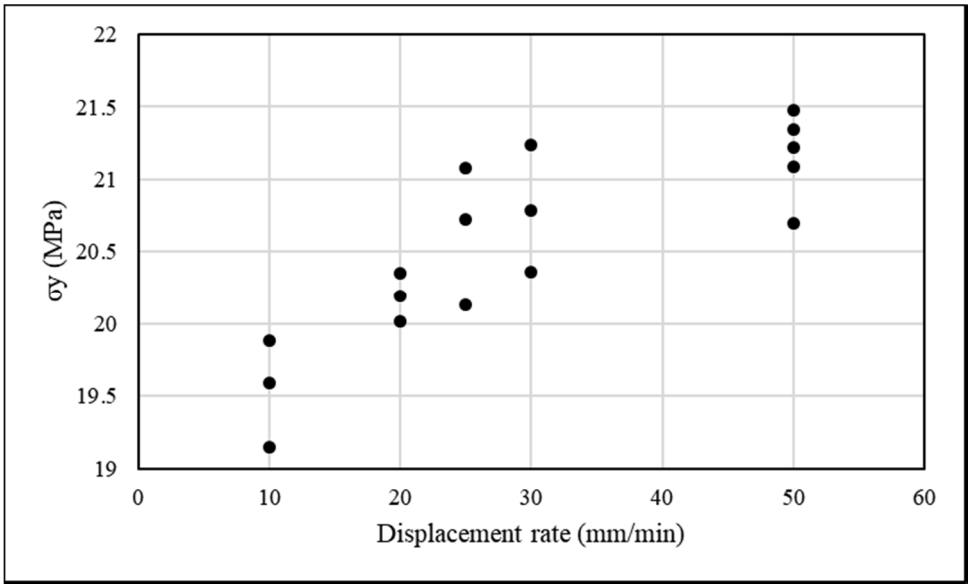

Figure 3.12 Yield stress versus displacement rate of 1 mm HDPE geomembrane

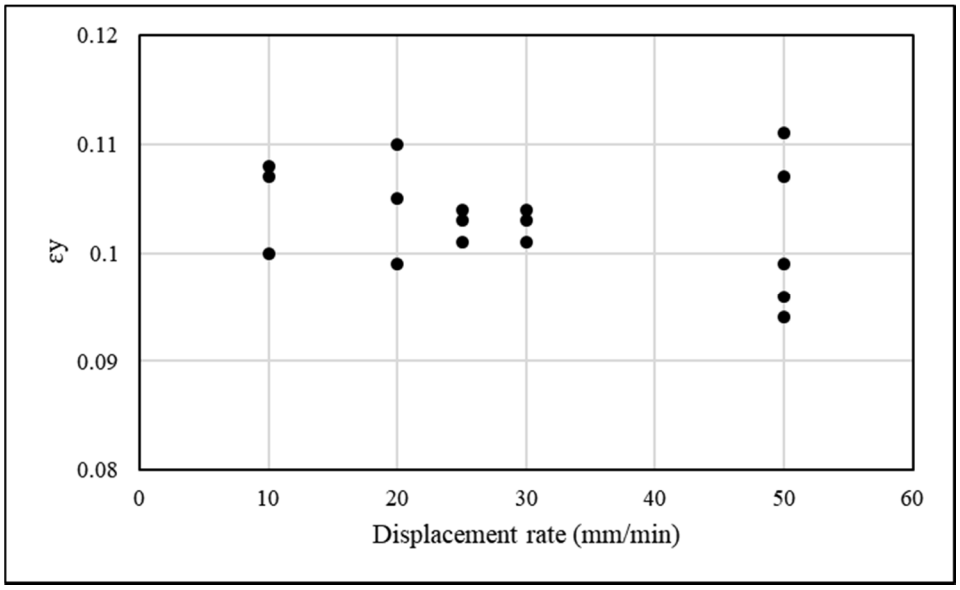

Figure 3.13 Yield strain versus displacement rate of 1 mm HDPE geomembrane

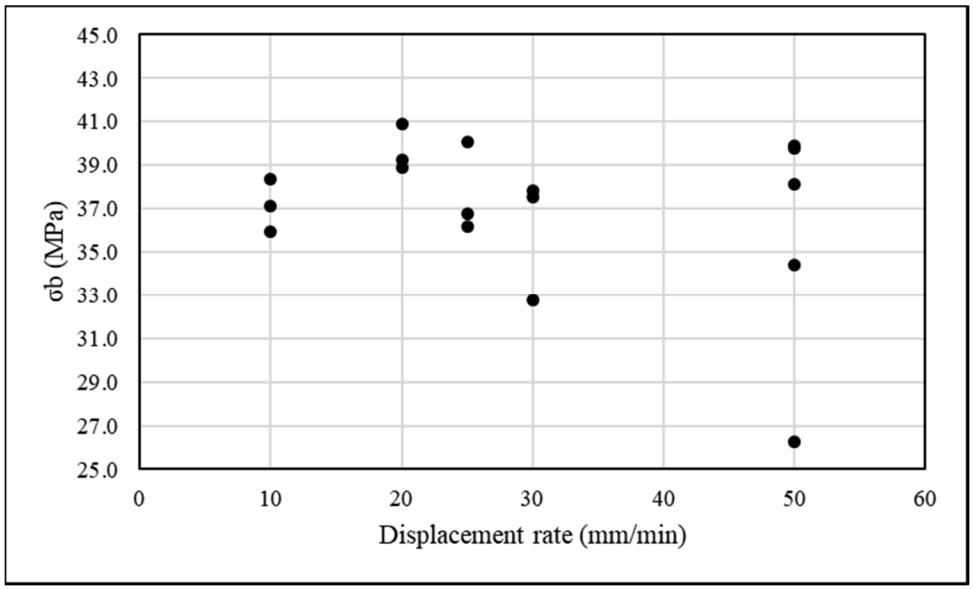

Figure 3.14 Break strength with displacement rate of 1 mm HDPE geomembrane

REFERENCES

[1] GRI Test Method GM13 (2016). Standard Specification for "Test Methods, Test Properties and Testing Frequency for High Density Polyethylene (HDPE) Smooth and Textured Geomembranes (Revision 10), *GSI Geosynthetic Institute, Folsom, PA, USA.*

[2] Tensile test properties of 1 mm HDPE geomembrane from GSE http://www.gseworld.com/content/documents/productsheets/DIS_GundSeal_METRIC.doc

[3] Rowe and Ewais 2014 Antioxidant depletion from five geomembranes of same resin but of different thicknesses immersed in leachate

[4] ASTM D638- 14 Standard Test Method for Tensile Properties of Plastics

[5] ASTM D6693/D6693M-04(2015) Standard Test Method for Determining Tensile Properties of Nonreinforced Polyethylene and Nonreinforced Flexible Polypropylene Geomembranes

[6] ASTM D4833-07 Standard Test Method for Index Puncture Resistance of Geomembranes and Related Products

[7] ASTM D8172-18 Standard Test Method for Shear and Peel Strength of Solvent-Welded Seams with Nonreinforced Geomembranes

[8] ASTM D1004-13 Standard Test Method for Tear Resistance (Graves Tear) of Plastic Film and Sheeting

[9] ASTM D5397-19 Standard Test Method for Evaluation of Stress Crack Resistance of Polyolefin Geomembranes Using Notched Constant Tensile Load Test

[10] ASTM D1693-15 Standard Test Method for Environmental Stress-Cracking of Ethylene Plastics

[11] Rowe and Sangam 2009 Ageing of HDPE geomembrane exposed to air, water and leachate at different temperatures

[12] Rowe et al 2008 Depletion of Antioxidants from an HDPE Geomembrane in a Composite Liner

[13] Rowe et al 2010 Antioxidant Depletion from a High Density Polyethylene Geomembrane under Simulated Landfill Conditions

[14] Havermans-van Beek, D. J. M., Delieck, R., McCarthy, M., Kloth, R., & Kurelec, L. (2010). An elegant and fast method to predict the slow crack growth behaviour of high density polyethylene pipe materials. In *Plastic Pipes XV Conference*.

[15] Engelsing, K. and Zanzinger, H. (2012). A new accelerated test method for stress Crack resistance of HDPE geomembranes. Segundo Congreso Panamericano de Géosintéticos, GEOAMERICAS 2012, 01-04 de Mayo, 2012, Lima, Peru, 8p.

CHAPTER 4

STANDARDIZED STRAIN HARDENING METHOD OF HIGH-DENSITY POLYETHYLENE GEOMEMBRANES

4.1 Introduction

In this chapter, the strain hardening modulus is calculated for unaged high-density polyethylene (HDPE) geomembrane specimens in tension at room temperature. The strain hardening behavior of HDPE geomembranes is non-linear, and the strain hardening modulus depends on the range of strain over which it is calculated. Tensile tests are performed at several displacement rates (high to low) to study their effects on strain hardening modulus. The purpose of this chapter is to select a displacement rate and strain interval that provide the most repeatable calculation of strain hardening modulus.

4.2 Background

Strain hardening is the strengthening of material by plastic deformation. The strengthening occurs as a result of dislocation movements within crystal structure of the material [1]. The Strain Hardening Method was studied by many researchers to evaluate service life and crack resistance of different polyethylene resins such as pipe resins [1, 2, 3,4, 5, 6, 7], bimodal HDPE pipe PE80 and PE100 [8, 9, 10, 11, 12, 13], unimodal resin [14], polytetrafluorethylene [15], LDPE and HDPE [16], aged pipe resin PE80 and PE100 [17], geomembrane resins [18], aged HDPE pond liner [19], aged geomembrane liner [20].

The strain hardening modulus is measured usually from tensile test that performed at high temperature. Researchers measured strain hardening for tensile test at 80 °C with displacement rate of 10 or 20 mm/min [4, 5, 8, 10,11, 12, 13, 14, 17, 18]. Oven chamber is manufactured in a way to allow performing tensile test at high temperature. Tensile specimen is pulled inside the chamber until the end of the test. The strain between gage marks are measured using video extensometers or contact extensometers. Oven chamber add limitation of using these extensometers during the test. The strain hardening modulus is measured as the slope of tensile curve after natural draw ratio. The x-axis of tensile curve is draw ratio while the y-axis is the trues stress that calculated assuming conservation of specimen volume between gage marks. The strain hardening modulus is calculated in literature between different draw ratio limits according material strain hardening region and test limitation. Several researchers select to calculate strain hardening at draw ratio limits of 8-12 [4, 6, 8, 11, 12]. Other researcher suggested λ limits of 9-12 [1, 10]. The minimum draw ratio limit ranged between 8 and 9 while the maximum draw ratio is mostly limited by oven chamber length while. Other researchers measure the slope of strain hardening part at load-displacement or stress-strain curve [2, 3, 9, 7, 15, 16, 19]. The strain hardening modulus method has been investigated for several PE pipe resins using a 0.3 mm sample thickness and a 20 mm/min displacement rate at 80 °C [5]. In this work, it was found that strain hardening method can easily distinguish between different PE types including PE100 and PE100RC produced from different resins manufacturers. The study also showed that the strain hardening values for the same materials tested at 8 different laboratories were very similar to a low variation coefficient. The strain hardening modulus method was published as an international

standard in 2015 to predict crack resistance of PE pipe resins [21]. According to this standard, the test is performed using a universal testing machine equipped with optical extensometer at a crosshead speed of 20 mm/min and at 80 °C chamber temperature.

Conducting strain hardening test at room temperature allow measuring strain by many extensometers and allow using more data of strain hardening region without the need to stop the test at the maximum length of chamber. The strain hardening test conducted on two blown molding HDPE resins tested at room temperature and 80 °C at a rate of 10 mm/min were examined. These resins have a low crack resistance of 58 hours and 103 hours respectively. It is reported that the stress-strain response after the onset of strain hardening of these two samples at the same room temperature has no significant difference. However, at 80 °C, significant difference was noticed between test curves [1]. It is further suggested to conduct strain hardening tests at room temperature and at a low displacement rate of 0.2 mm/min [1]. While a lot of material laboratories have tensile device to measure mechanical properties of different materials, oven chamber that allow performing strain hardening test are limited. Having a procedure to perform tensile test and measure strain hardening modulus at room temperature make the test more accessible in laboratories that have only tensile device with no oven chamber.

Various types of HDPE products such as blow mold, injection mold and HDPE pipe resins were also studied [2]. The tests follow ASTM D 638 using a dogbone sample with a narrow section being 41 mm and 1.8 mm in thickness. The specimen was stretched to extensions of 7 and 0.5 mm/min displacement rates at room temperature. Hardening stiffness was measured from the load displacement curve after the onset of hardening. It

was shown that hardening stiffness test detected differences in crack resistance of PE resins at both 0.5 and 7 mm/min.

At tensile test of five bimodal PE with different molecular parameters has been performed following the ASTM D638 at a 7 mm/min displacement rate at room temperature [9]. It is shown that the tensile strain hardening stiffness test was a fast and reliable method for evaluating crack resistance of PE [9]. However, no standard has been produced for measuring hardening stiffness in this research. In addition, the hardening stiffness in this research is measured using the total hardening zone of load displacement curve rather than a specific zone of displacement or strain values.

HDPE geomembrane is produced and used to cover a large area at the bottom of landfills and lagoon. Every geomembrane roll that used at site has to be tested to assure validity of using in landfills and lagoons. Researchers pointed out the need for a new test method to assess service life of HDPE geomembrane with more convenient test time and easier test performance [22, 23].

To date there is no standardized strain hardening modulus test for geomembrane resins. It must be recognized that suitable ovens for tensile test measurement are not always available in laboratories. In addition, many difficulties may be encountered performing the test inside oven chambers. The length of the heating chamber limits the maximum strain that can be used to measure strain hardening [1, 8]. Also, the high oven temperature results in the breaking of self-stick gage markers [4]. In this chapter, the strain hardening modulus is measured for HDPE geomembrane at room temperature. The displacement rate and draw ratio intervals will be selected based on test results. The

effect of measurement method and displacement rate on repeatability of data will be studied.

4.3 Materials and methods

In this chapter, tensile test data of HDPE geomembrane from chapter 3 will be further used to measure strain hardening modulus. Tests are performed at displacement rate of 50, 30, 25, 20, and 10 mm/min. Only three replicates are used for each displacement rate to study strain hardening. Several methods will be proposed to measure strain hardening modulus.

4.3.1 HDPE geomembrane

A 1 mm HDPE geomembrane is used for this study as received from the manufacturer. This geomembrane is available as a roll at the University of South Carolina Civil and Environmental Engineering Department and stored in the dark at room temperature for several years. The apparent view of the material shows a clean surface with a Tensile test of the material showed that the material is acceptable and met the requirement given by Geosynthetic Research Institute (GRI-GM13). The limited available area of the material control test number of tests thus tests are performed only at three replicates at each displacement rate.

4.3.2 Specimen shape and dimensions

A tensile test specimen is cut using a dogbone die produced by Pioneer Co, part number 16655. The cut specimen is type IV which is applicable for both ASTM D638 type IV and ASTM D6693 [24, 25]. Tensile test is performed according to ASTM D6693. However, because of limited material, only three replicates are performed. In

addition, tensile specimen exposed to preload of about 3 N to give a straight specimen under preload stress of 0.5 MPa which close to stress that applied for strain hardening test (0.4 MPa) [26, 27]. Specimen is 6.0 mm in width of narrow section and 33.0 mm in length of narrow section (Figure 4.1). The thickness of specimen is measured at three locations along the narrow section using a digital caliper of 0.02 mm accuracy and the average is determined for later calculation. Since the geomembrane is an anisotropic material, mechanical properties in one direction are expected to be different than the other one. For consistence, tests are performed at only cross machine direction (CMD).

4.3.3 Specimen gage length

The gage length is specified by ASTM D6693 to be 25 mm [25]. Since video extensometer is used to measure strain, two white marker dots applied on the specimen. Paint marker type edding 571 is used to apply white marker that contrast to specimen black color. This marker is come with calibration tool box of the tensile device. The instruction manual of video extensometer that used in the test advised to have a mark that cover the width of the specimen narrow section. The location of mark is located based on the center of mark between its upper and lower edges. Thus, a clear edge of mark gives better result of mark location and strain measurement. For this reason, a rectangular tape is punched from top and bottom using paper punch to form a Staedtler template. This tape sticked on the narrow section of the specimen and paint mark applied then the tape removes to give a rectangle marks with smooth edges. The marks are located to give approximately a 25 mm gage length within 33 mm long narrow section of the specimen (Figure 4.2). The specimen is subjected to a preload force of 3 N before measuring gage length. Gage length is measured from Bluhill2 software screen. Tensile specimen preload

is common practice in tensile test that conducted to get a data for measuring strain hardening modulus [26, 27].

4.3.4 Test matrix

Series of tests are performed on 1 mm GMB at displacement rates of 50 to 10 mm/min. At least three replicates are performed at each rate as it is common in Gp research [10, 13, 17]. Paint marker fade during the test and result in lack of strain data at some point as has been discussed in chapter 3.

Table 4.1 shows test matrix including sampling frequency and number of data point per mm for each test rate. Sampling frequency for test performed at 50 mm/min displacement rate is selected to be 0.10 sec. This frequency is selected to provide reasonable data point. Number of data point per millimeter for this rate is 13 points. The frequency has been factored according to displacement rate to give same data point when testing at lower displacement rate.

4.3.5 Tensile test equipment

The tensile test is performed using tensile device type Instron 5566. The device has a load cell with a capacity of 5 kN and (serial number 64833), manufactured by Instron Co. A specimen can be tested in this device at displacement rate of 0.5 to 1000 mm/min. A noncontact optical video extensometer type AVE is used to locate gage marks on tensile specimen before and during the test and measure strain. This extensometer locates marks within a field of view of 350 mm (Figure 4.3). A software Bluehell2 that come with the tensile device is used to input test properties including displacement rate and sampling frequency. Data including sampling time, load, displacement, and strain are collected and saved to excel sheet on a computer to treated

later. The amount of data is collected so that is can be saved to the computer and it can be treated at acceptable time. Sampling frequency has been selected as 0.1 second so that to allow reporting the stress to three significant figures according to ASTM D6693 [25]. As displacement rate decrease, test time become grater and sampling rate has to be modified to save acceptable data amount. Sampling rate has been decreased as displacement rate decrease to allow measuring load at acceptable accuracy and reasonable amount of data. At 50 mm/min, sampling is conducted at 0.1 per second while sampling frequency decreases for lower displacement rate.

4.3.6 Collected data and data treatment

The raw data of tensile test include time, displacement, force, and strain. Only the force and strain are used for this research. The engineering stress (σ) and engineering strain (ε) are used for calculating other data that will use to measure strain hardening. Engineering stress is calculated as the force divided by initial cross-sectional area of the specimen. The specimen narrow section of the specimen is 6 mm while the thickness is 1 mm. Thus, the force is divided by 6 mm^2. The engineering strain (ε) represent the change in length between gage marks to the initial gage length. It is directly measured from the video extensometer. Figure 4.4 shows engineering stress engineering strain curve of tensile test of three replicates tested at 50 mm/min.

Since the purpose of tensile test is to measure strain hardening modulus, different space of data is used. The strain hardening modulus is measured as the slope of the curve after onset of strain hardening at draw ratio-true stress space. Draw ratio is calculated on the basis of gauge length according to the equation [1]:

$$\lambda = \frac{\Delta L}{L} + 1 \quad \text{.....4-1}$$

Where λ is the draw ratio expressed as a dimensionless ratio, L_o is the initial distance between the gauge dots in millimeters and ΔL is the increase in the specimen length between the gauge dots marks in millimeters. According to its definition, draw ratio represents the engineering strain plus one unit.

The true stress is calculated assuming conservation of sample volume between the gauge dot marks:

$$\sigma_t = \frac{\lambda . F}{A} \quad \text{4-2}$$

Where σ_t is the true stress in MPa, F is the measured force in Newtons, A is the initial cross-sectional area of the narrow section of the specimen in square millimeters. Tensile test of three replicates tested at 50 mm/min in true stress-draw ratio space are shown in figure 4.5. True stress shows higher value compared to engineering stress. The strain hardening modulus (Gp) is measured as the slope of strain hardening region after the onset of strain hardening. The next section will describe several ways of measuring strain hardening modulus in this research.

In order to study the variation of strain hardening modulus and evaluate the results, the standard deviation and coefficient of variation have been measured. The standard deviation is measured based on a sample of data and is given by the equation:

$$\mathrm{SD} = \sqrt{\frac{\Sigma(\mathrm{X}-\mathrm{Mean})^2}{\mathrm{n}-1}} \quad \text{4.3}$$

While SD is standard deviation, X is each value in the data set, Mean is the mean of all values of strain hardening modulus in the data set, and n is number of values in the data set which represent the number of replicates which is 3.

While the coefficient of variation (COV) is measured according to the equation:

$$\mathrm{COV} = \frac{SD}{Mean} * 100 \quad \text{.....4.4}$$

4.3.7 Selected draw ratio limits

Gp calculated in literature using different λ limits according to method of calculation and test limitation and conditions. It is considered that the strain hardening part of the true stress- draw ratio is homogeneously deformed well above the onset of strain hardening [1]. Several researchers perform tensile test at 80°C and select to calculate Gp at λ limits of 8-12 [8, 11, 12]. Other researcher suggested λ limits of 9-12 at same temperature (80°C) [1, 10]. The maximum λ is mostly limited by oven chamber length while the minimum λ limit ranged between 8 and 9. Other researchers perform tensile test at room temperature and measure the slope of the total strain hardening part at load-displacement or stress-strain curve [9, 15, 16, 19].

In our experiment, true stress-draw ratio data is used to calculate Gp on the basis of sample volume conservation which allow compare geomembranes with different thicknesses. The test is performed at room temperature. Several ways of measuring Gp are used in this research:

1- The two points method: Gp is measured as the slope between two points on strain hardening region. The first point is the onset of strain hardening which is determined visually by observing an increase in true stress after a constant value of true stress after yield point. The second point is the point of maximum draw ratio measured by extensometer. It should be mentioned here that the maximum draw ratio is not necessary represent draw ratio at break point since at most of tests the video extensometer failed to reach this point.

2- The best line fit through two points method: Gp is measured as the slope of best

fit line through all points between onset of strain hardening and maximum draw ratio points.

3- The best fit through a specific draw ratio method: Gp is measured at several selected zones of draw ratio and at different increments. There is a curvature zone after strain hardening onset. It is found that after λ of 6.5 mm/mm, the behavior of true stress-draw ratio is more linear. Thus, minimum draw ratio that used for Gp is 6.5 mm/mm. On the other hand, maximum calculated draw ratio at most of tests reach or exceed 8 mm/mm. Thus, the maximum used draw ratio is 8 mm/mm.

4.3.8 Scanning electron microscope (SEM)

A scanning electron microscopy (SEM) (model Tescan Vega-3) is used to observe appearance of fracture surfaces at break zone of the selected specimens (Figure 4.6). Tensile specimens that tested at a rate of 50, 20, and 10 mm/min are selected to visualize break zone. One side of break zone of each specimen is selected and cut to about 5 mm in length. The three selected portions are inserted vertically in a split mount holder that allows the scanning of breaking zone (Figure 4.7). Specimens are prepared, and gold coated by a sputter coater model Denton Vacuum Desk II under vacuum for 60 seconds (Figure 4.8).

4.4 Results

4.4.1 Strain hardening modulus measurement methods

The tensile tests were performed at displacement rates of 50, 30, 25, 20, and 10 mm/min. The maximum displacement rate (50 mm/min) is referenced in ASTM 6693 for the tensile test of polymer materials [25]. Three replicate tests were performed for each

displacement rate in order to examine variations in the results. The strain hardening modulus was calculated using three different methods: the two points method, the best fit through the two points method, and the best fit through a specific draw ratio method. In the first and second methods, the total strain hardening region data from the onset of strain hardening to the last measured point on the curve was used. The onset and end points on the strain hardening region for test U1-50 are shown in Figure 4.9. In the third method, the strain hardening modulus is measured at several selected draw ratio limits within the strain hardening region with different increments of draw ratio.

4.4.1.1 Two points method

In this method the strain hardening modulus is calculated as the slope between two points of the strain hardening region. The first point is at the onset of strain hardening region, and the second is at the final point on the strain hardening region (Figure 4.10). The onset of strain hardening is located visually. While the final point on curve represents the last point on the strain hardening region with detected draw ratio. The video extensometer failed to detect paint mark dots in many tests in this study because of fading. Depending on detected strain, the final point on tensile curve could be the break point or the point with maximum measured strain. If the video extensometer detects the location of paint marks up to the breaking point, then the final point is the break point. If the extensometer fails to detect the break point and the strain measurement stops at some point during the test because of a faded mark, then the final point is the point with the maximum measured strain. Table 4.2 shows the coordinates of the onset and end points that are used to measure strain hardening moduli (Gp) for three replicates at each displacement rate. The onset of strain hardening was around a draw ratio of 6.00,

while the maximum measured draw ratio varied between 7.82 and 9.43. The strain hardening region shows a concave down directly after the onset followed by a concave up after a draw ratio of 6.5 (Figure 4.10). The strain hardening moduli that were measured using two points are shown in table 4.2 column 7. At each displacement rate, the strain hardening modulus increases in relationship to the maximum draw ratio measured. Table 4.3 shows the mean value and variation of the data represented by standard deviation and the coefficient of variation at each displacement rate using a two points method (column two to four). The mean value of the strain hardening modulus is roughly between 64 and 80 MPa. There is no displacement rate effect on the mean of the strain hardening modulus. However, the lower mean of the strain hardening modulus has been measured at 10 mm/min compared to other rates. The low value of the mean of Gp agrees with both low values of true stress and low draw ratio that is measured at 10 mm/min. The coefficient of variation of Gp has been calculated at each displacement rate. Its value is between 3.5% and 8.3%. The value of the strain hardening modulus in this method is based on only two points on the strain hardening region. Since the initial point (onset of strain hardening) has a similar draw ratio and true stress value, then strain hardening has been affected mainly by the end point with measured maximum draw ratio and true stress. The variation of Gp found through this method is controlled mainly by end point coordinates (maximum draw ratio and true stress). However, it can be noticed that the line between these two points does not necessarily represent the data points that make up the strain hardening region well. Thus, measuring strain hardening as the slope between two points is not a reasonable method.

4.4.1.2 Best fit through two points method

Another way to measure strain hardening between two points is best fit through a set of data between the onset of the strain hardening and the end point on a curve. Figure 4.10 shows the best fit line through data at the strain hardening region in test U1-50. The best fit line is less steep than the line between two points. This lower slope occurs mainly because of the large amount of data forming a concave up part of the curve. Column 8 in table 4.2 shows a strain hardening modulus measured as the best fit line through points between the same two points used in previous methods. The strain hardening moduli that were measured using best fit are lower than the Gp measured between two points for all tests. Table 4.3 shows the mean value and variation of data represented by standard deviation and the coefficient of variation at each displacement rate using best fit through the two points method (column five to seven). Similar to measurement based on two points, the displacement rate has no effect on the mean of the strain hardening modulus based on best fit measurement. In addition, the coefficients of variation of the Gp of best fit measurements are much higher than comparative values from a two points strain hardening modulus. While best fit is more representative as a data set on the strain hardening region, results show a higher variation. From the curve of the strain hardening region in figure 4.10, it is observed that both methods were not representative of a linear part of the curve. It is more accepted to have a strain hardening measurement that passes through a mostly linear segment of the curve. A method of measuring strain hardening modulus through linear portions will result in better representative measurement and high repeatability. In the next section, several segments will be selected to get the most acceptable measurement method.

4.4.1.3 Best fit through specific draw ratio method

From above sections it is clear that the measurement of strain hardening modulus has to be at a selected draw ratio limits rather than the total strain hardening region. In this section, the modulus will be measured at several limits of draw ratio and increments. The effect of the displacement rate on a hardening modulus will be discussed. The variation of a hardening modulus will be studied in combination with the effect of the displacement rate. This will allow a proper measurement method to be selected and recommended as the most accurate. Because we are dealing with a large amount of data in this method of measuring Gp, only three displacement rates have been selected for study. These rates are the highest displacement rate of 50 mm/min and two lower displacement rates, which are 20 and 10 mm/min. The high displacement rate represents the standard test (ASTM D6693) while the low displacement rates are expected to be more sufficient for measuring Gp, according to the literature.

4.4.1.3.1 The selection of draw ratio limits, displacement rates, and increments

Figure 4.11a shows the overall draw ratio versus the true stress curve of the selected tensile tests of each displacement rate of 50, 30, 25, 20, and 10 mm/min. It is noticed in this figure that the data points of the curves end a little after the draw ratio (λ) value of 8 for all rates of displacement. The strain stopped in many tests at some point during the test, mainly because of the high extensibility of the HDPE geomembrane. This extensibility caused a failure to continue to capture the increase in the strain. Failure occurs when the narrow section of the specimen extends beyond a certain point, and the paint dot marker color fades away. The extensometer requires a sufficient contrast between the specimen's surface color and the marked color throughout the duration of the

test. When the extensometer fails to capture one or two dots, an operational error message appears, and the strain measurement stops in spite of the dots that are within the field of view (FOV) of the video extensometer. Thus, the maximum draw ratio for strain hardening modulus in this research is selected to be 8. On the other hand, a strain hardening modulus test can be performed to evaluate aged geomembrane. Aged HDPE geomembrane becomes brittle and breaks at a lower strain than a sample that is not aged. Thus, it is wise also to measure the strain hardening modulus in lower draw ratios so that the test can be standardized for use on both aged and unaged geomembranes.

Figure 4.11b illustrates the onset of strain hardening and the shape of the curves beyond the onset region. With the exception of the displacement rate of 20 mm/min, the lower displacement rates of 10 and 25 mm/min shows early strain hardening onset compared to that for higher displacement rates of 30 and 50. At the lower displacement rates (10 and 20 mm/min), curves are more linear after the onset of strain hardening, in contrast to the nonlinear plot for the high displacement rates (50, 30, and 25) up to 6.7 λ. The strain hardening modulus needs to be measured at the most linear part of the hardening region. The data from tensile tests at high curvature zones will be excluded. The minimum initial draw ratio ($\lambda_{\cdot}$) used for strain hardening modulus calculation is 6.5, which is well above the curvature zone for most displacement rates.

The strain hardening modulus will be measured with this method at draw ratio increments of 0.1, 0.25, 0.5 and 1 starting from the initial draw ratio ($\lambda_{\cdot}$) of 6.5 and ending at λ= 8. Strain hardening modulus is measured as the slope of the best fit line through data in selected zones of draw ratio limits. Figure 4.12 shows a segment of draw ratio-true strain data that is used to measure the strain hardening modulus at increment of

0.1 for test U1-50. There are 63 data points between a draw ratio of 6.5-6.6. The strain hardening modulus is 36.17 MPa. The data at this range of draw ratio are close to the fitted regression (R^2=0.999).

The next section will discuss values of strain hardening modulus and variation at selected draw ratio limits and increments. Figure 4.11c shows the strain hardening zone of interest in this study which lay between draw ratios of 6.5 and 8. It is clear that the curves are not perfectly linear at any displacement rates. There is a noticeable concave up at each displacement rate. In addition, while the curves show an increase in true stress with an increase in true strain, there are some locations on the curve that show less increase compared to adjacent zones. This behavior results in a decline in measured Gp at some zones as will be shown in the next section.

4.4.1.3.2 Gp measured at fine draw ratio increment (0.1)

Figure 4.13 shows Gp measured in three replicates which are tested at the displacement rates of 50 20, and 10 mm/min with an initial draw ratio (λ ▪) at a zone of interest from 6.5 to 8 draw ratios at a reading increment (Δλ) of 0.1. Tests performed at 50 mm/min show a slight reduction in Gp at λ ▪ =6.6 followed by a consistent linear increase in Gp for the three replicates up to a minimum initial draw ratio λ ▪ of 7.2 (Figure 4.13a). This trend however is followed by a slight increase in measured Gp up to the maximum λ of interest. A Gp of three replicates of 20 and 10 mm/min tests, shows more fluctuation in Gp values over the entire zone of interest. However, Gp at these low displacement rates (10 and 20 mm/min) show a linear positive trend throughout the strain region extending from 6.5 up to 8 (Figure 4.13 b and c).

Tables 4.4, 4.5, 4.6 cover the averages of the Gps and their variations for the λ limits of 6.5 to 8, which are measured at an increment of 0.1 for the displacement rates of 50, 20 and 10 mm/min respectively. It can be seen in Table 4.4 that at a 50 mm/min displacement rate there is a slight reduction in the average slope measured at 50 mm/min and at draw ratio limits of 6.6 to 6.7. This occurs mainly because of a substantial curvature of the draw ratio-true stress curve close to the onset of strain hardening. The concave part of the curve after the onset of strain hardening results in a higher strain hardening modulus followed by a lower value. This is followed by a gradual increase in average values of Gp. However, at low displacement rates (20 and 10 mm/min), the Gp average values show only an increase when there is an increased draw ratio. The variations of Gp have been measured and are presented in column four of each rate in Tables 4.4, 4.5, and 4.6. It is noticed that the coefficient of variation of Gp measured at a rate of 50 mm/min had a higher range of 2.2 to 19.4%. A similar range was noticed for the coefficient of variation of Gp at two other lower displacement rates (20 and 10 mm/min). It can be concluded that at low increments (0.1), Gp measurements shown unpredicted variation no matter what the displacement is.

4.4.1.3.3 Gp measured at course draw ratio increment (0.25, 0.5, and 1)

Figure 4.14 shows Gp for the test performed at 50, 20, and 10 mm/min at the zone of interest with 6.5 to 8 draw ratios at reading increments of 0.25 and 0.5. Figures 4.14 a, b, and c represent Gp measured at reading increment of 0.25 at displacement rates of 50, 20, and 10 mm/min respectively. While figures 4.14 d, e, and f represent Gp measured at reading increment of 0.5 at displacement rates of 50, 20, and 10 mm/min respectively. Similar to the Gp measured at an increment of 0.1, a Gp at reading segment 0.25 for 50

mm/min rate shows fluctuations to become more pronounced at a λ · of 7 (Figure 4.14a). Gp measured at an increment of 0.5 at 50 mm/min shows a bilinear response throughout the selected region of the draw ratio (Figure 4.14d). At a displacement rate of 20 mm/min, Gp measured at a reading increment of 0.25 exhibits a lower variation (Figure 4.14b). At the same displacement rate with a 0.5 increment of draw ratio, Gp shows a linear response for the λ limits of 6.4 to 8 for two replicates of the test U1-20 and U3-20 (Figure 4.14e). Finally, slopes measured at a 0.25 reading increment for 10 mm/min show a linear response for the three replicates with a minor reduction in Gp at the last measurement of test U3-10 (Figure 4.14c). However, Gp measured at a 0.5 draw ratio increment for tests performed at a 10 mm/min displacement rate show a linear trend for all three replicates (Figure 4.14f). It is therefore clear that the increase in Gp has become more consistent in tests performed at lower displacement rates rather than high rates.

Tables 4.7, 4.8, and 4.9 shows mean values of Gp and the coefficient of variation measured at three selected replicates (50, 20 and 10 mm/min) at draw ratio increment of 0.25, 0.5, and 1 respectively. There is a normal relation between measured Gp and draw ratio limits at all course increments and rates. The coefficient of variation of the Gp is measured at a rate of 50 mm/min tests at an increment of 0.25 are within a range of 0.7 to 14.6% (Table 4.7). There is a slight reduction in variation of the Gp measured at the same increment of 0.25 at lower rates (20 and 10 mm/min).

Measuring Gp at a 0.5 increment of draw ratio shows a coefficient of variation between 3.3 and 8.1% at a 50 mm/min displacement rate. However, the variation decreases to a coefficient of variation roughly between 2 and 5% for 20 and 10 mm/min

displacement rates (Table 4.8). The values of Gp and the variation are further studied at 1 increment of draw ratio. At this higher increment, there is a reduction in the measured mean of Gp as displacement rates decrease (Table 4.9). This is more in line with results found in the literature. In addition, the coefficient of variation of Gp in the tests performed at a 50 mm/min displacement rate was 6.8%, while Gp at lower displacement rates show high repeatability with a coefficient of variation of only 0.8 and 0.9 % for displacement rates of 20 and 10 mm/min respectively. The variation of Gp measured at these two low displacement rates were very low compared to the variation of all mechanical properties measured for same material in chapter 3.

4.4.1.3.4 Compare of Gp values at selected course increment (Δλ) with displacement rates

Figure 4.15-18 shows Gp values for the various displacement rates covering four preselected draw ratio ranges of 6.5-7, 7-7.5, 7.5-8, and 7-8 respectively. In these figures, the filled symbols represent Gp for each of the three replicates while the unfilled symbols represent the average Gp of the three replicates.

Several unique features of curves are observed for the λ segment of 6.5 to 7 (Figure 4.15). There is a reverse relationship between the slope and the displacement rate. This trend, however, is different from what is found in the literature where a direct relation between strain hardening and displacement rate measured at room temperature [2] and at a high temperature of 80 □ [23] is observed. The reason behind this is that at this increment of draw ratio, Gp is being measured near the onset location. Within this onset location, the plotted data produces a curved profile formation which results in this unexpected behavior.

In contrast to this observation, for the increment of draw ratio from 7 to 7.5 (Figure 4.16) the Gp indicates a direct linear relationship with the displacement rate. This trend is more in line with the literature cited [23].

For Gp measured at draw ratio increments of 7.5 to 8 (Figure 4.17) and 7 to 8 (Figure 4.18), two trends are noticeable. For the first section of the profile at displacement rates of 10 to 25 mm/min, the average strain hardening modulus values showed a linear direct positive increase with the displacement rates. This trend is reasonable and in line with literature findings. It is also observed from the average Gp values at displacement rate of 25 to 50 mm/min that the curve exhibits another constant linear value. That is, the strain hardening modulus value remains constant and independent of displacement rates for this region. This could be the role that the amorphous and crystalline phases play in tensile tests. The onset of strain hardening commences after the amorphous phase is fully stretched [2]. In this segment the molecular network could not be pulled out any more before the crystalline lamellae starts breaking up and gradually unfolds into mosaic blocks dominating the hardening process for the high displacement rates [28]. At a low displacement rate, the material has sufficient time for relaxation which results in a lower strain hardening modulus, while at higher displacement rates, the orientation of HDPE is favored over relaxation because of the increase in entanglement density leading to increased strain hardening modulus [23]. Figure 4.18 shows the variation in Gp with displacement rates at this 7-8 λ limits. Similarly, linear profiles are observed for the high displacement rates of 30 to 50 mm/min. It should be noticed that for this particular HDPE geomembrane, the transition

point at which the amorphous effect is overshadowed by the crystalline effect takes place around a displacement rate of 30 mm/min.

4.4.2 Scan Electron Microscopy Results

The fracture surface of the specimen tested at three selected displacement rates were examined using scan electron microscopy. Figure (4.19) shows SEM fractograph of HDPE specimens tested at rates of 50, 20, and 10 mm/min. At the highest displacement rate (50 mm/min), the break surface of the specimen shows some fibril microstructure. However, at a low displacement rate (10 mm/min), fracture morphology of the break test specimen shows a higher density of small fibril microstructures. This suggests a brittle like failure at a low displacement rate. Specimens that were tested at the rate of 20 mm/min show a fracture surface similar to that at the higher rate of (50 mm/min).

4.5 Conclusions and Recommendations

4.5.1 Conclusions

From this research, the followings can be concluded:

- The limitation of a video extensometer to capture the total curve of tensile tests, even though the marked dots are within the FOV of the extensometer, represents a significant drawback to obtaining additional valuable λ data which represents nearly half of the tested specimens.
- Minimum λ to measure representative strain hardening is specified to be 7 in order to avoid the curved profile zone at draw ratio-true stress curve after onset of strain hardening. While the maximum λ is specified as 8, at which the first significant number of tests successfully reached this value of λ. Second, it

provides enough of a span to evaluate and compare aged geomembrane that has small strain hardening region.

- The variation in Gp is noticeably low for the three replicates measured at low displacement rates (10 and 20 mm/min) vs those tested at higher displacement rates. Also, Gps measured at coarse increments (0.5 and 1.0) show lower variation compared to those for fine increments (0.1 and 0.25) regardless of the displacement rate.
- Gp measured at draw ratio of 7.5-8 and 7-8 shows linear increase with the increase in displacement rate up to 30 mm/min and a horizontal line with no effect of displacement rate above 30 mm/min.

4.5.2 Recommendations

- The evaluation of the strain hardening modulus should be further investigated for other geomembrane resins at the same set of displacement rates to further evaluate the role of the HDPE amorphous and the crystalline phases.
- The measured strain hardening modulus data can be correlated with Stress Crack Resistance data made available for the same HDPE resin. This correlation shall prove useful and less time consuming to determine SCR compared with ASTM 5397.
- The conventional applied dot technique needs to be modified and a new method is required to obtain continuous test results and hence avoid specimen retesting, which was encountered throughout the present experimentations. The proposed method should show a continuous, clear contrast between the sample and gage marker.

Table 4.1 Text matrix of tensile test experiment at selected displacement rates

Specimen Designation	Displacement rate (mm/min)	Sampling Frequency (sec)	Number of data points per 1 mm of displacement
U1-50	50	0.10	13/mm
U2-50			
U3-50			
U1-30	30	0.16	13/mm
U2-30			
U3-30			
U1-25	25	0.20	13/mm
U2-25			
U3-25			
U1-20	20	0.25	13/mm
U2-20			
U3-20			
U1-10	10	0.50	13/mm
U2-10			
U3-10			

Table 4.2 Strain hardening modulus measurement between two points

Rate	Test	λ_{min}	σ_{min} (MPa)	λ_{max}	σ_{max} (MPa)	Gp two points (MPa)	Gp regression (MPa)	*R^2
50	U1-50	6.12	92.96	9.08	324.77	78.31	72.4	0.982
	U2-50	6.00	92.53	9.04	343.09	82.42	75.93	0.981
	U3-50	6.00	91.1	7.98	231.4	70.86	63.84	0.986
30	U1-30	6.11	97.25	8.38	268.27	75.34	68.57	0.986
	U2-30	6.06	95.01	9.18	347.2	80.83	76.81	0.98
	U3-30	5.92	88.83	9.17	344.33	78.62	74.16	0.982
25	U1-25	6.08	97.53	8.02	228.52	67.52	63.03	0.992
	U2-25	6.00	93.79	9.02	326.61	77.09	74.31	0.983
	U3-25	5.90	90.59	8.85	317.17	76.81	72.92	0.982
20	U1-20	6.11	95	9.72	397.16	83.70	81.16	0.981
	U2-20	6.04	92.24	9.14	334.19	78.05	73.77	0.981
	U3-20	6.11	94.01	9.43	360.9	80.39	76.54	0.984
10	U1-10	6.02	91.47	8.95	298.7	70.73	67.75	0.987
	U2-10	5.97	89.5	7.9	206.7	60.73	57.5	0.995
	U3-10	6.01	93.73	7.82	206.69	62.41	59.16	0.996

*R^2 is for Gp regression method

Table 4.3 Mean and variation of strain hardening modulus between two points

Rate	Two points Gp			Regression Gp		
	Mean (Mpa)	SD	COV %	Mean (Mpa)	SD	COV %
50	77.20	5.86	7.6	70.72	6.22	8.8
30	78.26	2.76	3.5	73.18	4.21	5.7
25	73.81	5.45	7.4	70.09	6.15	8.8
20	80.71	2.84	3.5	77.16	3.73	4.8
10	64.62	5.36	8.3	61.47	5.50	9.0

Table 4.4 Gp and variation for 50 mm/min at $\Delta\lambda$ 0.1

Limits of λ	Mean Gp (MPa)	SD	COV (%)
6.5-6.6	40.6	4.3	10.7
6.6-6.7	38.7	6.0	15.4
6.7-6.8	43.4	2.3	5.3
6.8-6.9	45.9	1.0	2.2
6.9-7	49.6	3.6	7.2
7-7.1	57.6	2.4	4.2
7.1-7.2	62.0	5.3	8.5
7.2-7.3	72.8	3.9	5.3
7.3-7.4	75.9	14.7	19.4
7.4-7.5	76.0	7.1	9.3
7.5-7.6	76.8	4.0	5.2
7.6-7.7	78.7	8.1	10.2
7.7-7.8	84.6	6.3	7.4
7.8-7.9	88.8	6.8	7.7
7.9-8	86.6	5.9	6.9

Table 4.5 Gp and variation for 20 mm/min at Δλ 0.1

Limits of λ	Mean Gp (MPa)	SD	COV (%)
6.5-6.6	46.0	7.8	16.9
6.6-6.7	47.1	4.7	10.0
6.7-6.8	53.8	6.5	12.1
6.8-6.9	54.6	2.7	5.0
6.9-7	55.4	6.3	11.4
7-7.1	55.8	7.7	13.9
7.1-7.2	59.0	6.0	10.1
7.2-7.3	73.6	9.2	12.5
7.3-7.4	69.7	4.2	6.0
7.4-7.5	69.9	4.5	6.4
7.5-7.6	69.1	1.9	2.8
7.6-7.7	78.7	3.3	4.2
7.7-7.8	78.3	16.8	21.5
7.8-7.9	84.6	3.8	4.5
7.9-8	77.1	4.3	5.5

Table 4.6 Gp and variation for 10 mm/min at Δλ 0.1

Limits of λ	Mean Gp (MPa)	SD	COV (%)
6.5-6.6	47.8	2.5	5.2
6.6-6.7	49.6	2.1	4.1
6.7-6.8	53.4	6.0	11.2
6.8-6.9	57.1	3.4	6.0
6.9-7	54.7	6.7	12.2
7-7.1	64.8	5.8	9.0
7.1-7.2	61.0	6.2	10.1
7.2-7.3	66.9	3.4	5.1
7.3-7.4	65.3	3.4	5.2
7.4-7.5	64.4	3.6	5.6
7.5-7.6	66.4	11.1	16.7
7.6-7.7	72.8	8.2	11.2
7.7-7.8	79.9	6.5	8.1

Table 4.7 Gp and variation for 50,20, and 10 mm/min at Δλ 0.25

Rate (mm/min)	Limits of λ	Mean Gp (MPa)	SD	COV (%)
50	6.5-6.75	40.1	5.4	13.4
	6.75-7	47.1	1.1	2.3
	7-4.25	62.7	2.5	4.0
	7.25-7.5	76.9	11.2	14.6
	7.5-7.75	77.9	6.7	8.6
	7.75-8	86.7	0.6	0.7
20	6.5-6.75	47.0	1.9	4.0
	6.75-7	54.8	2.7	4.9
	7-4.25	59.6	2.8	4.8
	7.25-7.5	69.6	4.4	6.3
	7.5-7.75	77.2	1.6	2.0
	7.75-8	80.9	3.1	3.9
10	6.5-6.75	49.8	2.1	4.1
	6.75-7	55.7	2.1	3.8
	7-4.25	61.4	3.0	4.8
	7.25-7.5	65.8	2.6	3.9
	7.5-7.75	72.5	3.6	5.0
	7.75-8	73.8	6.9	9.4

Table 4.8 Gp and variation for 50,20, and 10 mm/min at Δλ 0.5

Rate (mm/min)	Limits of λ	Mean Gp (MPa)	SD	COV (%)
50	6.5-7	43.5	2.5	5.8
	7-7.5	71.2	5.8	8.1
	7.5-8	83.1	2.7	3.3
20	6.5-7	51.3	1.6	3.2
	7-7.5	66.6	3.2	4.8
	7.5-8	78.7	3.2	4.1
10	6.5-7	52.9	1.9	3.5
	7-7.5	64.0	1.3	2.1
	7.5-8	75.5	2.2	2.9

Table 4.9 Gp and variation for 50,20, and 10 mm/min at Δλ 1

Rate (mm/min)	Limits of λ	Mean Gp (MPa)	SD	COV (%)
50	7-8.	77.3	5.3	6.8
20	7.-8.	72.3	0.6	0.8
10	7-8.	67.8	0.6	0.9

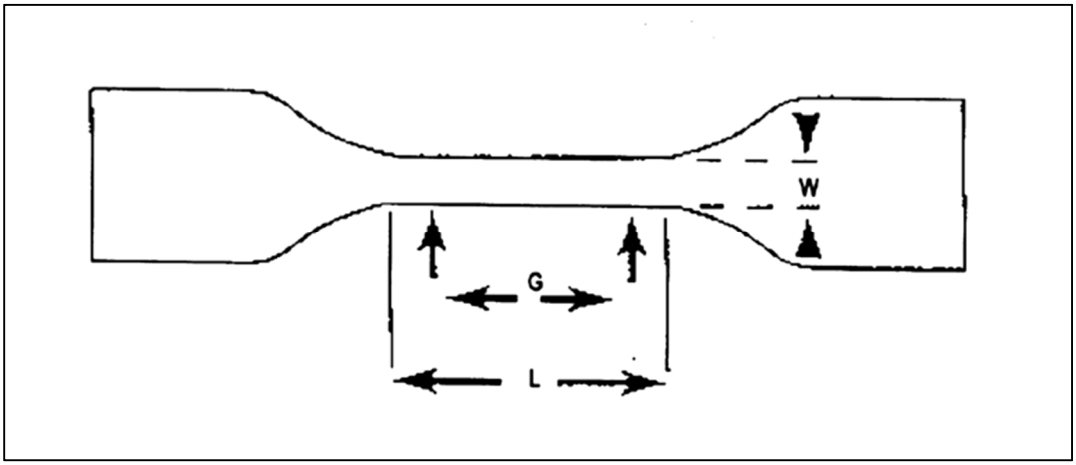

Figure 4.1 Dogbone specimen that used in the experiment L=33mm, w=6 mm, and G=25 mm (modified from ASTM D6693)

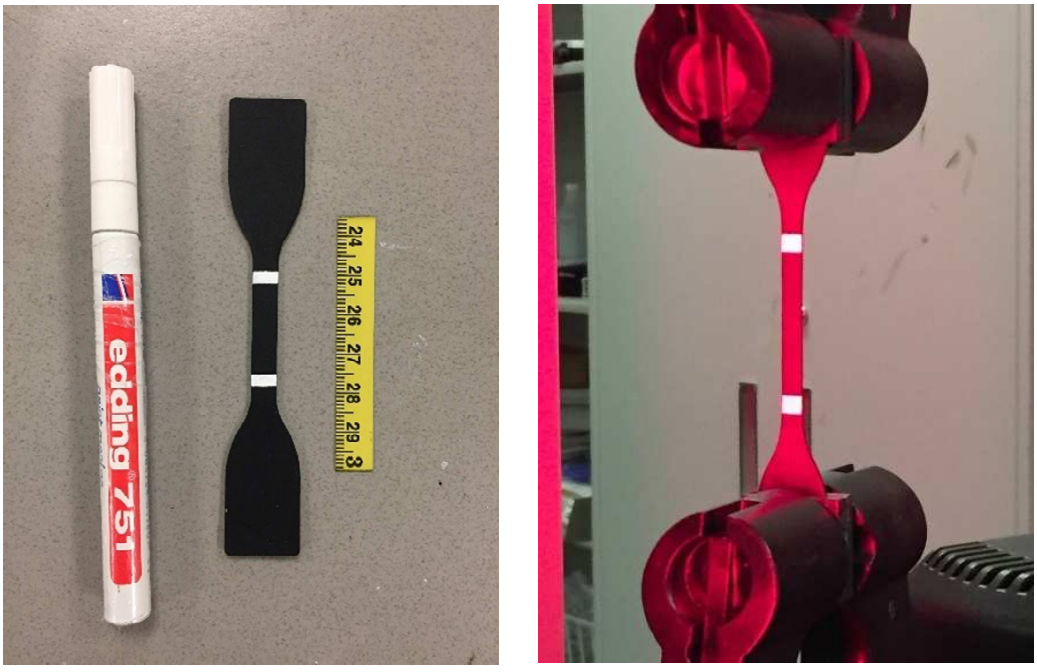

Figure 4.2 Locating gage marks on tensile specimen

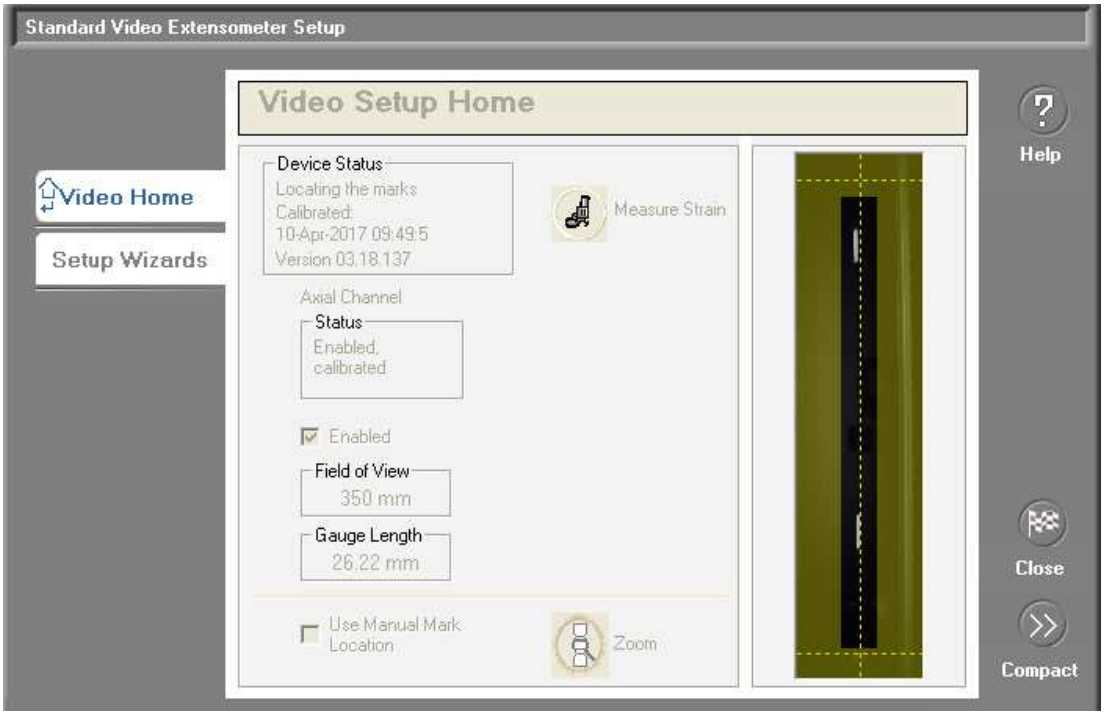

Figure 4.3 Photoshoot of extensometer video setup of Bluhill2 software shows locating of marks and measuring gage length

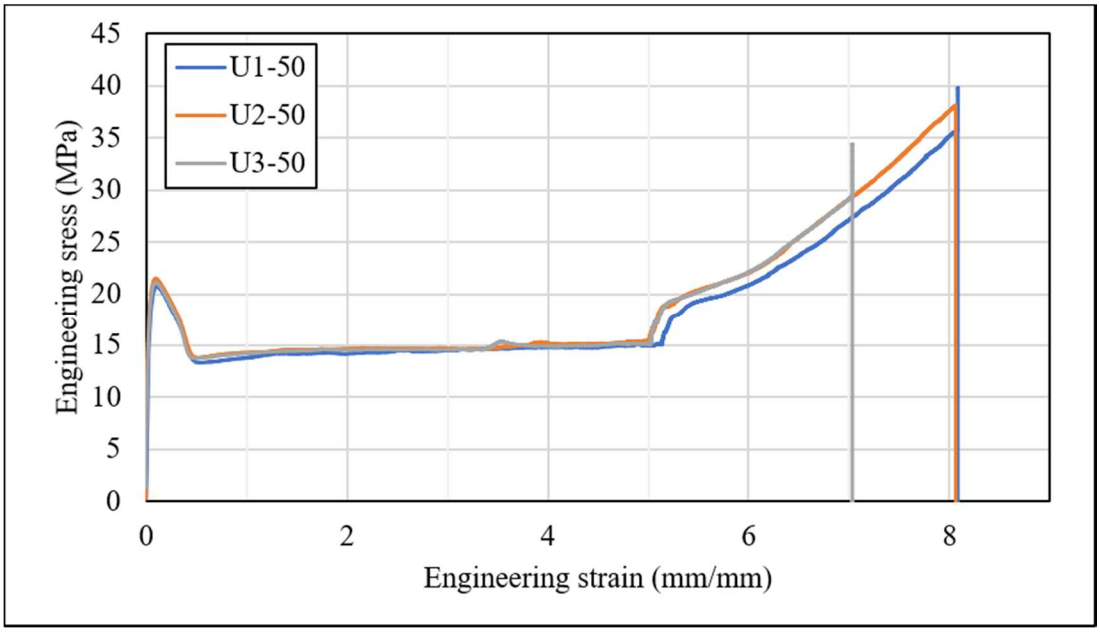

Figure 4.4 Engineering stress-engineering strain curves for three replicates at 50 mm/min

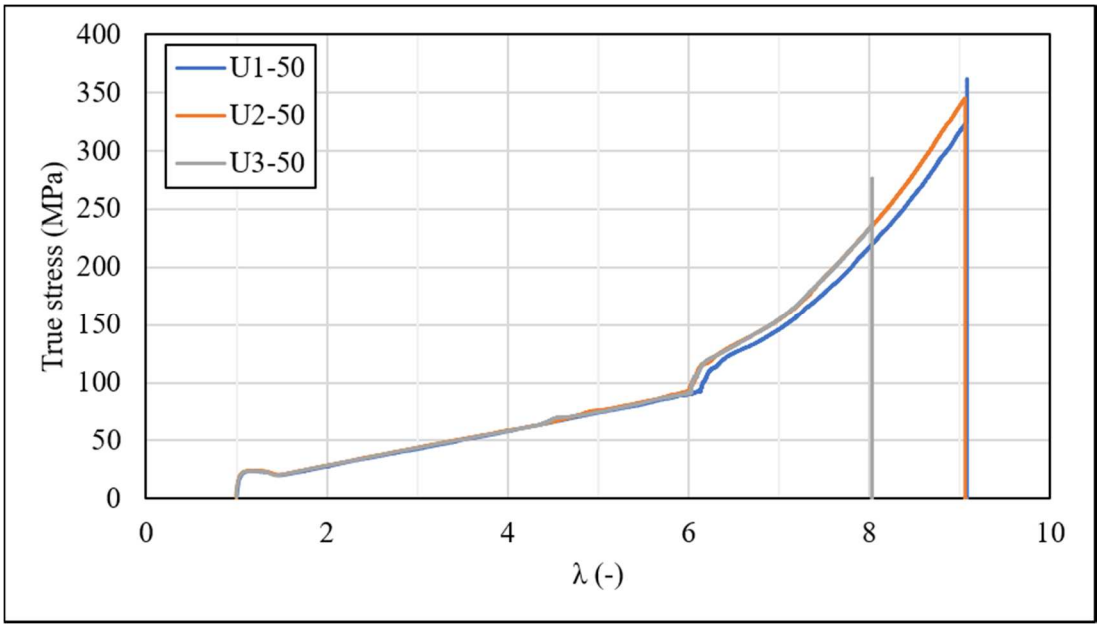

Figure 4.5 Draw ratio (λ) vs true stress for three replicates at 50 mm/min

Figure 4.6 Tescan Vega-3 scan electron microscopy for imaging break surface of specimens

Figure 4.7 Portions of break specimens in Split Mount Holder

Figure 4.8 Denton Vacuum Desk II for coating samples with gold

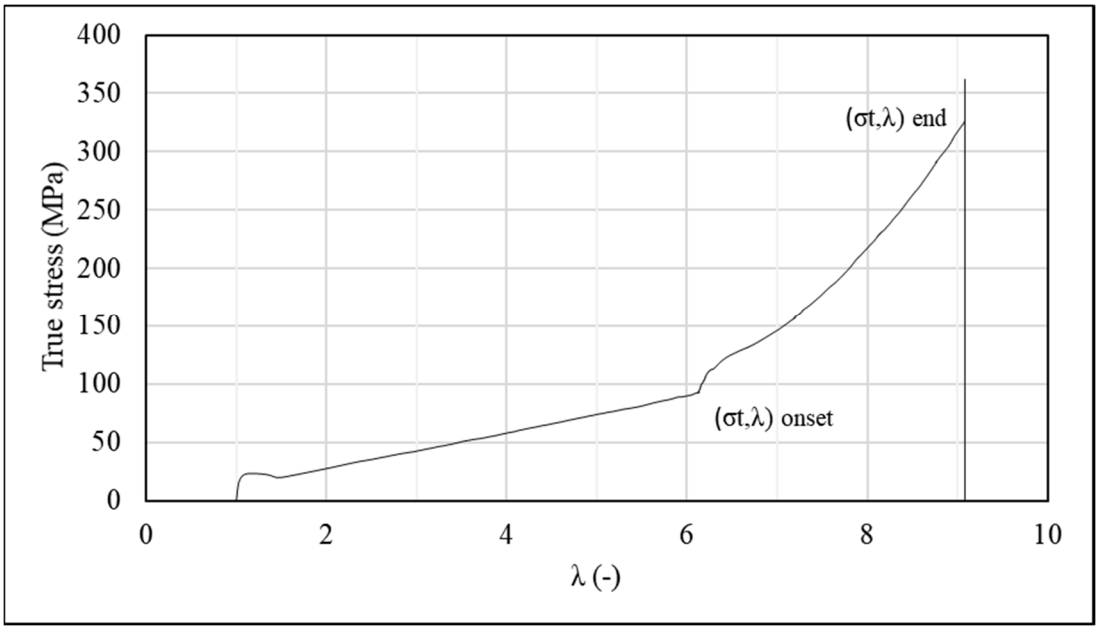

Figure 4.9 Draw ratio versus true stress of test U1-50 shows onset of strain hardening

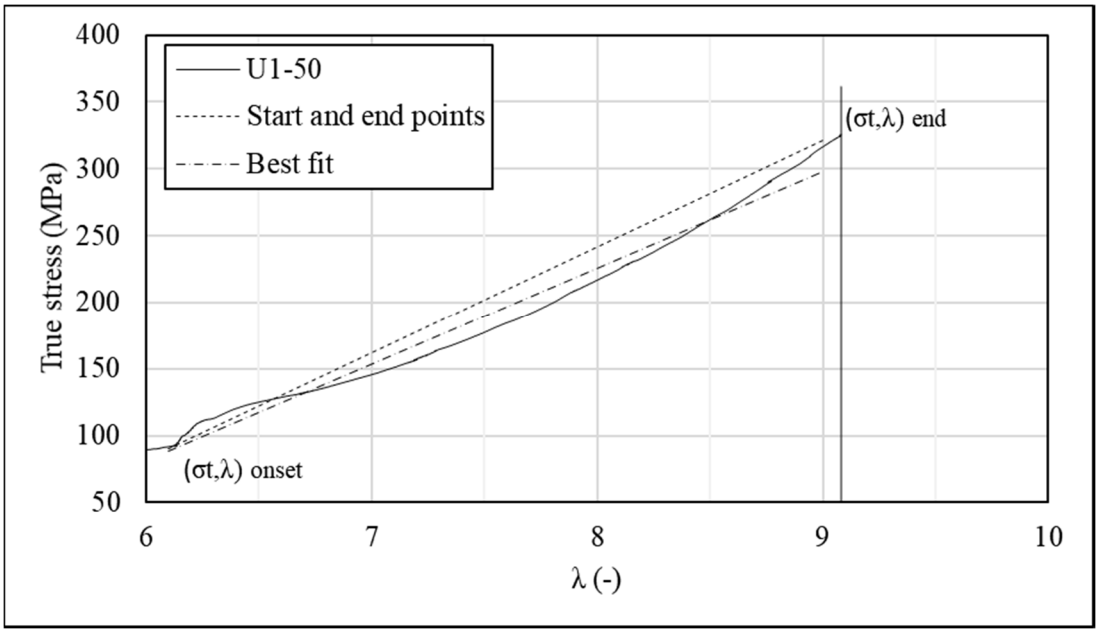

Figure 4.10 Strain hardening region of test U1-50 shows strain hardening region and measuring strain hardening modulus between two points (start and end point method and best fit method)

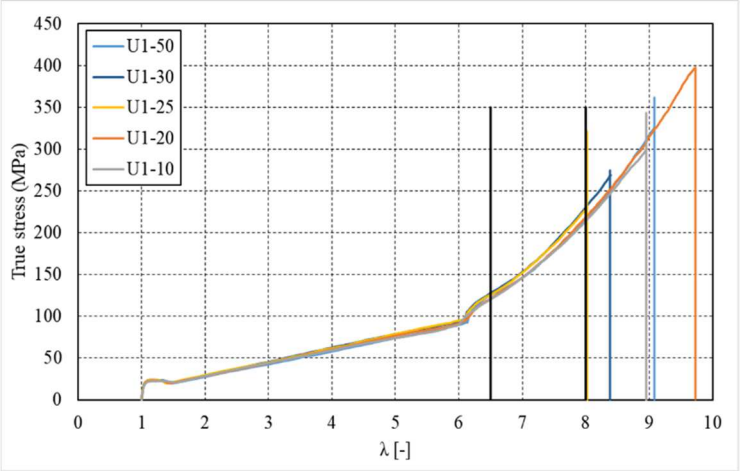

(a)

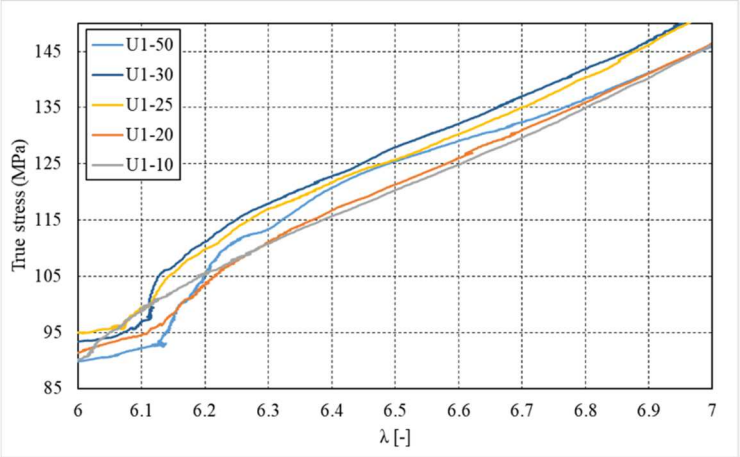

(b)

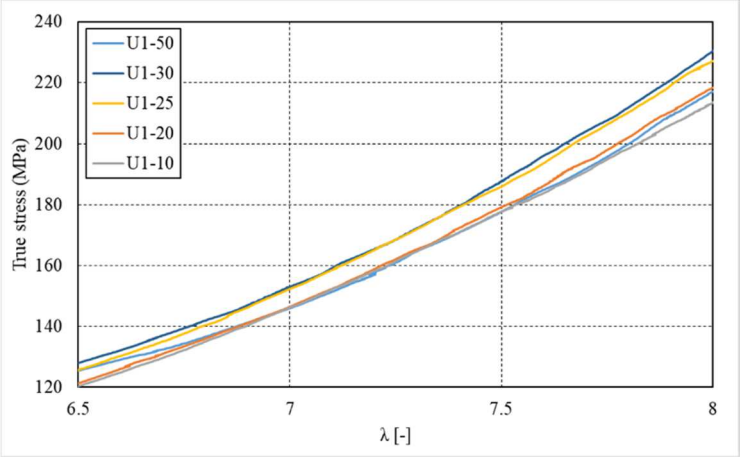

(c)

Figure 4.11 True stress-draw ratio curves of unaged specimens tested at displacement rate 50, 30, 25, 20, and 10 mm/min (a) total curve; (b) onset and start of hardening portion of curve (b) portion of true stress-draw ratio where slopes (Gp) are being measured.

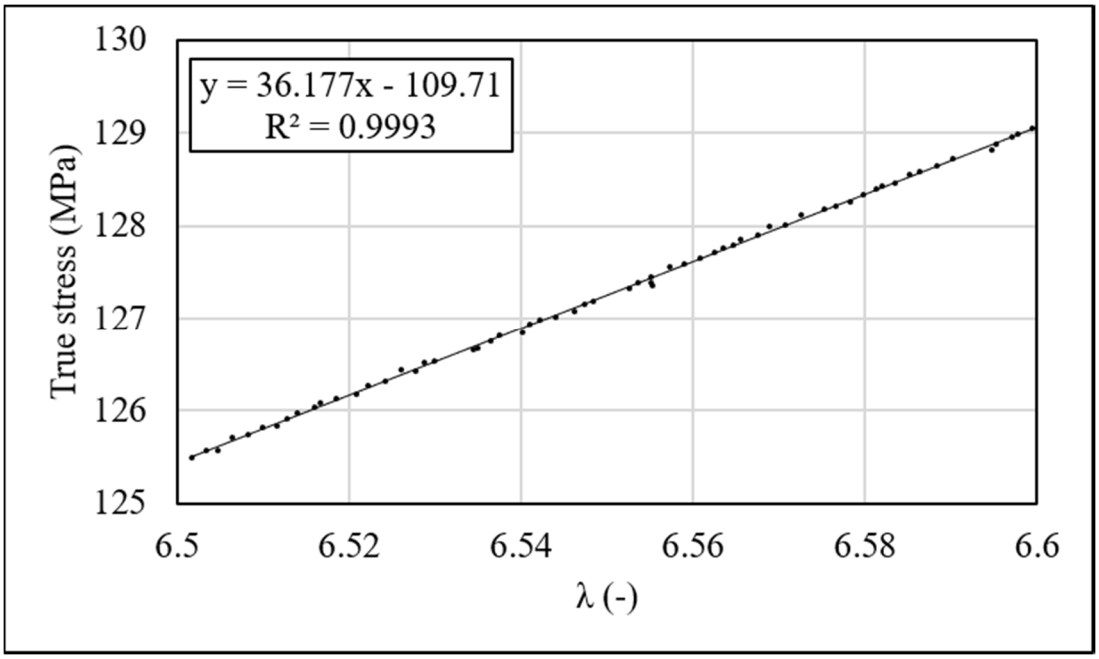

Figure 4.12 Slope of curve at λ of 6.5-6.6 for test U1-50 (number of data point is 63 points)

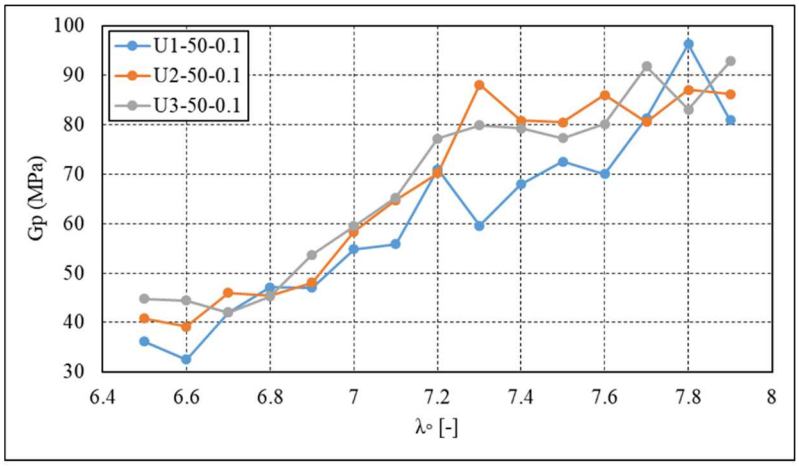

(a)

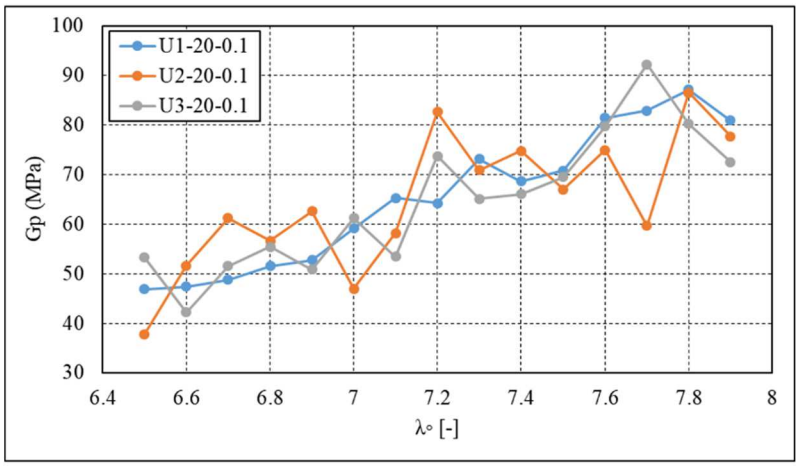

(b)

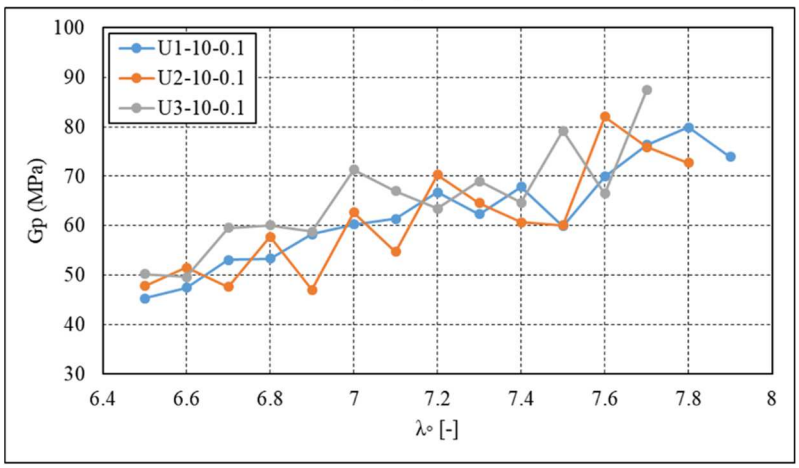

(c)

Figure 4.13 Strain hardening modulus (Gp) against initial draw ratio (λ ▪) of three replicates tested at 0.1 increment at a) 50, b) 20, and c) 10 mm/min

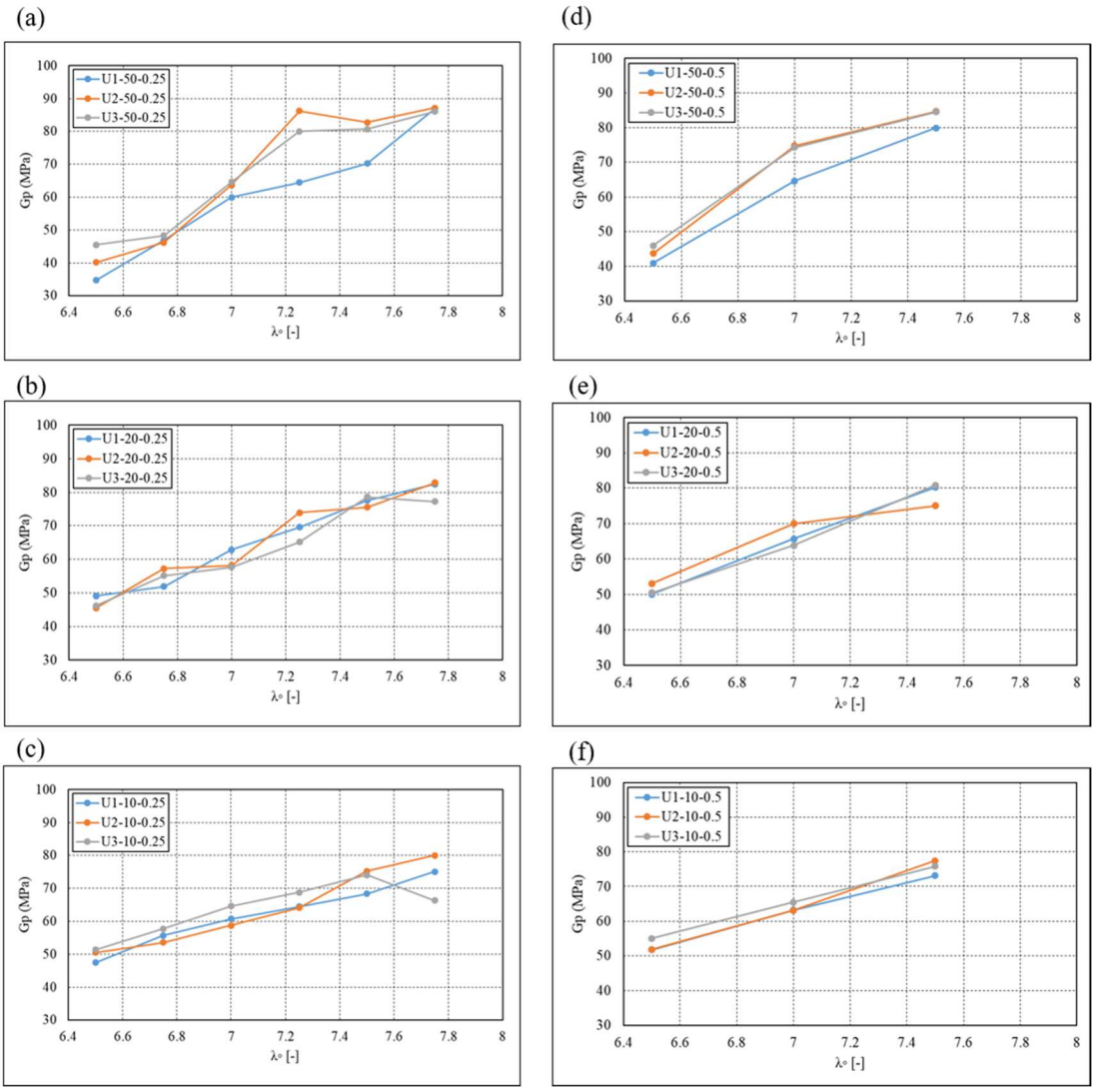

Figure 4.14 Gp vs initial draw ratio increment (λ ▪) of three replicates tested at 50, 20, and 10 mm/min a, b, c at 0.25 and d, e, f at 0.5 increments.

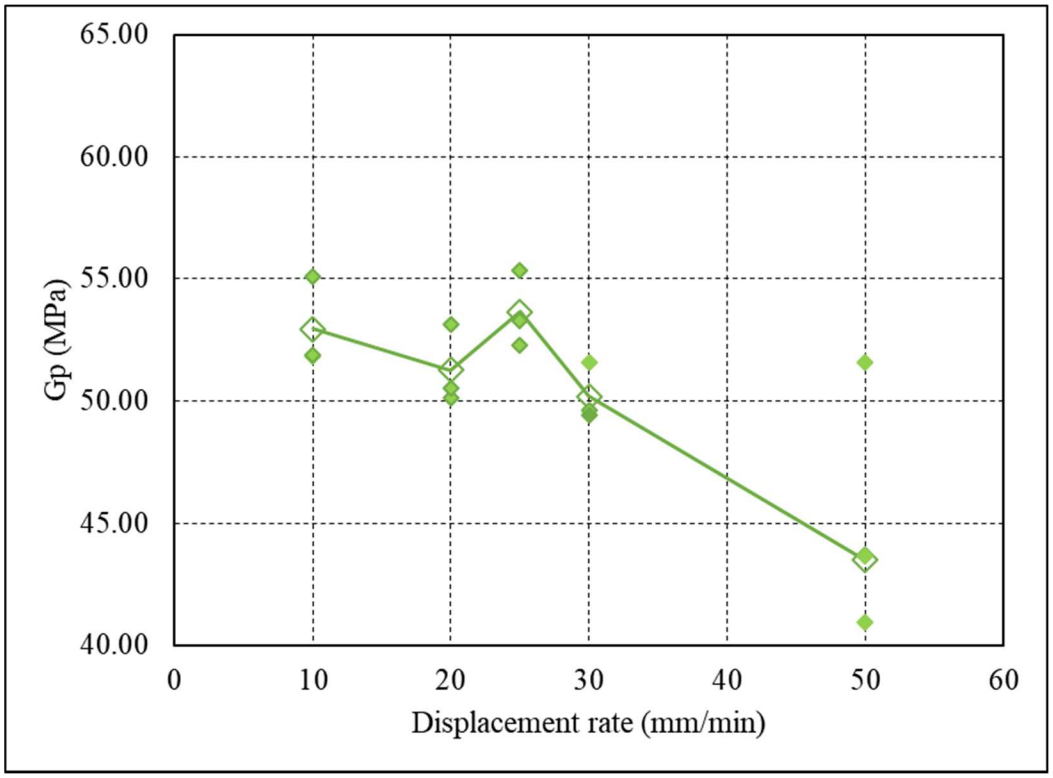

Figure 4.15 Gp versus displacement rates calculated at draw ratio of 6.5-7

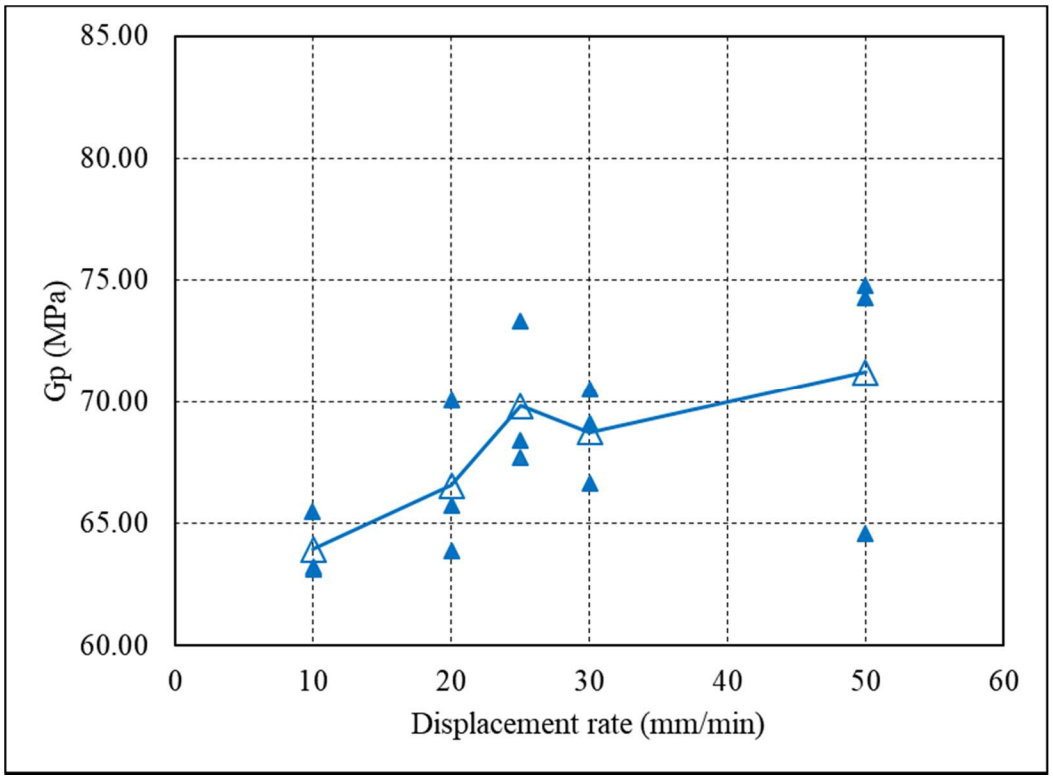

Figure 4.16 Gp versus displacement rates calculated at draw ratio of 7-7.5

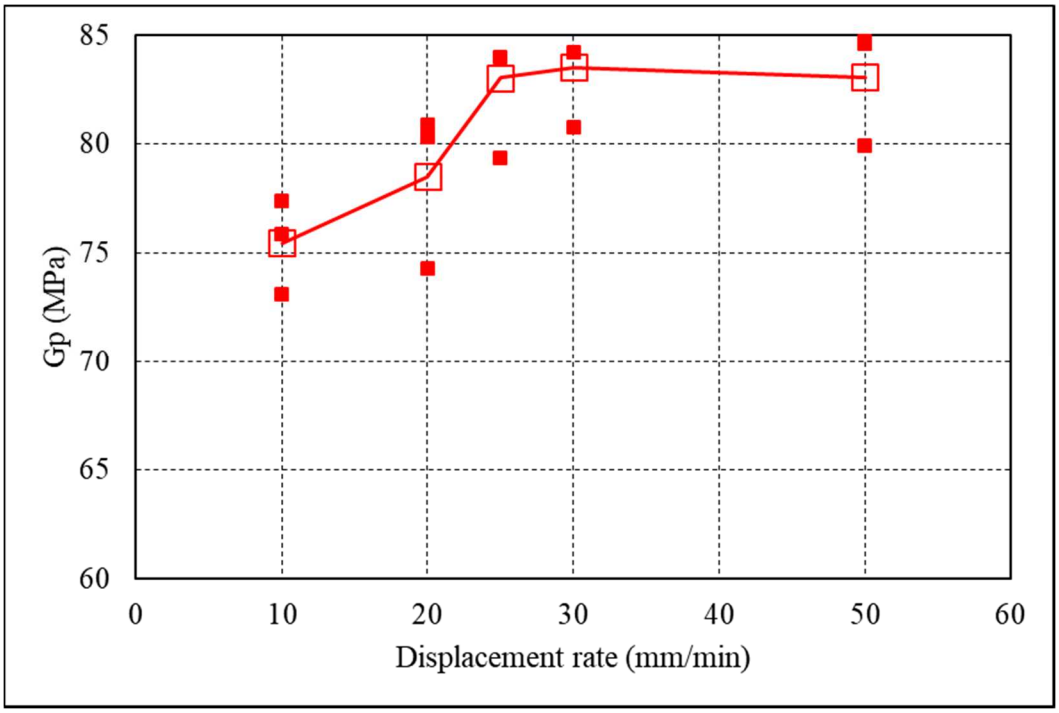

Figure 4.17 Gp versus displacement rates calculated at draw ratio of 7.5-8

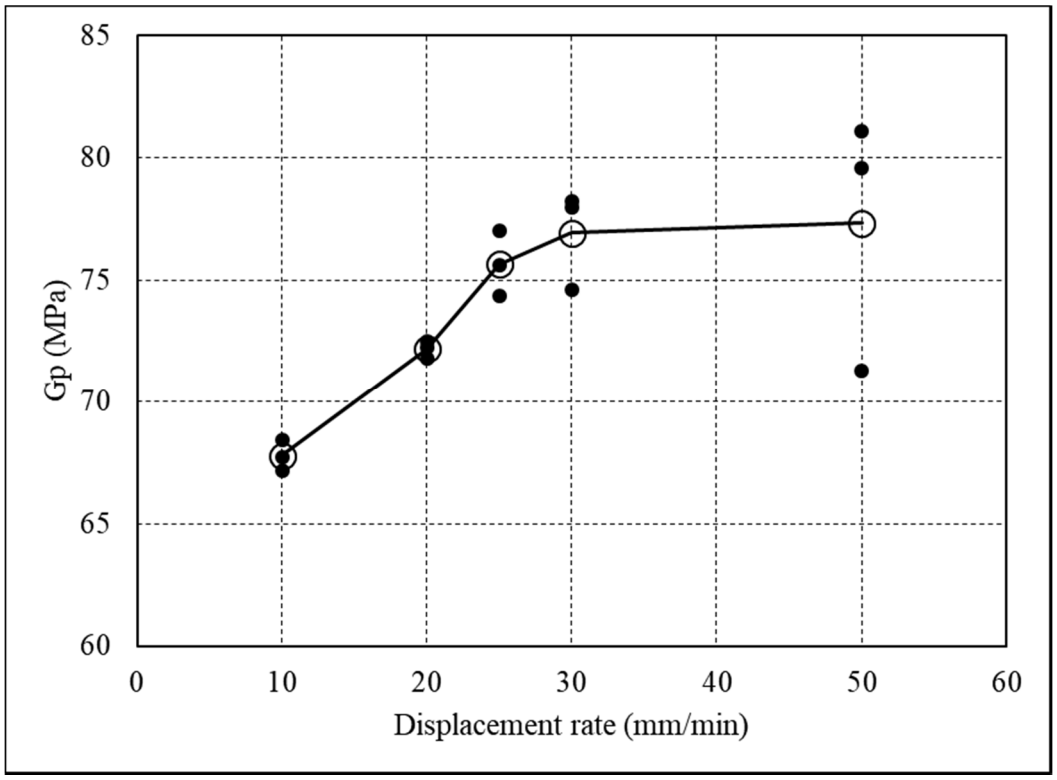

Figure 4.18 Gp versus displacement rates calculated at draw ratio of 7-8

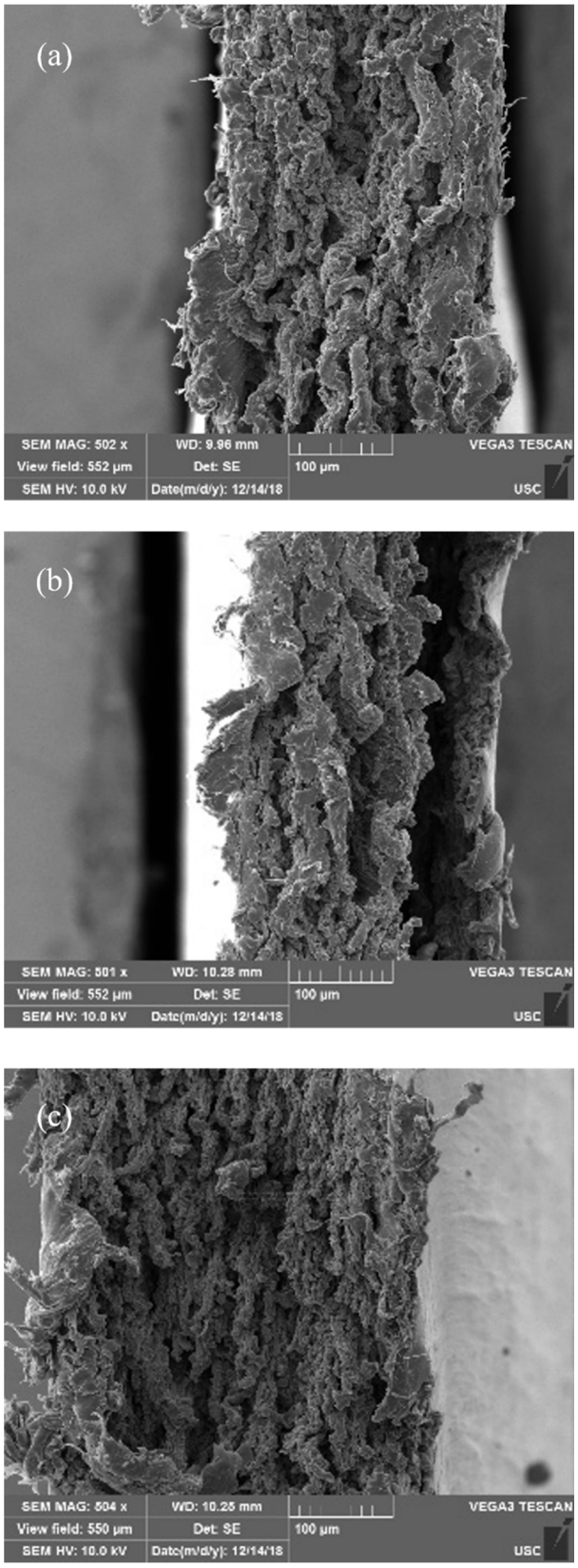

Figure 4.19 SEM image of fracture surface of specimens tested at displacement rate of a) 50 mm/min, b) 20 mm/min, and c) 10 mm/min

REFERENCES

[1] Kurelec, L., Teeuwen, M., Schoffeleers, H., & Deblieck, R. (2005). Strain hardening modulus as a measure of environmental stress crack resistance of high density polyethylene. *Polymer*, *46*(17), 6369-6379.

[2] Cheng, J. J., Polak, M. A., & Penlidis, A. (2008). A tensile strain hardening test indicator of environmental stress cracking resistance. *Journal of Macromolecular Science®, Part A: Pure and Applied Chemistry*, *45*(8), 599-611.

[3] Cheng, J. J., Alvarado-Contreras, J. A., Polak, M. A., & Penlidis, A. (2010). Chain entanglements and mechanical behavior of high density polyethylene. *Journal of Engineering Materials and Technology*, *132*(1), 011016.

[4] Havermans, L., Kloth, R., & Deblieck, R. (2012). Strain hardening modulus: an Accurate measure for slow crack growth behavior of HDPE pipe materials. *Proceedings Plastic Pipes XVI, Barcelona, Spain*.

[5] van der Stok, E., & Scholten, F. (2012). Strain hardening tests on PE pipe materials. *Plastic Pipes XVI, Barcelona*.

[6] Pomperton et al, 2014 DEVELOPMENT OF A SLOW CRACK GROWTH RESISTANCE (STRAIN HARDENING) TEST FOR ASSESSMENT OF AGEING PE PIPELINE MATERIALS

[7] Wu, T., Yu, L., Cao, Y., Yang, F., & Xiang, M. (2013). Effect of molecular weight distribution on rheological, crystallization and mechanical properties of polyethylene-100 pipe resins. *Journal of Polymer Research,20*(10). doi:10.1007/s10965-013-0271-9

[8] McCarthy, M., Deblieck, R., Mindermann, P., Kloth, R., Kurelec, L., & Martens, H. (2008). New accelerated method to determine slow crack growth behaviour of polyethylene pipe materials. *Plastics Pipes XIV, Budapest*, *31*(35), 121.

[9] Chen, Y., Lei, Y., Zou, H., Liang, M., & Cao, Y. (2014). Structural and rheological property relationship of bimodal polyethylene with improved environment stress cracking resistance. *Polymer Science Series A*, *56*(5), 671-680.

[10] Adib, A., Domínguez, C., Rodríguez, J., Martín, C., & García, R. A. (2015). The effect of microstructure on the slow crack growth resistance in polyethylene resins. *Polymer Engineering & Science*, *55*(5), 1018-1023.

[11] Robledo, N., Domínguez, C., & García-Muñoz, R. A. (2017). Alternative accelerated and short-term methods for evaluating slow crack growth in polyethylene resins with high crack resistance. *Polymer Testing*, *62*, 366-372.

[12] Nezbedová, E., Pinter, G., Frank, A., Hutař, P., Poduška, J., & Hodan, J. (2017, June). Accelerated Tests for Lifetime Prediction of PE□HD Pipe Grades. In *Macromolecular Symposia* (Vol. 373, No. 1, p. 1600096).

[13] Gerets, B., Wenzel, M., Engelsing, K., & Bastian, M. (2017). Slow Crack Growth of Polyethylene—Accelerated and Alternative Test Methods. In *Deformation and Fracture Behaviour of Polymer Materials* (pp. 177-187). Springer, Cham.

[14] Havermans-van Beek, D. J. M., Delieck, R., McCarthy, M., Kloth, R., & Kurelec, L. (2010). An elegant and fast method to predict the slow crack growth behaviour of high density polyethylene pipe materials. In *Plastic Pipes XV Conference*.

[15] Frick, A., Sich, D., Heinrich, G., Stern, C., Gössi, M., & Tervoort, T. A. (2013). Relationship between Structure and Mechanical Properties of Melt Processable PTFE: Influence of Molecular Weight and Comonomer Content. *Macromolecular Materials and Engineering,298*(9), 954-966. doi:10.1002/mame.201200172

[16] Sardashti, A. (2014). Methodologies for Obtaining Reliable Indicators for the Environmental Stress Cracking Resistance of Polyethylene.

[17] Zanzinger, H., Engelsing, K., & Hausmann, S. (2014). Durability of polyethylene geopipes for landfill applications after several years in service. In *Proceedings of the 10th International Conference on Geosynthetics, Berlin, Germany, 21-25 September 2014*.

[18] Engelsing, K. and Zanzinger, H. (2012). A new accelerated test method for stress crack resistance of HDPE geomembranes. Segundo Congreso Panamericano de Géosintéticos, GEOAMERICAS 2012, 01-04 de Mayo, 2012, Lima, Peru, 8p.

[19] Peggs, I. D. Liner Performance: Interesting Observations and Test Results. In *Geotechnical Frontiers 2017* (pp. 148-159).

[20] Zanzinger, Helmut & Peggs, Ian. (2013). Stress cracking resistance of HDPE Geomembranes with very high densities.

[21] SHT test_ISO 18488: Polyethylene (PE)materials for piping systems _ Determination of Strain hardening Modulus in relation to slowcrack growth_Test method.

[22] Zanzinger, H., Wenzel, M., and Engelsing, K. (2015) Determination of the Stress Cracking Resistance of HDPE Geomembranes by using Accelerates Test Methods

[23] Zanzinger 2012 Good-better-best HDPE Geomembrane in Engineering Geoinvironemtnal (HS design)

[24] ASTM D638- 14 Standard Test Method for Tensile Properties of Plastics

[25] ASTM D6693/D6693M-04(2015) Standard Test Method for Determining Tensile Properties of Nonreinforced Polyethylene and Nonreinforced Flexible Polypropylene Geomembranes

[26] Havermans-van Beek, D. J. M., Delieck, R., McCarthy, M., Kloth, R., & Kurelec, L. (2010). An elegant and fast method to predict the slow crack growth behaviour of high density polyethylene pipe materials. In *Plastic Pipes XV Conference*.

[27] Engelsing, K. and Zanzinger, H. (2012). A new accelerated test method for stress crack resistance of HDPE geomembranes. Segundo Congreso Panamericano de Géosintéticos, GEOAMERICAS 2012, 01-04 de Mayo, 2012, Lima, Peru, 8p.

[28] Contreras, J.A.A. Micromechanical Modelling of Polyethylene; Department of Civil Engineering, University of Waterloo, 2007.

CHAPTER 5

A SYSTEM METHOD FOR MEASURING STRAIN USING A NEW MARK TYPE

5.1 Introduction

Strain at tensile test measured using different techniques including video extensometer. Video extensometer needs to track the location of dot on a specimen to measure strain. The dot can be a stick dot or paint marker dot. These conventional dot types have many limitations. The purpose of this research was to compare the stress-strain curve of the two methods and get approved a new method. The limitations of conventional test methods were presented, and the new dot design has been reviewed with an explanation of how it overcomes the disadvantage of conventional methods. Moreover, the new design of dot allows testing various materials from hard to soft using any optical extensometer such as video extensometer and digital image correlation (DIC). The results show the ability to use the modified dot. Further improvement of the new dot type and manufacturing process has been discussed.

5.2 Background

The tensile test has been used to characterize the mechanical properties of a variety of materials types. Many standards required to measure strain for different materials types such as metal [1] and plastic [2,3,4]. Measuring strain involved in many

material types and forms such as metal [5], polymer (6, 7, 8, 9, 10, 7], rubber [11], biological tissues [12, 13, 14, 15, 16, 17], foam material [18], and textile materials [19].

Strain can be measured using a different type of extensometers. Extensometers divided into two categories: contact and noncontact extensometers. Contact extensometers mounted directly onto a tensile specimen via knife edges. Examples of contact extensometer are clip-on extensometer for a few millimeters displacement and long travel extensometer for high elongation measurement. Contact extensometers sharp knife can cause notching to specimen surface ,which affects its mechanical properties ,especially for low stiffness materials such as polymers and biomedical materials. Noncontact extensometer is the other type extensometer at which optical device measures strain between specific targets on the specimen without direct contact. Noncontact extensometer allows measuring the strain of highly extensible materials up to break point accurately [20].

A video extensometer is an example of a noncontact type. They required attaching measurement marks to the specimen such as stick dot or paint marker dot that are in contrast to specimen color. The location of these marks is evaluated by a software algorithm ,and during the test, mark movement is converted to extension values [20]. Several researchers who used this technique with the aid of an optical device have reported many problems with its results. This is mainly due to paint markers or stick dots shape deformation [21]. The paint marker with specific dimensions is located on a tensile specimen for easy detection by the video extensometer. Highly ductile materials such as high-density polyethylene HDPE exhibit very high strain that results in appreciable change of dot mark size and color fading. This low color contrast highly impacts

extensometer reading accuracy. Another source of error is the sample elongation becoming very narrow in a direction perpendicular to the extension. This leads to a loss of a significant part of the stress strain curve with strain measurement undetected prior to reaching break point. For this reason, for highly extensible materials, the adhesive (stick) marker method is preferred to maintain a sufficient color contrast with a fixed dimension (22).

Several workers have studied the effect of types of paint markers and physically attached markers on the mechanical response of biomedical materials and biological tissues (20,23,17,24). It is found that markers can modify mechanical response and inducing local stiffening of a specimen. Cyanoacrylate, for example, as a marker adhesive affects local and overall mechanical response of elastomer 300 SIL 50-BL and synthetic mesh. Caution is recommended with the use of cyanoacrylate for attaching markers on biomedical materials [24]

The physical properties of a sample can limit the use of paint and stick dot markers. Sample surface texture -such as a nonuniform surface of synthetic meshes- affects the dot type selection and accuracy of measured strain [25]. Current markers types are not suitable for the rough surface of high-density polyethylene textured geomembrane. The sample's dimensions and shape dictate the selection of dot type. For example, thin wire specimens do not provide enough visible area for video extensometers measurements [20].

In addition to the physical properties, testing conditions such as high temperatures can adversely impact test results. It is reported that some tensile tests that are performed at high temperature resulted in breakage of stick dot gage marker which led to

discontinuity of tensile test curve and hardening modulus [26]. In addition, stick dot may results in strain error measurement because it does not necessarily represent a specific point on a specimen. It rather slides randomly during tensile test ,especially with high extensible materials.

From above, there is a need in the strain measurement field for a new dot type that overcomes the above-mentioned limitations of conventional stick dots and paint marker dots. In this research, a novel design of a dot marker will be introduced. This dot marker can be used for any material types with any sample dimensions and thickness. It can withstand and resist high temperatures and last up to the end of the tensile test giving continuous strain measurement. This proposed design will be tested by performing a tensile test for HDPE geomembrane. In order to validate the new dot type design, its results will be compared with those from stick dot and paint marker dots. Replicates will also be performed to test its accuracy and repeatability.

5.3 Materials and Methods

5.3.1 Material

A commercial High-density polyethylene geomembrane was selected for this investigation. The material is a smooth 1 mm thickness with an anonymous source. It is stored in the dark in good condition at the University of South Carolina at room temperature. The initial mechanical and physical properties are unknown.

5.3.2 Sample preparation

Dogbone samples type IV were cut according to ASTM D638 for tensile testing. The geomembrane is considered as an anisotropic material. Because of the limiting area

of the material, samples cut in only one direction, which is cross to the machine direction. The specimen is 115 mm total length, and the narrow section is 6 mm width. The length of the narrow section is about 33 mm allow locating dot with a gage length of about 25 mm.

5.3.3 Tensile machine

The tensile test performed using dual column Instron 5566 with a load cell of 5.0 kN (Figure 5.1). Strain measured using a video extensometer with the field of view of 350 mm. The test performed at a displacement rate of 10 mm/min and with a sampling frequency of 0.5 seconds to allow capturing elastic region of the stress-strain curve before the yield point. Tensile test data are collected and stored during the test and stored in an excel sheet. Stored data include time, displacement, load, and strain. Figure 5.2 shows an example of part of data in the excel sheet as received from the tensile machine for tests using a paint marker. The specimen is preloaded for 2-3 N so that to have a straight narrow section to get an acceptable measurement of gage length and strain values.

5.3.4 Data analysis

Four tensile properties were measured in the investigation: yield stress, yield strain, break stress, break strain except at paint marker. The yield point and break point are essential data of the tensile test and it is worth to evaluate stress and strain measurements at these points on tensile curve and to find their repeatability. Paint marker dots fade during tensile test thus video extensometer loos tracking marks and strain measurement stop. For this reason, break strain has not measured for the test performed using paint marker dots. Evaluation of tensile properties give an indication of

repeatability of data at test performed at each dot type and shows if there any effect of the newly manufactured dot on tensile properties.

Stresses at specific strain values (6.00, 6.50, and 7.00 mm/mm) were measured. These strains values all above the onset of strain hardening and within recommended draw ratio limits, which are 7-8 that used to measure strain hardening modulus as described in chapter 4. Also, replicates using all three dot types have reached or exceed the maximum selected strain (7 mm/mm). Three replicate tests were performed, and average values of stresses at these strains are reported for each dot type.

One main reason to design a new dot is to have enough data to measure strain hardening modulus. Thus, the strain hardening modulus is measured using three dot types as a slope of the true stress-draw ratio(λ) curve at draw ratio limits of 7-8. Values and repeatability have been compared among three dots types.

5.3.5 Dot types used in the study

Three types of the dot will be used in this research: Stick dot, paint marker dot, and new designed dot. Stick dot and paint markers represent conventional dot type. New design dot represents the dot that has been produced to overcome the limitation of conventional dots. Below is a description of each dot type:

5.3.5.1 Conventional dots

5.3.5.1.1 Stick dot

Stick dot is prepared by cutting 7 mm diameter stick paper using a paper punch. Two stick dots apply to a specimen at the narrow section with a gentle pressure of hand thumb to assure good contact. A 25 mm distance between dots is used as a gage length (Figure 5.3a).

5.3.5.1.2 Paint marker dot

The paint marker is located on the specimen with specific dimensions that specified in video extensometer user manual (22). Care has been taken to apply paint marker with the same shape and with specific dimensions. A tape has been punched from two sides with rectangle holes using coil punch, stuck on a specimen and dot applied using a white paint marker edding 751 that recommend for black materials. The tape then removed to lift two rectangle dots with a height of 3 mm and cover the total specimen width with a gage distance of 25 mm center to center (Figure 5.3b).

5.3.5.2 New design dot (center dot)

Figure 5.4 shows a sketch diagram of the new dot design. The designed dot is a compromise of a white solid plastic disc with a thickness of 0.3 mm and a steel pin with a pointy end that penetrate the disc in the middle. The center of the disc located visually using a regular 1 mm space ruler. The measured strain required a correction when the sample thickness exceeds 1 mm from the calibrated surface. Thus, the penetration of pin is barely set on the specimen at a point so that the disc is on specimen surface with no gap can be seen between sample and disc edges. The other side of pin tilt in a spiral way and extend to the other side of the specimen with a round end parallel to the specimen surface. The benefit of the round end is first to allow sliding on the specimen while pointy end set on other and maintain vertical alignment of pointy part of a steel pin to the specimen surface. This design allows video extensometer to locate the disc that sticks continuously to a point on specimen surface thus this dot is named “centered dot.” Figure 5.5 shows a prototype centered dot located on dogbone geomembrane sample.

5.4 Results

Tensile tests are performed using three different dot types with three replicates for each type. Below description of tensile curve of each dot type:

5.4.1 Tensile test using conventional dots type

5.4.1.1 Paint marker dots

Figure 5.6 show three replicates of the stress-strain curves of tensile test using paint marker dot. Paint marker deform as specimen exposed to an extension, and video extensometer locates the center of each dot from its deformed height. The three replicates curves are coincided up to the onset of strain hardening at a strain of about 5 mm/mm. After onset, two curves coincide while the third curve has a little steeper slope. Because of the high extensibility of HDPE geomembrane, paint marker dot fade at high strain and video extensometer loss dot tracking of two test curves at a strain of about 7 mm/mm and the third test curve at 8 mm/mm. This problem results in losing significant data of tensile test and prevent measuring property such as break strain.

5.4.1.2 Stick dot

Figure 5.7 show three replicates of a tensile test using stick dot. Since stick dot is made of paper, it is considered as a rigid dot. Rigid dot can not deform with deformation of the specimen. Instead, while specimen deform, the dot stick to the specimen in some area but slide in some another area on the specimen with unpredicted form. The three replicates curves coincide at yield zone suggested a good strain measurement in this low strain zone. However, high variation occurs in measured strain at and after the onset of strain hardening. Each test of the three replicates shows different onset of strain hardening above and below 5 mm/mm strain. This variation in strain increase as

measured strain increase to give higher variation in break zone when compare three replicates strain at same stress. Stick dots have successfully survived up to the end of the test for all replicates and give a complete stress-strain curve, but it fails to give a consistency data at strain hardening part after onset.

5.4.2 Tensile test using center dot

Figure 5.8 shows three replicates of centered dot tensile tests. This dot is nondeformable, and its location represents a single point on the specimen. The three replicates curves of the tensile test using this dot coincide at yield zone. They continue to coincide at the onset of strain hardening at about strain of 5 mm/mm and also above onset at strain measured up to the end of each curve. Centered dot gives a continuous curve up to break point for all three replicates. It should be noticed that one of the three replicates has significantly lower break stress and break strain which suggested a premature break.

5.4.3 Compare tensile curves of three dot types

Figure 5.9 compare engineering stress-engineering strain curves of a selected test of each dot type. All three dot types show a yield point in the same zone. Figure 5.10 show the elastic region of each dot type. Paint marker failed to show elastic relation and strain decrease after stress reaches 3 MPa up to 6 MPa. On the other hand, both centered dot and stick dot show a linear respond at the elastic region below stress of 8 MPa. However, a different trend in compared strain noticed at the higher strain. The onset of strain hardening of paint marker dot and centered dot are located at a strain of 5 mm/mm while the stick dot onset located above 5 mm/mm (Figure 5.9). Curves parts of both paint marker and centered dot are coincided after the onset of strain hardening all the way to the last point of detected strain in the test using a paint marker. Stick dot show lower

stress as strain increase and the curve bias from both other curves using paint marker and centered dot.

Figure 5.11a shows stress-strain curve at a strain of 6-6.1 mm/mm of three dots method. Paint marker shows a high variation in measured strain with a noticed increase and decreases at some data on the curve. Figure 5.12 shows deformed paint marker under tensile extension. The deformation of paint marker on tensile specimen shows a nonhorizontal nonsmooth rectangle. Instead, it shows an inclined surface with the pointy (rocky) shape of dot edges. The video extensometer needs the location of the upper and lower edge of the dot to locate the center by averaging these locations. The nonsmooth edges result in an increase or decrease in measured strain. However, this may not affect properties measured from tensile test since it happens only at some segment of data (Figure 5.11). In apposite to paint marker dot, centered dot and stick dot show smooth stress-strain curve with no fluctuation in measured strain at same segment of strain (6-6.1 mm/mm) (Figure 5.11 b and c). The smooth curve in later dot types attributed to their solid un-deform property which gives sharp edges allow video extensometer to locate the center of dot accurately.

5.4.4 Tensile properties

Tensile properties have been calculated at yield point and break point. Table 5.1-5.3 show mean and variation of each tensile property in addition to stress measured at selected strain values after strain hardening onset at engineering stress-engineering strain space. The mean and variation of yield stress were different among dot types. The mean yield stress of three replicates is ranging from lower values using stick dots followed by centered dots and then paint marker dots. Scattering of yield stress increase with the

increase of average yield stress. The relatively higher variation in yield stress of tests using centered dot and paint marker suggest that these dots may have some effect on yield properties. Similar to yield stress, values of average and coefficient of variation of yield strain are ranging from lower values using stick dots followed by centered dots and then paint marker dots.

Average break stress of centered dot was very low compared to average of other dots types with coefficient of variation values of five times of other dots. Both stick dot and paint marker dots tests show similar average break stress and scattering (Table 5.1 and table 5.2). Break strain has not been measured for paint marker dot tests since the strain stop at some value before reaching break point (Table 5.2). The average break strain of stick dots tests was higher than average break strain of centered dot while the later show higher scattering. One specimen of centered dot tests break earlier than other two replicates result in increase scattering and decrease average break strain (Table 5.3). Break stress decrease by 4 MPa and break strain decrease by 1 mm/mm compared to stick dot results. The early break of this test suggests either intrinsic variation of the tested material or premature break resulted from centered dot sharp end that set on the specimen.

Tensile test of stick dot shows high average break strain and high average break stress with a low scattering of both break properties. Stick dot has no damage effect on specimen surface which yield lower scattering in break properties. It is found that most tensile specimen using centered dot break close to dot location. Based on this assumption, the pointy part of centered dot should be redesigned by decreasing gripping force, changing pointy part material, or make a less pointy end to prevent any possible damage

to specimen surface. However, the pointy part should be tested whether it sick well at a location on the specimen after adjustment. In order to check pointy part stability on a specimen, centered dot attached to a specimen and another arm of dot move up and down 2-3 mm. If the pointy part stable during this check and does not move, then stability is good. It is recommended to made pointy part of the centered dot of a material with lower rigidity compared to tested material. Break stress of centered dot should be compared with three replicates of specimen tested without any dot type to assure a good adjustment.

Paint marker tests show average break stress very close to that of stick dot suggest that paint marker does not cause any damage to specimens. The process of design centered dot is shown in Figure 5.13. Many considerations have to be taken when design centered dot such as specimen shape and thickness, tested material properties, cost of production, and dot production ease. Most important is that making sure that dot will not cause damage of specimen surface and not causing a premature break.

5.4.5 Properties at strain hardening region

5.4.5.1 Stresses at selected strains

It is worth to compare the part of the stress-strain curve after the onset of strain hardening since data at this region are used to measure important property which is strain hardening modulus. Stresses are calculated at strain values of 6, 6.5, and 7 mm/mm. These strains values are within draw ratio limits which is 7-8 that used to measure hardening modulus. Stick dot show lower values of average stresses at selected strains compared to other methods, and as the strain increase, more reduction in stress compared to relevant stresses are noticed. Also, a scattering of stresses of the tensile test using stick dot is much higher than both other two methods and the coefficient of variation of

stresses increase as strain increase. Paint marker dot and centered dot show similar average stress at selected strains. The variation of stress using paint marker dot is very low at a strain of 6.5 mm/mm compared to variation of stresses at a strain of 6 and 7 mm/mm. However, centered dot shows a consistent low variation at selected strains with coefficient of variation around 0.6 %.

From above, tensile test using centered dot show low scattering of stresses at selected strains after strain hardening onset. It is important to keep in mind that centered dot has been produced in this research manually as a prototype product and strain measurement is very sensitive to the location of the center of the dot. The scattering of calculated properties using centered dots may be enhanced and result in lower variation when dot produced in highly accurate devices and repeatable process.

5.4.5.2 Onset and strain hardening modulus

Table 5.4 shows average and coefficient of variation of both of strain hardening modulus and onset of strain hardening that measured from true strain-draw ratio space. The average of onset of strain hardening are close to each other using all dot types. However, coefficient of variation of the onset using stick dot shows very high value reach about 12 times the coefficient of variation using paint marker and center dot. On the other hand, the average of strain hardening modulus using both paint marker dot and center dot are very similar. However, strain hardening modulus using stick dot is lower than average of modulus of both other dots by more than 10% and coefficient of variation of this property using stick dots is more than tenfold variation of the property using paint marker and stick dot.

5.5 Conclusions and recommendations

5.5.1 Conclusions

In this research, a new design of dot (center dot) has been introduced that allows video extensometer to measure strain. The tensile test has been performed using geomembrane specimens. Conventional dot types have been evaluated to show the pros and cons of each type. Paint marker dots result in failure in measuring strain using video extensometer at high strain because of dot fading problem. Stick dot shows lower average stresses at strain hardening region and higher variation compared to paint marker at same strain which can be accused to a high error in measured strain using stick dot. The new dot design (centered dot) overcome the limitations of both paint marker dots and stick dots and decrease the variation of measured properties. The accuracy of measured tensile properties using centered dot is expected to increase by producing dot in manufacturer with more accurate tools and precise machine to locate the center of dots. Design chart can be used to produce a centered dot that works properly with material and specimen dimension.

5.5.2 Recommendations

Although of promised result found in this research using centered dots, further aspects in the development of the new dot are still required. These are listed below:

1- Locating center of centered dot should be done accurately using machine auto method. This will definitely increase repeatability and give more consistent results that will overcome even paint marker results. A further test needs to be performed using machine produced centered dots and compare with results in this work.

2- Investigate the ability to adopt centered dot for a group of materials with similar properties such as high strength, soft tissue, and very ductile materials to specify centered dot features such as grabbing force, dot material, and sharpness of pointy part for each material. The designed dot should also be relevant to specimen dimensions such as thickness and specimen color to specify dot color that provides the required contrast.

3- Investigate the repeatability of a tensile test using centered dot by performing round-robin test using same HDPE geomembrane. The stress-strain curve in this work should be compared with results at another lab with the different tensile machine and different video extensometer.

Table 5.1 Tensile properties using stick dot

Property	Mean	SD	COV (%)
yield stress (MPa)	18.32	0.11	0.578
yield strain (mm/mm)	0.12	0.00	0.256
break stress (MPa)	37.61	1.32	3.502
break strain (mm/mm)	9.09	0.40	4.347
Onset (mm/mm)	4.94	0.34	6.976
Gp (7-8) (Mpa)	59.67	8.07	13.518
stress (MPa) at 6 strain	19.25	1.63	8.451
stress (MPa) at 6.5 strain	21.62	2.02	9.367
stress (MPa) at 7 strain	24.28	2.42	9.977

Table 5.2 Tensile properties using paint marker dot

Property	Mean	SD	COV (%)
yield stress (MPa)	19.54	0.37	1.881
yield strain (mm/mm)	0.11	0.01	4.974
break stress (MPa)	37.13	1.21	3.260
break strain (mm/mm)	-	-	-
Onset (mm/mm)	5.00	0.02	0.417
Gp (7-8) (Mpa)	67.79	0.63	0.924
stress (MPa) at 6 strain	21.04	0.30	1.446
stress (MPa) at 6.5 strain	23.64	0.03	0.147
stress (MPa) at 7 strain	26.34	0.32	1.205

Table 5.3 Tensile properties using centered dot

Property	Mean	SD	COV (%)
yield stress (MPa)	18.88	0.23	1.231
yield strain (mm/mm)	0.11	0.00	0.817
break stress (MPa)	33.49	5.47	16.325
break strain (mm/mm)	8.09	0.68	8.417
Onset (mm/mm)	4.88	0.03	0.710
Gp (7-8) (Mpa)	67.62	0.78	1.155
stress (MPa) at 6 strain	20.42	0.15	0.739
stress (MPa) at 6.5 strain	23.25	0.16	0.676
stress (MPa) at 7 strain	26.28	0.13	0.503

Table 5.4 Average and coefficient of variation of both of strain hardening modulus and onset of strain hardening using three dot types

Dot type	Property	Mean	SD	COV (%)
Paint marker	(lamda) Onset (-)	6.00	0.02	0.347
	Gp (7-8) (Mpa)	67.79	0.63	0.924
Stick dot	Onset (-)	5.94	0.34	5.803
	Gp (7-8) (Mpa)	59.67	8.07	13.518
Center dot	Onset (-)	5.88	0.03	0.589
	Gp (7-8) (Mpa)	67.62	0.78	1.155

Figure 5.1 Tensile machine Instron 5566

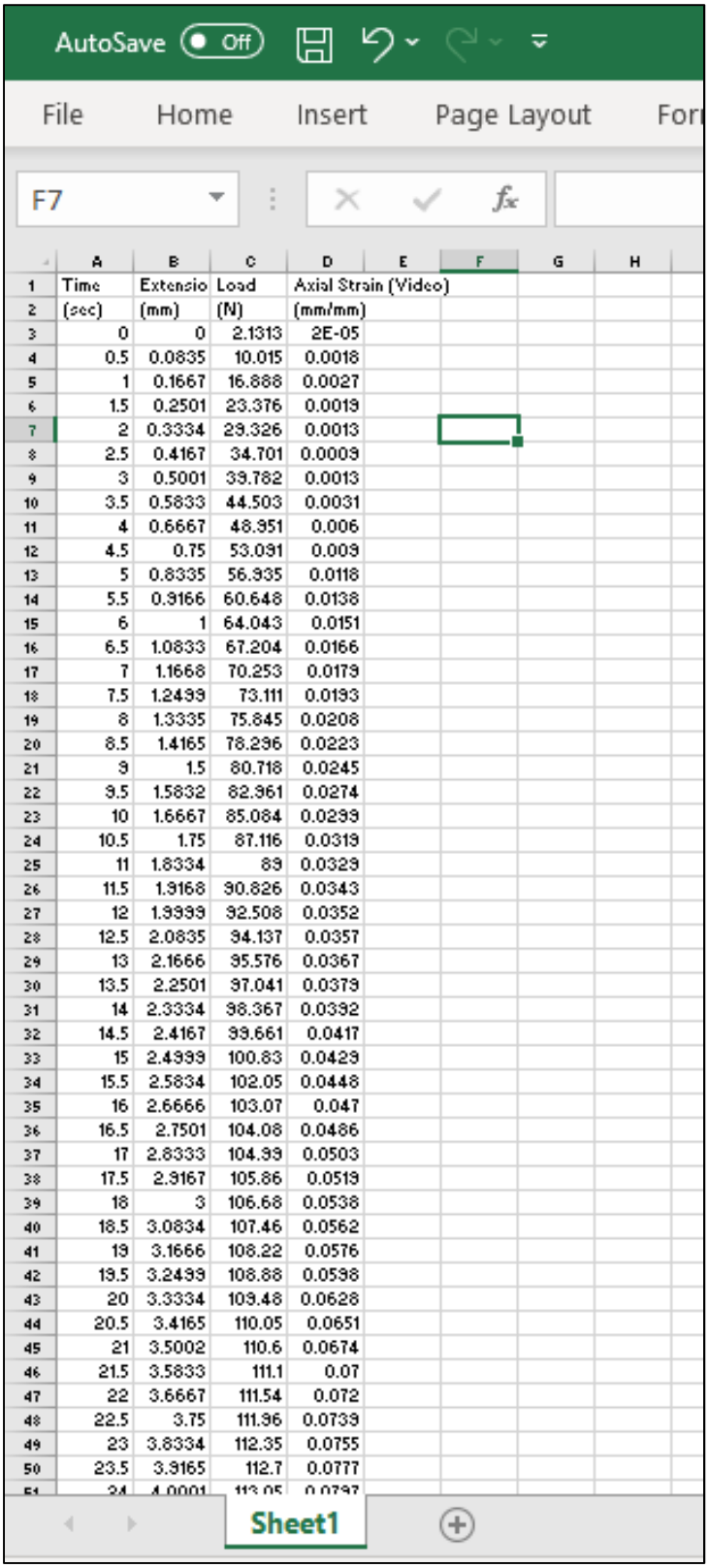

	A	B	C	D
1	Time	Extensio	Load	Axial Strain (Video)
2	(sec)	(mm)	(N)	(mm/mm)
3	0	0	2.1313	2E-05
4	0.5	0.0835	10.015	0.0018
5	1	0.1667	16.888	0.0027
6	1.5	0.2501	23.376	0.0019
7	2	0.3334	29.326	0.0013
8	2.5	0.4167	34.701	0.0009
9	3	0.5001	39.782	0.0013
10	3.5	0.5833	44.503	0.0031
11	4	0.6667	48.351	0.006
12	4.5	0.75	53.031	0.009
13	5	0.8335	56.935	0.0118
14	5.5	0.9166	60.648	0.0138
15	6	1	64.043	0.0151
16	6.5	1.0833	67.204	0.0166
17	7	1.1668	70.253	0.0179
18	7.5	1.2499	73.111	0.0193
19	8	1.3335	75.845	0.0208
20	8.5	1.4165	78.296	0.0223
21	9	1.5	80.718	0.0245
22	9.5	1.5832	82.961	0.0274
23	10	1.6667	85.084	0.0299
24	10.5	1.75	87.116	0.0319
25	11	1.8334	89	0.0329
26	11.5	1.9168	90.826	0.0343
27	12	1.9999	92.508	0.0352
28	12.5	2.0835	94.137	0.0357
29	13	2.1666	95.576	0.0367
30	13.5	2.2501	97.041	0.0379
31	14	2.3334	98.367	0.0392
32	14.5	2.4167	99.661	0.0417
33	15	2.4999	100.83	0.0429
34	15.5	2.5834	102.05	0.0448
35	16	2.6666	103.07	0.047
36	16.5	2.7501	104.08	0.0486
37	17	2.8333	104.99	0.0503
38	17.5	2.9167	105.86	0.0519
39	18	3	106.68	0.0538
40	18.5	3.0834	107.46	0.0562
41	19	3.1666	108.22	0.0576
42	19.5	3.2499	108.88	0.0598
43	20	3.3334	109.48	0.0628
44	20.5	3.4165	110.05	0.0651
45	21	3.5002	110.6	0.0674
46	21.5	3.5833	111.1	0.07
47	22	3.6667	111.54	0.072
48	22.5	3.75	111.96	0.0739
49	23	3.8334	112.35	0.0755
50	23.5	3.9165	112.7	0.0777

Figure 5.2 Data at excel sheet as received from Bluhill 2 software of tensile test performed using paint marker dot at 10 mm/min displacement rate

a) b)

Figure 5.3 Conventional dots: a) Stick dots, b) Paint marker dots

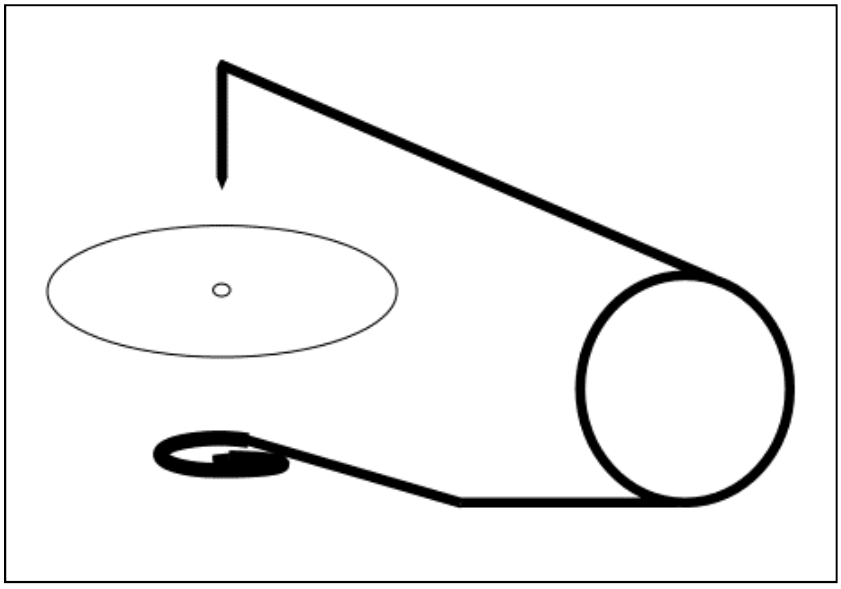

Figure 5.4 Sketch of centered dot

Figure 5.5 Center dot attached to a geomembrane specimen

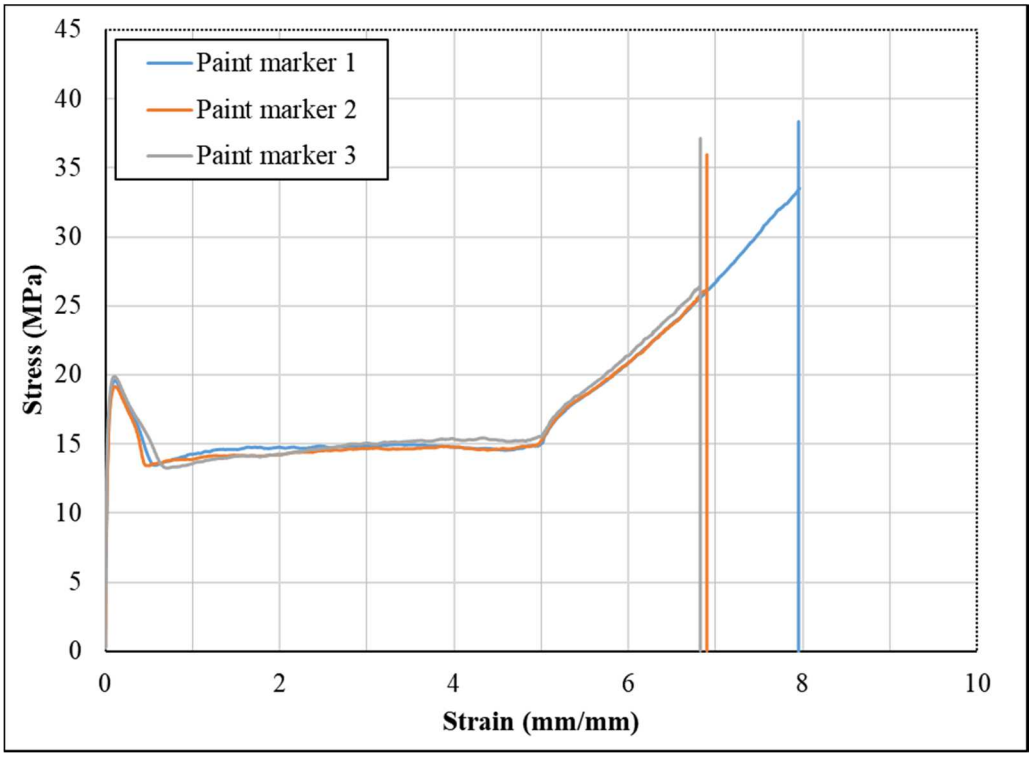

Figure 5.6 Stress-strain curves of three replicates using paint marker dots

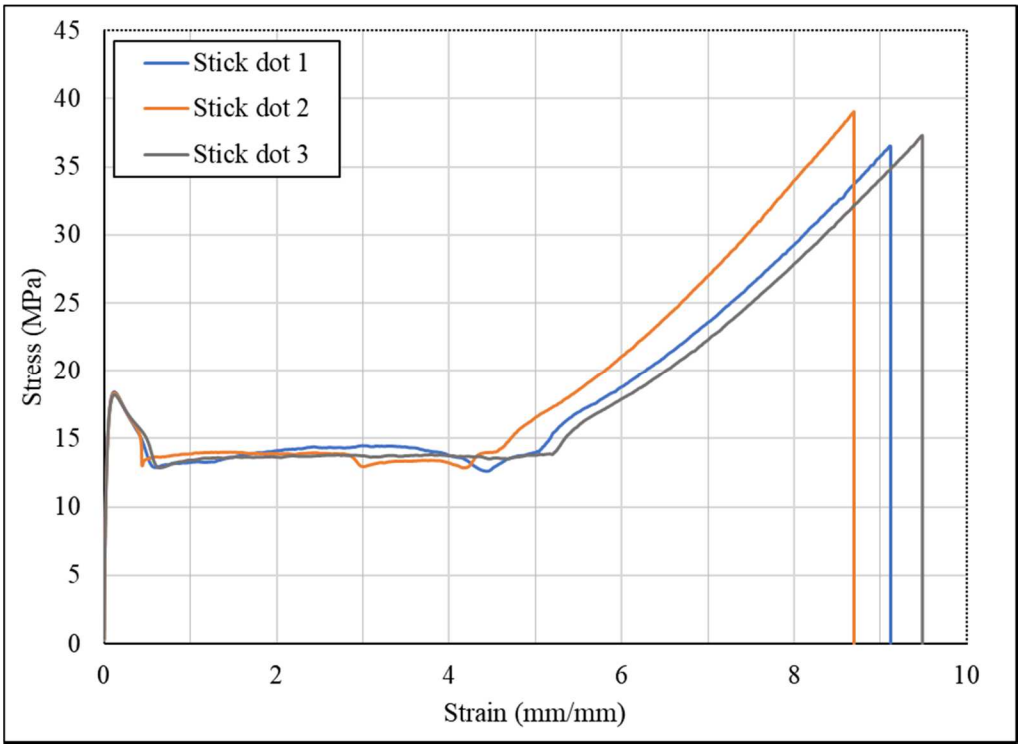

Figure 5.7 Stress-strain curves of three replicates using Stick dots

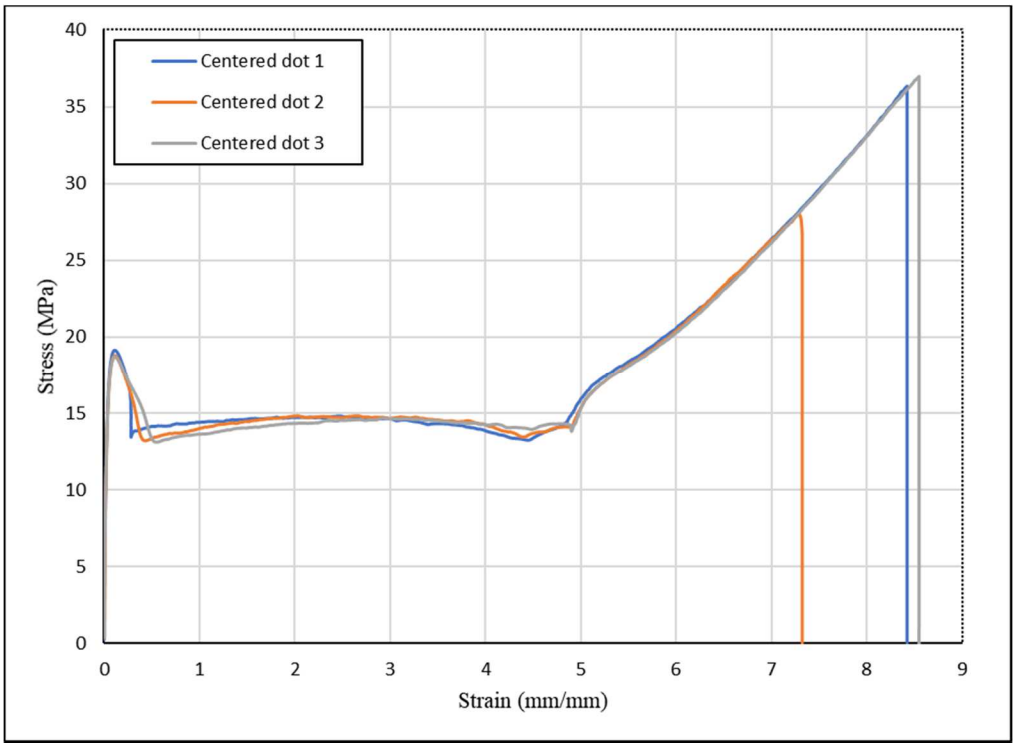

Figure 5.8 Stress-strain curves of three replicates using centered dots

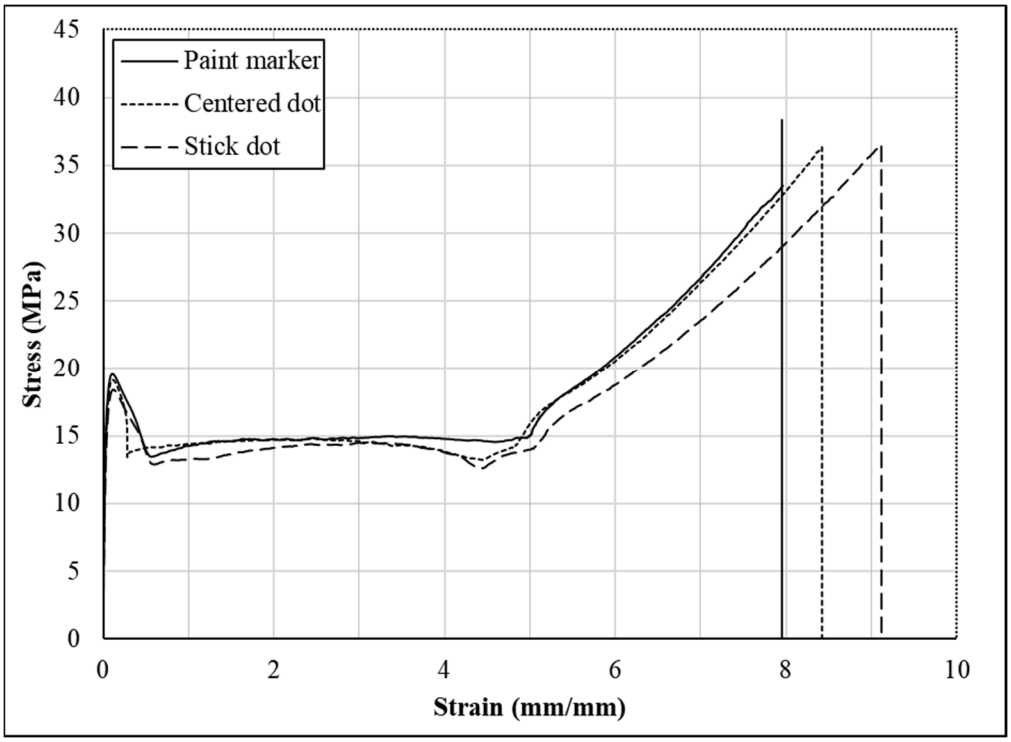

Figure 5.9 Compare of stress-strain curves using different dot types: Paint marker, centered dot, and stick dot

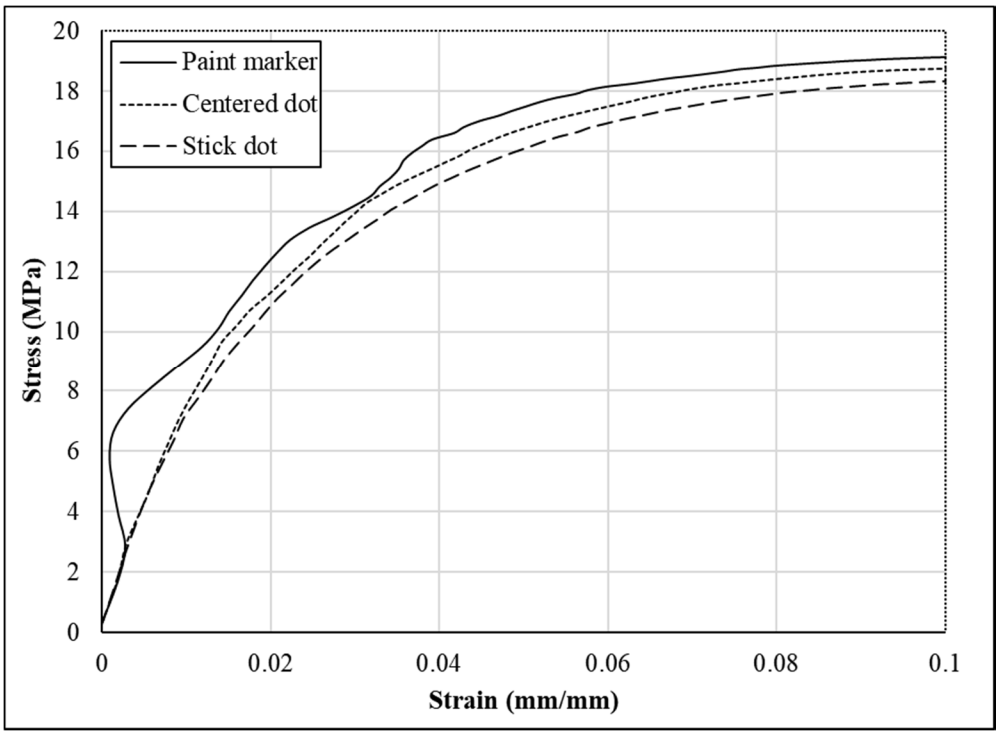

Figure 5.10 Zone up to yield of stress-strain curves using different dot types: Paint marker, centered dot, and stick dot.

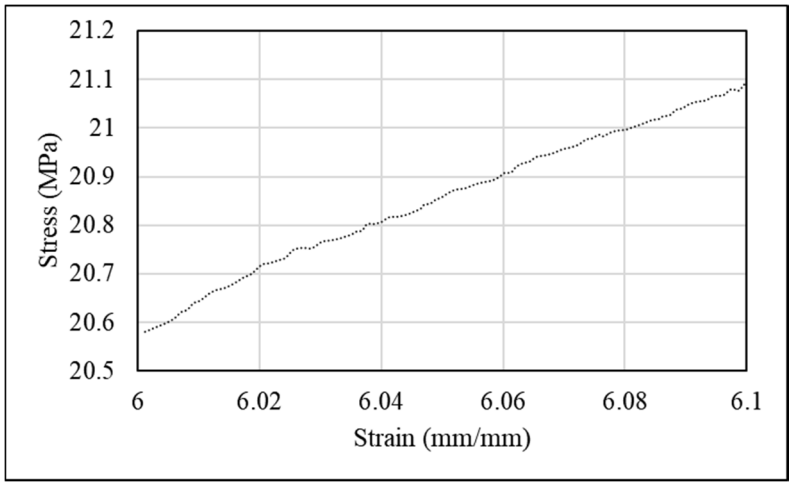

a) Centered dot

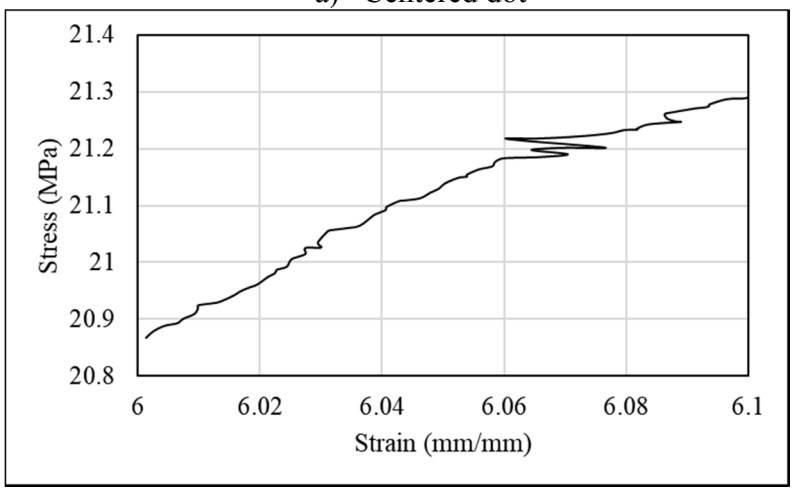

b) Paint marker

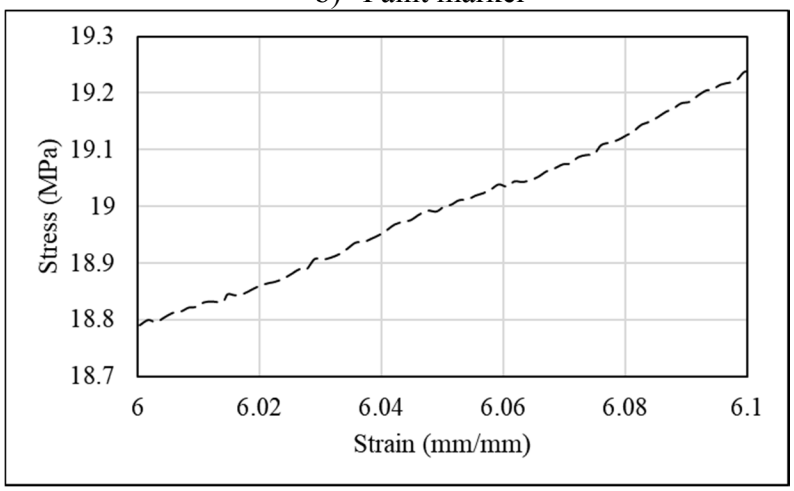

c) Stick dot

Figure 5.11 Stress-strain at strain of 6-6.1 mm/mm using three dot types: a) centered dot, b) paint marker dot, c) stick dots

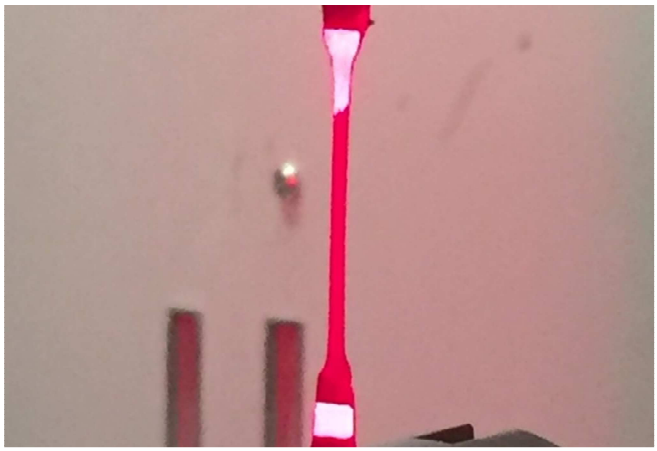

Figure 5.12 Nonuniform deformation of paint maker during tensile test

Manufacturing process:

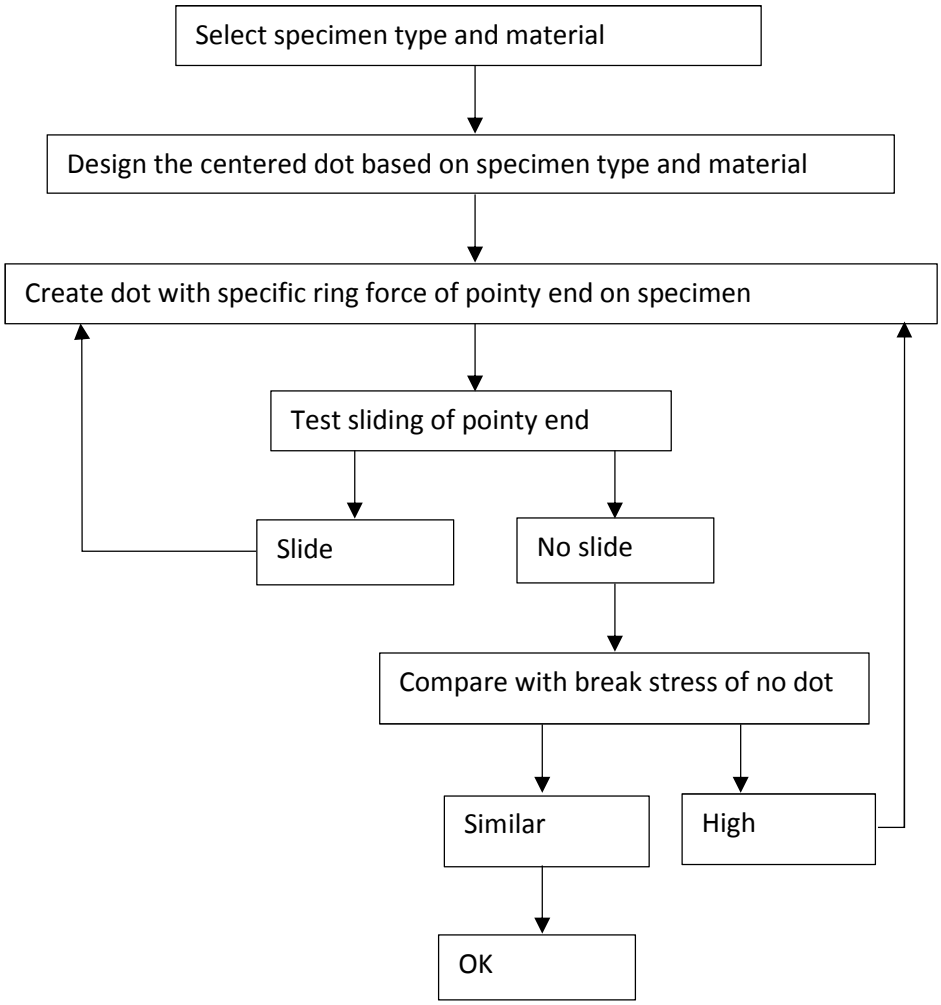

Figure 5.13 Design process of centered dot

REFERENCE

[1] DIN EN ISO 6892: Metallic Materials – Tensile Tests.

[2] DIN EN ISO 527: Thermo-plastics and duro-plastics – Determination of Tensile Characteristics.

[3] ASTM D638. Standard test method for tensile properties of plastics, Annual Book of Standards, vol. 8.01.

[4] SHT test_ISO 18488: Polyethylene (PE)materials for piping systems _ Determination of Strain hardening Modulus in relation to slow crack growth Test method.

[5] Hsu, Q. C. (2003). Comparison of different analysis models to measure plastic strains on sheet metal forming parts by digital image processing. *International Journal of Machine Tools and Manufacture*, *43*(5), 515-521.

[6] Jerabek, M., Major, Z. and Lang, R.W., 2010. Strain determination of polymeric materials using digital image correlation. *Polymer Testing*, *29*(3), pp.407-416.

[7] E. Fauster, P. Schalk, and P. L. O'Leary, "Evaluation and calibration methods for the application of a video-extensometer to tensile testing of polymer materials," Proc. SPIE 5679, 187–198 (2005).

[8] Kweon, S., & Benzerga, A.A. (2016). Strain localization in determining the constitutive response of polymers. ASME International Mechanical Engineering Congress and Exposition, Proceedings (IMECE), 14.

[9] Poulain, X., Kohlman, L. W., Binienda, W., Roberts, G. D., Goldberg, R. K., & Benzerga, A. A. (2013). Determination of the intrinsic behavior of polymers using digital image correlation combined with video-monitored testing. International Journal of Solids and Structures, 50(11–12), 1869–1878.

[10] Uchida, M., & Tada, N. (2011). Sequential evaluation of continuous deformation field of semi-crystalline polymers during tensile deformation accompanied by neck propagation. International Journal of Plasticity, 27(12), 2085–2102.

[11] Sasso, M., Palmieri, G., Chiappini, G., & Amodio, D. (2008). Characterization of

hyperelastic rubber-like materials by biaxial and uniaxial stretching tests based on optical methods. Polymer Testing, 27(8), 995–1004.

[12] D. S. Zhang, C. D. Eggleton, and D. D. Arola, "Evaluating the mechanical behavior of arterial tissue using digital image correlation," Exp. Mech. 42(4), 409–416 (2002).

[13] Freutel, M., Schmidt, H., Durselen, L., Ignatius, A., & Galbusera, F. (2014). Finite element modeling of soft tissues: Material models, tissue interaction and challenges. Clinical Biomechanics, 29(4), 363–372.

[14] Mazza, E., & Ehret, A. E. (2015). Mechanical biocompatibility of highly deformable biomedical materials. Journal of the Mechanical Behavior of Biomedical Materials, 48,100–124.

[15] Todros, S., Pachera, P., Baldan, N., Pavan, P. G., Pianigiani, S., Merigliano, S., et al. (2018). Computational modeling of abdominal hernia laparoscopic repair with a surgical mesh. International Journal of Computer Assisted Radiology and Surgery, 13(1),73–81.

[16] Pavan, P. G., Pachera, P., Todros, S., Tiengo, C., & Natali, A. N. (2016). Mechanical characterization of animal derived grafts for surgical implantation. Journal of Mechanics in Medicine and Biology, 16(3), 1650023. https ://doi.org/10.1142/S0219 51941 6500238.

[17] Volk, B. L., Lagoudas, D. C., & Maitland, D. J. (2010). Characterizing and modeling the free recovery and constrained recovery behavior of a polyurethane shape memory polymer. Paper presented at the ASME 2010 Conference on Smart Materials, Adaptive Structures and Intelligent Systems, SMASIS 2010, 1, pp. 253–260.

[18] Feng, B., Xu, M. L., Zhao, T. F., Zhang, Z. J., & Lu, T. J. (2010). Triaxial extensometer for volumetric strain measurement in a hydro-compression loading test for foam materials. *Measurement Science and Technology*, *21*(11), 115705.

[19] Tourlonias, M., Bueno, M. A., Bigué, L., Durand, B., & Renner, M. (2005). Contactless optical extensometer for textile materials. *Experimental mechanics*, *45*(5), 420-426.

[20] Becker and M. Dripke, "Choosing the right extensometer for every materials testing application," Adv. Mater. Process. 169(4), 17–21 (2011).

[21] Qiuhong, T., Zhengrong, S., Zhongping, L., Yanna, L., Lijian, Z., & Sendong, X. (2014). Strain measurement based on laser mark automatic tracking line mark on specimen. Optical Engineering, 53(12), 122412.

[22] Instron Video Extensometer AVE and SVE Reference Manual - quipment M26-14185-EN Revision K (Manuall)

[23] Roeder, R. K. (2013). Mechanical characterization of biomaterials. Characterization of biomaterials (pp. 49–104). Amsterdam: Elsevier.

[24] Todros, Silvia, et al. "Marker Tracking for Local Strain Measurement in Mechanical Testing of Biomedical Materials." *Journal of Medical and Biological Engineering* (2018): 1-9.

[25] Todros, S., Pavan, P. G., & Natali, A. N. (2017). Synthetic surgical meshes used in abdominal wall surgery: Part I - materials and structural conformation. Journal of Biomedical Materials Research. Part B, Applied Biomaterials, 105(3), 689–699.

[26] Havermans, L., Kloth, R. and Deblieck, R., 2012. Strain hardening modulus: an accurate measure for slow crack growth behavior of HDPE pipe materials. *Proceedings Plastic Pipes XVI, Barcelona, Spain*.

CHAPTER 6

STRAIN HARDENING METHOD FOR AGED GEOMEMBRANE

6.1 Introduction

Strain hardening modulus is performed through tensile test inside the oven at high temperature to evaluate the performance and service life of high density polyethylene (HDPE) geomembrane. This research proposes a more simplified test by conducting of strain hardening test at room temperature. HDPE geomembrane samples have been aged at 120 □ and retrieved at a specific aging time. Strain hardening test performed at room temperature. A significant change in the tensile curve has been noticed as a result of aging. According to these changes in tensile curves, several ways have been used to measure the strain hardening modulus. Methods have been studied, evaluated, excluded, or approved based on expected results of modulus values from the literature. Besides, samples at the same aging time of strain hardening test have been selected and send to the lab to measure stress crack resistance. The strain hardening method in this research is a viable alternative for evaluating failure resistance of HDPE geomembrane.

6.2 Backgroaund

HDPE geomembrnae is used widely as a liner under landfills and lagoons to protect ground water from polution. During their service life, geomembranes are exposed to harsh conditions such as heat, UV light, chemicals, and mechanical stresses. These conditions result in accelerating the aging process which impact material chemical and

phsical properties and finally stress crack resistance. Stress crack is defined by ASTM D5397 as an "external or internal crack in a plastic caused by tensile stresses less than its short-time mechanical strength.[1]" There are two methods to evaluate crack resistance of HDPE geomembranes refrenced by ASTM. The first method is a bent strip test according to ASTM D1693[2], which is not recommended to rank geomembrnae samples' crack resistance [3]. The second method is the Notch Constant Load Test (NCTL) according to ASTM D5397, which is favored to evaluate geomembrnae crack resistance[1].

Crack resistance tests are not limited to HDPE geomembrane. They are also used to evaluate other HDPE and polymeric materials such as pipe reisns, geotextiles, etc. With the improvement of materials, polymeric resins become more resistant to cracks and have a longer service life. The conventional method to evaluate crack resistance requires a very long time, and these tests are not feasible for such improved materials. Thus, researchers explored other alterantive test methods to evalute crack resistance within shorter time frame.

Researchers studied new alternative methods to replace conventional stress crack resistance (SCR) test with a more simplified approach. Among these methods, the strain hardening method has been used to evaluate SCR of HDPE. This method simulates the fibrils conditions developed in craze formation and predicts resistance to slow crack propagation in HDPE products from a tensile measurement performed at 80 °C [4]. It is found that the slope of the stress-strain curve above its natural draw ratio -strain hardening modulus - correlates well with failure time determined by conventional SCR tests.

The prediction of SCR of PE pipe resins using the strain hardening method was published as an international standard ISO18488 [5]. The test is performed using a universal testing machine equipped with optical extensometer at a crosshead speed of 20 mm/min and a 80 □ chamber temperature.

Recently there is an attempt to study the strain hardening method for HDPE geomembrnane at University of South Carolina. A measurement methods at simplified room temperature conditions have been established for the measurment of strain hardening modulus of unaged geomembrnane specimens. However, these methods have not been yet approved for the use for aged materials where HDPE chemicals, mechanical, and morphological properties are degraded with aging.

It is reported that many features occur when HDPE geomembranes aged such as additive and stabilizer loss, brittleness, and change in the molecular weight etc. [6]. Depending on the exposure conditions and the HDPE resin used, several ageing and degradation mechanism can occur. Aging can occur because of ultraviolet degradation, chemical degradation, biological degradation, extraction and the depletion of antioxidant, oxidative degradation, and thermal degradation, etc. [7,8].

There are three distinct stages for HDPE GMB degradation [9]. (A) Stage I: antioxidant depletion. Depletion of antioxidant (AO) is a consequence of two processes: chemical reactions of AO with oxygen that diffuse into the GMB and AO physical loss form the geomembrane. AO depletion rate is highly affected by the initial AO concentration in GMB, the nature of site environment, and temperature. (B) Stage II: induction time at which polymer react with oxygen forming very low amount of hydroperoxide (ROOH). ROOH does not decompose readily into free radicals thus

oxidation occurs extremely slowly. (C) Stage III: polymer degradation at which additional ROOH molecules are formed, then reach a critical level, and decompose, resulting in a substantial increase in the free radicals concentration. The Oxidation process produces alkyl radical (free radical polymer chains), which can result in further reactions, leading to cross-linking of chain scissions. With these degradations, the physical (such as melt index) and the mechanical properties (break strength and break strain) start to change. Thus, the tensile test properties and stress-strain curve is affected by the aging process. Researchers studied the slope of strain hardening part of tensile test to evaluate SCR of aged polyethylene resins. The serviceability of aged polyethylene geopipes has been evaluated from three different landfills locations using Full Notch Creep Test (FNCT) and strain hardening method [10]. The variation of these properties indicates that these materials have not met the service life of the 100 years and the requirements for geopipes suitable for landfill applications.

The performance of three different lining systems that were used for pond and landfill liners have been evaluated using elongation at break and slope of strain hardening of load displacement curve performed at room temperature. One of the liners is a 1.5 mm HDPE geomembrane and has a stress crack after 6 months of installation. It is found that the material easily met the specification in machine direction (MD) for elongation at break with noticed strain hardening segment while transvers machine direction specimen has lower elongation at break with no rising strain-hardening segment. It is suggested that the material in TMD has a lower SCR than in MD [11].

The strain hardening modulus of several aged HDPE geomembrane has been tested following the standard (ISO 18488). It has been shown that modulus is proportional to the stress crack resistance of aged liners [12].

The stress crack resistance of 1.5 and 2.0 mm HDPE geomembranes from three sites after two years of exposure from a lagoon, a water reservoir, and a landfill have been studied [13]. The results compared to the strain hardening in the same cross machine direction CMD. A good correlation has been found between NCTL failure times for CMD and the measured modulus. It is also found that the strain hardening modulus of HDPE geomembrane decreased by ageing the material in lab at 80 °C and 50 bar oxygen pressure. It is suggested that the reduction in the mechanical properties starts after the depletion of the entire antioxidant content.

The natural draw ratio is defined as a ratio of a sample strain at the onset of strain hardening and its initial length. There is evidence of a relationship between polymer extensibility (and hence NDR) and entanglement density in melt-spun fibers [14]. Apractical approach has been adopted by performing strain hardening tests for several HDPE resins at room temperature at low displacement rates [15]. It is found that both hardening stiffness and the natural draw ratio are a good indicator of ESCR of HDPE. The NDR was inversely proportional to ESCR and suggested that NDR can be used as an indicator of ESCR. It was suggested that the onset of strain hardening increases with the decrease of entanglement density within amorphous phase of the ultra-high molecular weight polyethylene [16].

It is hypothesied that with aging of HDPE, the extensibility increases and thus the onset of strain hardening also increases. The increase of the onset in the aged samples

affects strain zone at which the strain hardening modulus is measured. Thus, there is a need to carry out strain hardening modulus measurments for the aged HDPE geomembrane.

In this research, we will evaluate and validate the strain hardening method to characterize aged HDPE geomembrane. Geomembrane sheets will be oven aged to accelerate the degradation process. The effect of aging on tensile test curve will be studied. Samples will be retrieved and tested using strain hardening methods. Strain hardening modulus will be measured in several methods according to the change in tensile curve with aging. The results and measurements methods will be analyzed and compared for unaged and aged samples. Another unaged and aged geomembrane samples of selected aging time will be tested using stress crack resistance test. The variation of the strain hardening modulus for the aged samples shall be compared with the variation of SCR of geomembrane samples that aged at the same time. This correlation shall prove useful to characterize geomembrane with appreciable time saving in comparison with the stress crack resistance following ASTM 5397. Because of limitation of paint marker dot which results in failure to get a continuous measurement of strain up to break point which is necessary for measuring strain hardening modulus, center dot will be used for all aged samples in this research. Center dot has been approved as a good replacement for conventional marker as described in chapter 5.

6.3 Materials and methods

6.3.1 Materials

The material that is used in this study is a 1 mm HDPE geomembrane. A roll of

this geomembrane is available at the University of South Carolina Civil and Environmental Engineering Department and stored in the dark at room temperature for several years. The apparent view of this geomembrane shows a clean surface and tensile test of the material showed that the material is acceptable and met the requirement given by Geosynthetic Research Institute (GRI-GM13). The limited available area of the material control replicates number of tests thus tests are performed only at three replicates at each displacement rate for both unaged and aged samples.

6.3.2 Experimental method

6.3.2.1 Specimen shape/dimensions

Dogbone die produced by Pioneer co is used to cut specimen for tensile test from unaged and aged geomembrane sheets. The specimen dimensions are as specified by ASTM D638 for tensile test for polymer materials such as geomembrane specimen. The narrow section width of the specimen is 6 mm while the length is 33 mm [17] (Figure 6.1).

6.3.2.2 Test Preparation

The test is performed using an Instron 5566 tensile device with a load cell of ±5 kN capacity and has a video extensometer for strain measurement (Figure 6.2). Test parameters such as displacement rate and sampling per second, are assigned as input to Bluehell 2 software. The test is performed at displacement rate of 10 mm/min and sampling frequency is 0.5 second. All tests are performed at room temperature.

The video extensometer required two markers on the specimen to measure strain during the test. Markers are applied using paint marker edding 571 for unaged specimens. Video extensometer failed to track paint marker of many unaged tested specimens. While

unaged HDPE geomembrane available for test, aged material samples are very limited. A new design marker "Centered dot" will be used for aged samples so that no strain measurement failure occurs. Figure 6.3 shows the two types of markers that used in this study. Centered dot overcome the limitation of conventional markers and allow measuring strain up to specimen break point. Unaged and aged specimens are cut in cross machine direction which represent the weak one.

6.3.2.3 Exposure condition

GM coupons (110 x 130 mm) were incubated inside the oven at 120 'C. The coupons held vertically with space between them to allow a fare exposure condition (Figure 6.4). Aging temperature was selected based on literature that show that maximum exposure temperature for aging experiment should not exceed melting temperature of the geomembrane. Since melting temperature of HDPE geomembrane is about 130 □, 120 □ is selected. This temperature will result in aging and dropping in mechanical properties (stage three of aging stages) within months rather than years in low temperature such as at 80 □ and lower incubation temperatures.

6.3.2.4 Test matrix

Test will be performed for both unaged and aged geomembrane to compare variation in tensile test curves and to study and adjust several measurement methods of strain hardening modulus test. According to results at Chapter 4, Low displacement rates result in lower coefficient of variation of strain hardening modulus (Gp). Thus, all tensile tests have been performed at displacement rate of 10 mm/min. Aged materials will be monitored by testing sacrifice specimen. One specimen will be tested every week to notice any significant change in stress-strain curve. Changes include variation in stress

and strain hardening region, shifting in onset of strain hardening, and change in tensile properties. When change noticed at sacrifice specimen, two more specimens are retrieved for tensile test to have a set of three specimen per sample. At the same time of tensile test sampling, another sample is retrieved for stress crack resistance. It is expected that strain hardening modulus measured from tensile test at low displacement rate can be representative to evaluate crack resistance of the material. Table 6.1 shows test matrix at selected aging time. Because of the limited samples, sampling has been retrieved only for tensile test at 41 days. Sampling stopped when tensile test shows a significant reduction in mechanical properties and no strain hardening region. At this condition, the material become brittle and reach end of service life [10]. Geomembrane sheets for strain hardening modulus test are collected and marked with cutting direction (CMD) and aging time and kept in dark at room temperature so that specimens cut later. SCR samples are collected and marked with cutting direction (CMD) and aging time and kept in dark at room temperature to send later to TRI environmental lab.

6.3.2.5 Calculation Method and Data Treatment for strain hardening test

Draw ratio is calculated on the basis of gauge length according to the equation [4]:

$$\lambda = \frac{\Delta L}{L} + 1 \quad \text{.....6-1}$$

Where λ is the draw ratio expressed as a unit less, L_o is the initial distance between the gauge dots in millimeters and ΔL is the increase in the specimen length between the gauge dots marks in millimeters.

The true stress is calculated assuming conservation of sample volume between the gauge dot marks:

$$\sigma_t = \frac{\lambda . F}{A} \quad \text{6-2}$$

Where σ_t is the true stress in MPa, F is the measured force in Newtons, A is the initial cross-sectional area of the narrow section of the specimen in square millimeters.

In this research Gp is calculated as a linear regression of the curve between specified λ limits [18]. The effect of aging on tensile curve will be consider while measuring strain hardening modulus. The strain hardening modulus will be measured at three different methods: Constant limits method, total strain hardening region method, and ratio method. In constant limits method, modulus will be measured as the slope of best linear fit through data points on draw ratio-true stress curve at a specific limits of draw ratio. Draw ratio λ increments of 0.5 and 1 will be used between draw ratio of 7 and 8 according to Chapter 4. In total strain hardening region method, modulus will be the slope of the best fit line through data points between onset of strain hardening and break point. In ratio method, modulus will be measured as the slope of best linear fit through curve at strain hardening region between a specific draw ratio limits. These limits are justified according to onset and break draw ratio values. The results will be compared with unaged results that measured at same method. Gp measurement methods will be discussed and validated based on literature and exist tensile data.

6.4 Results

6.4.1 Effect of aging on tensile curve

In order to study the effect of aging on strain hardening property, 1 mm GM has been aged inside the oven at 120'C for up to 180 days. Sample retrieved, and tensile test performed for three replicates at 10 mm/min displacement rate to evaluate the change in strain hardening and tensile curve. Figure 6.5 shows tensile test curves of unaged and 41

days aged GM specimens tested at 10 mm/min. Three significant differences were observed in this figure between unaged and aged specimens. First, the nick width of aged specimen is obviously lower than that of unaged one. Aged specimen showed lower nick width and higher yield stress. Researchers indicate that neck width measured for specimen tested at low displacement rate was proportional to tie molecules concentration [20, 21]. Material with high tie molecules content has homogenous deformation resulted from shearing crystal blocks, while low tie molecule content materials exposed heterogenous deformation due to crystal block sliding [20]. Second observation is the increase in the onset of strain hardening of aged specimen from 5 to 5.6. The onset or natural draw ratio NDR is related to extensibility of the material network after yield. He et al 2016 found that the NDR of UHMWPE blends decreased with improvement of tie molecule probability and the crystallization rate indicating improvement in material long term properties [22]. Chain entanglements control extensibility of polymer with no crosslinks [23]. The increase in the onset of strain hardening of aged specimen may resulted from a reduction in tie molecule and or entanglement density. Third noticeable observation, there is a significance stress drop of aged specimen after onset of strain hardening. The total hardening part of stress-strain curve of 41 days aged GM is located below the comparative part of the curve of unaged GM specimen curve.

Similar to our finding, the effect of UV light on Ultra high molecular weight polyethylene (UHMWPE) has been studied [22]. It is found that the slope after onset of plastic region decrease with exposure to UV light. This is attributed to the reduction in entanglement density and increase in crystallinity with aging which yield easier deformation. In addition, stress is shifted upward at region between yield and strain

hardening onset for aged specimen. That could be attributed to the increase in crosslinking as a result of annealing of HDPE in the oven. Figure 6.6 shows change in tensile curve of unaged and oven aged samples up to 180 days. There is a clear reduction in slope of strain hardening region with aging. Also, the onset of strain hardening increase and maximum draw ratio decrease with aging. The 180 days aged sample show no onset or strain hardening region and suggest very low stress crack resistance value.

6.4.2 Measurement methods of Gp of unaged and aged samples

Three different methods of measuring Gp of unaged and aged geomembrane samples have been discussed below.

6.4.2.1 Constant limits method

Table 6.2 shows strain hardening modulus (Gp) and coefficient of variation (COV) with aging time using constant limits method. Course limits of draw ratio has been selected based on suggestion of Chapter 4 of unaged samples. Minimum draw ratio at constant limits method is 7 while maximum value is 8. Gp increase as draw ratio limits increase at limits of 7-7.5, 7.25-7.75, and 7.5-8. These increase in Gp suggest a nonlinear relation of draw ratio-trues stress curve after onset of strain hardening. However, Gp measured at draw ratio of 7-8 were lower than those measured at 7.5-8 at all unaged and aged samples. It is interesting that Gp measured at draw ratio of 7.25-7.75 are similar to those measured at draw ratio of 7-8 for each aging time up to 82 days. This suggest that Gp measured at draw ratio of 7.25-7.75 can be representative to Gp measured at 7-8 draw ratio. In addition, Gp values decrease with aging at all selected limits. The reduction in Gp with aging time accompanied by an increase in COV specially in samples aged at 82 and 150 days.

Figure 6.7 shows change in Gp that normalized to initial value of unaged specimen with aging time. Gp measured at draw ratio limits (λ) of 7-7.5, 7.25-7.75, 7.5-8, and 7-8. Gp measured at λ limits of 7-7.5 shows a decline in Gp value at 41 and 82 days followed by a little increase in Gp up to 150 days. Gp measured at other draw ratio limits (7.25-7.75, 7.5-8, and 7-8) show a similar decline at 41 days and 82 days aging time and a continuous decrease in Gp at 150 days aging time. Since crack resistance is expected to decrease with aging time, the reduction in Gp up to 150 days at draw ratio limits of other than 7-7.5 is more acceptable to represent crack resistance.

6.4.2.2 Total hardening region method

In this method, Gp measured as the best fit line through data points on tensile curve between the onset of strain hardening and the maximum point of the draw ratio-true stress curve before specimen breaks. Table 6.3 shows Gp and COV of unaged and aged samples using total hardening region method. The values of average Gp of unaged and aged samples up to 82 days show values around 62 MPa. There is no reduction in Gp with aging at this period of experiment time. Also, high COVs has been measured for unaged and 82 days aged samples compared with low variation of Gp at same aging time using previous method (constant limits method). The last data point on ensile curve represented by maximum draw ratio and maximum true stress. These points have high variation as shown in Chapter 3. This interpret the high COV of Gp using total strain hardening method compared to previous constant limits method. However, clear reduction in Gp has been noticed at sample aged 150 days.

Figure 6.8 shows Gp measured using total hardening region method with aging time. It is likely from average curve that Gp has negligible change with aging up to 82

days. However, Gp dropped at 150 days of aging. As can seen in this figure, the data has a high scatter from average value. The reason behind this is that the hardening zone of the curve is not linear portion and true stress increase exponentially with strain. While the initial selected draw ratio is at onset, the final draw ratio is not necessary at same value. Based on above, Gp measured using total hardening region can be very high when break point occurs at high draw ratio and vice versa.

6.4.2.3 Ratio method

There are several changes in tensile test curve occur after aging. These changes include:1) increase in onset of strain hardening with aging, 2) decrease in break strength and break strain, and 3) reduction in the slop of hardening part of the curve. An approach has been modified to measure strain hardening modulus considering these changes. This approach called ratio method.

Figures 6. 9, 6.10, 6.11, and 6.12 show draw ratio-true stress curves of strain hardening region of a selected unaged, 41 days, 82 days, and 150 days aged samples. Dot line is a guide to show the curvature of hardening region of the curve above onset and below break point. There is a linear part in the middle third of the strain hardening region of unaged and aged samples. When testing strain hardening modulus at high temperature, it is easy to find a straight line at hardening zone of tensile test. However, the linear part shows only at this middle third in test performed at room temperature. Based on above, the strain hardening modulus is measured according to ratio of strain hardening region. Thus, this method named “the ratio method”. Table 6.4 include data treatment and GP measurement using ratio method. Column 1 in table 6.4 shows specimen number and aging time. The ratio method can be summarized by steps below:

1- Specify draw ratio at onset (λ_{onset}) of three replicates and get average (column 2).

2- Find draw ratio at break point (λ_{break}) of each of three replicates (column 3).

3- Find the difference of hardening region of each replicate (λ_{break}-λ_{onset}) (column 4).

4- Find maximum difference of three replicates (column 5).

5- Locate initial draw ratio by adding λ_{onset} to one third of the maximum difference (column 6).

6- Locate end draw ratio by subtracting one third of the maximum difference from λ_{break} (column 7).

7- Find the strain hardening modulus as the best fit line through data points between initial draw ratio (column 6) to end draw ratio (column 7).

Red rectangles on tensile curves at figures 6.9-6.12 represent the limit of draw ratio at which Gp is measured at unaged and aged samples according to ratio method. The zone length between draw ratio limits at which Gp measured using the ratio method has a revers relation with aging time. This occurs because of the increase in onset and decrease in break point that result in reduction in measurement zone and thus lower increment on draw ratio. In addition, the strain hardening zone becomes more linear with aging to give almost linear behavior among the total hardening zone at sample aged for 150 days. Table 6.5 shows Gp and COV of unaged and aged samples using ratio method. There is a clear reduction in Gp with aging time. The COV of unaged and 41 days aged samples show very low values compared to other methods at same aging time. However, COV increases at samples aged at 82 days and 150 days. Figure 6.13 shows Gp measured using ratio method with aging time. There is a gradual decrease in Gp with aging time up to 82 days followed by a clear drop in Gp at sample aged for 150 days. It is noticed from this

figure that data has low scattering compared to previous method "total strain hardening method".

6.4.3 SCR test results of aging experiment

In order to validate measurement methods of strain hardening modulus, unaged and aged samples of same geomembrane have been retrieved for stress crack resistance test. The test is performed according to ASTM D5397 at TRI environment lab. Table 6.6 shows results of stress crack resistance test for each replicates of tested samples in hours and days. Currently, only two specimens are failed out of five replicates of unaged sample. All other specimens of aged samples are failed. Results are consistence at each aging time accept unaged sample that shows a clear different results of the two known results with time of 1176 and 4245 hours. The other three replicates of unaged specimen have not failed yet. The low time of crack resistance of unaged specimen 1 (1176 hours) may results from a manufacturer imperfection. It is likely that other three not failed unaged specimens will fail at or exceed 5000 hours. Based on this, the average SCR of unaged sample is assumed to be 5000 hours. Table 6.7 shows average of SCR and coefficient of variation (COV) with aging time. Sampling times are selected based on change in tensile curve from tensile test. Unaged samples and sample aged at 82 and 150 days have results of Gp. Sample that aged at 180 days has no Gp results because tensile curve shows no strain hardening region. Only SCR test results is available for sample aged for 180 days. There is a clear reduction in SCR failure time with aging. Samples that aged at 82 days and 150 days show low COV compared with sample aged at 180 days. However, according to results of two specimen of unaged sample, high COV is expected for unaged sample. It is known that scattering of failure time in SCR is quite high

compared to negligible scattering of strain hardening modulus test that measured inside the oven at 80 □[19].

Table 6.7 shows average of SCR and COV of geomembrane samples at selected aging time. While all aged samples results have been received, unaged samples are not available at time of submitting this thesis. It is expected for unaged geomembrane that used in this research to reach 5000 hrs of average crack resistance failure time. There is a clear reduction of SCR with aging time. Assuming that average failure time of SCR test is 5000 hours, it is dropped to the half within 82 days of aging time. In addition, within 6 months of aging, sever damage in material has been noticed with SCR of only 26 hours. This low value of SCR suggest reaching the end of service life of the geomembrane. The COV increase at low SCR samples such as samples aged at 150 and 180 days. In order to present SCR on figure, logarithm scale is used. The logarithm scale is used to present SCR results for HDPE geomembrane research [13, 15, 19]. Figure 6.14 shows average SCR with aging time in this experiment. There is a bilinear relationship between log SCR and aging time. This bilinear respond suggests the three phases of degradation. The first reduction in SCR was shallow and can represent antioxidants depletion and induction time. While the SCR at this stage dropped to the half of initial value, the material still has a considerable mechanical strength by showing high crack resistance. The second respond shows a clear reduction in crack resistance to reach a very low value of 26 hours of failure time at 180 days aging time. This reduction suggests reaching third stage of aging which is degradation stage. The following section will discuss the validation of strain hardening modulus measurement methods using SCR test results.

6.4.4 Validating Gp measurement methods according to SCR test results

Figure 6.15 shows the strain hardening modulus (Gp) measured constant limits method against failure times in SCR test. With exception to Gp measured at draw ratio limits of 7-7.5, Gp increase with increase in SCR failure time. However, there is no clear correlation between the two tests results. Figure 6.16 shows the strain hardening modulus measured in total hardening region method and ratio method plotted against the failure time in SCR test. While Gp measured in total hardening method increases with increase in SCR failure time at low value of SCR, it has a reverse relation with crack resistance at higher failure time. This suggest that total strain hardening method is not sufficient to represent SCR of HDPE geomembrane. On the other hand, Gp measured using ratio method shows a good correlation with SCR failure time. The higher the value of Gp by ratio method, the higher the failure times in SCR tests. For this particular 1 mm HDPE geomembrane, that aged inside the oven at 120 □, Gp measured by ratio method dropped from 69.54 to 52.51 MPa within 180 days. On the other hand, SCR failure time of samples dropped from 5000 hours to only 36 hours at the same aging time. The linear plot between logarithm of SCR failure time and Gp by ratio method suggest ability to evaluate crack resistance of aged geomembrane by strain hardening method measured from tensile test at room temperature.

6.5 Conclusions and recommendations

6.5.1 Conclusions

- Several signs of aging can be observed at tensile test curve of aged specimen (41 days aged specimen) such as decrease of width of yield zone, increase of strain hardening onset, and decrease in Gp at 10 mm/min. These factors are considered

while designing Gp measurement methods.

- Minimum λ to measure Gp found to be 7 to avoid curvature zone that represent widening part of the specimen adjacent to narrow section more than strain hardening modulus property. While maximum λ is specified as 8 at which first, significant number of tests reach this value of λ, second, it provide enough zone to compare slopes at strain hardening region, third, it allow to give fare evaluation of aged specimens that expected to show according to literature a reduction in break tensile properties (break strength and break strain) compared to unaged specimens with higher break tensile properties.
- Three methods have been modified to measure Gp. These methods give different values of Gp and variation. All methods show a reduction in Gp with aging time.
- Data of measurement methods has been corelated with SCR test results. Among the three methods of measuring Gp, ratio method shows a good correlation with SCR test results.

6.5.2 Recommendations

- The strain hardening modulus in this research should be further investigated for geomembrane with same resins but different thickness to study the effect of thickness on results.
- The methods should be applied to several new geomembrane with similar thicknesses but different SCR results. Correlations between Gp and SCR results should be constructed to select the most represented Gp measurement method.

Table 6.1 Sampling procedure for aged geomembrane.

Aging time	Tensile test at displacement rate of 10 mm/min.	SCR (hours)
0	X	X
41 days	X	
82 days	X	X
150 months	X	X
180 months	X	X

Table 6.2 Gp with aging time by constant limits method at λ limits of 7-7.5, 7.25-7.75, 7.5-8, and 7-8

Aging time (days)	limits	Gp mean	SD	COV %
0	7-7.5	63.96	1.33	2.08
	7.25-7.75	67.27	1.58	2.35
	7.5-8	75.47	2.18	2.89
	7.-8.	67.79	0.63	0.92
41	7-7.5	54.05	1.27	2.35
	7.25-7.75	59.31	2.10	3.54
	7.5-8	64.54	1.77	2.75
	7.-8.	59.24	1.34	2.25
82	7-7.5	52.63	1.16	2.21
	7.25-7.75	56.22	2.71	4.82
	7.5-8	61.85	3.23	5.23
	7.-8.	56.72	2.30	4.06
150	7-7.5	53.82	5.79	10.76
	7.25-7.75	48.67	1.82	3.74
	7.5-8	56.04	10.90	19.45
	7.-8.	53.40	2.12	3.97

Table 6.3 Strain hardening modulus using total strain hardening method with aging time

Time (days)	Gp mean (MPa)	SD	COV
0	61.25	5.29	8.64
41	63.09	4.84	7.68
82	62.04	5.00	8.06
150	53.56	0.79	1.48

Table 6.4 Data treatment and Gp calculation using ratio method

Specimen	λ_{onset}	λ_{break}	λ_{break}- λ_{onset}	Maximum difference	λ_{onset} + (maxdiff/3)	λ_{break} - (max diff/3)	Gp
0-1	6.25	8.95	2.7	2.7	7.15	8.05	69.24
0-2	6.25	7.9	1.65	2.7	7.15	8.05	69.76
0-3	6.25	7.82	1.57	2.7	7.15	8.05	69.62
41-1	6.55	9.07	2.52	2.52	7.39	8.23	65.81
41-2	6.55	8.05	1.5	2.52	7.39	8.23	65.52
41-3	6.55	8.68	2.13	2.52	7.39	8.23	66.1
82-1	6.77	8.5	1.73	2.19	7.5	8.23	68.09
82-2	6.77	8.26	1.49	2.19	7.5	8.23	61.7
82-3	6.77	8.96	2.19	2.19	7.5	8.23	63.03
150-1	7.13	7.36	0.23	1.76	7.72	8.30	54.31
150-2	7.13	8.89	1.76	1.76	7.72	8.30	50.76
150-3	7.13	8.11	0.98	1.76	7.72	8.30	52.48

Table 6.5 Strain hardening modulus using ratio method with aging time

Time (days)	Gp Mean (MPa)	SD	COV (%)
0	69.54	0.27	0.39
41	65.81	0.29	0.44
82	64.27	3.37	5.25
150	52.51	1.78	3.38

Table 6.6 Results of five replicates of SCR test

Aging time (days)	SCR hrs/days				
	Specimen 1	Specimen 2	Specimen 3	Specimen 4	Specimen 5
0	1176/49	4245/176.8	-	-	-
82	2435.8/101.5	2431.4/101.3	2494.3/103.9	2504.8/104.4	2440.2/101.7
150	65.8/2.70	64.4/2.70	73.2/3.00	64.8/2.70	69.1/2.90
180	22.8/0.95	20.4/0.85	43.8/0.93	22.3/0.96	23.2/

Table 6.7 SCR with aging and variation

Aging time (days)	SCR (Hrs)	SD	COV (%)
0	*5000	-	-
82	2461.30	35.30	1.43
150	67.50	3.70	5.48
180	26.50	9.70	36.60

*Expected range of SCR test of unaged sample

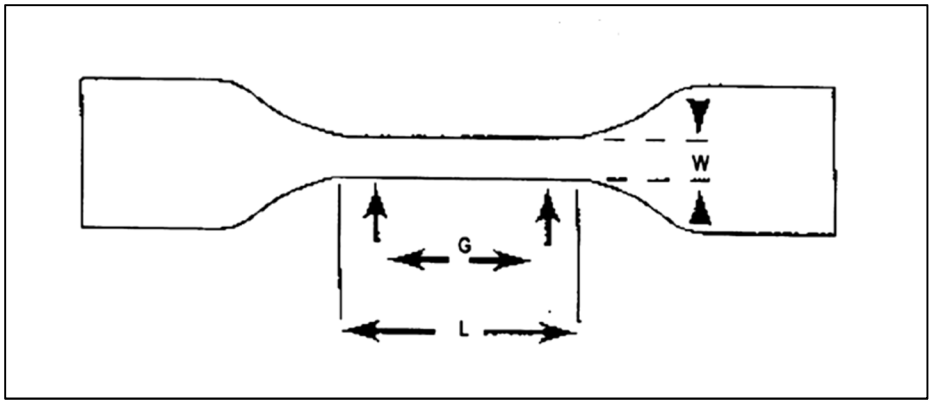

Figure 6.1 Dogbone specimen that used in the experiment L=33mm, w=6 mm, and G=25 mm (modified from ASTM D6693)

Figure 6.2 Tensile machine Instron 5566

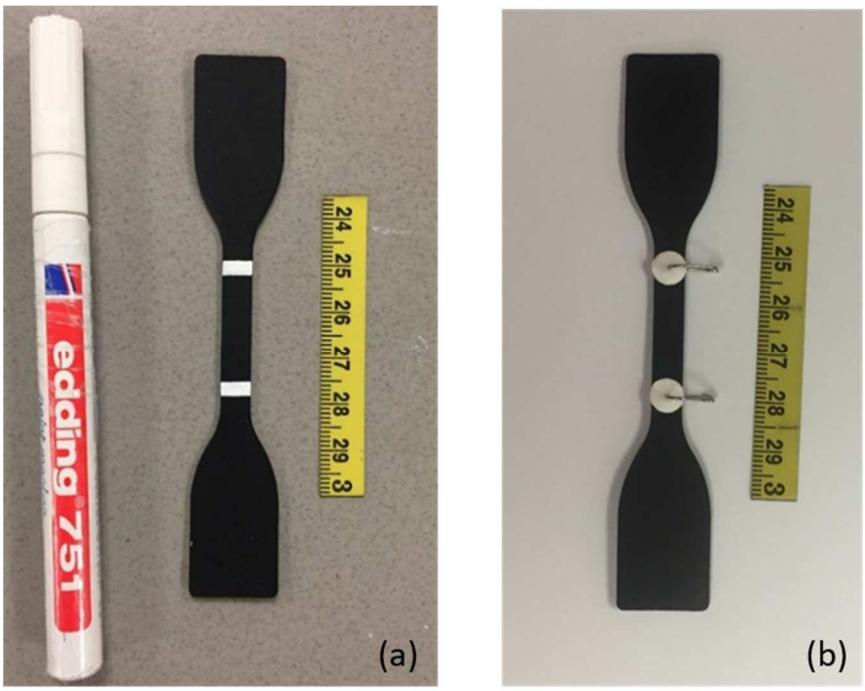

Figure 6.3 Marker used for samples a) paint marker for unaged specimens, b) center dot for aged specimens

Figure 6.4 A view of the HDPE GMB sheets inside the air forced oven

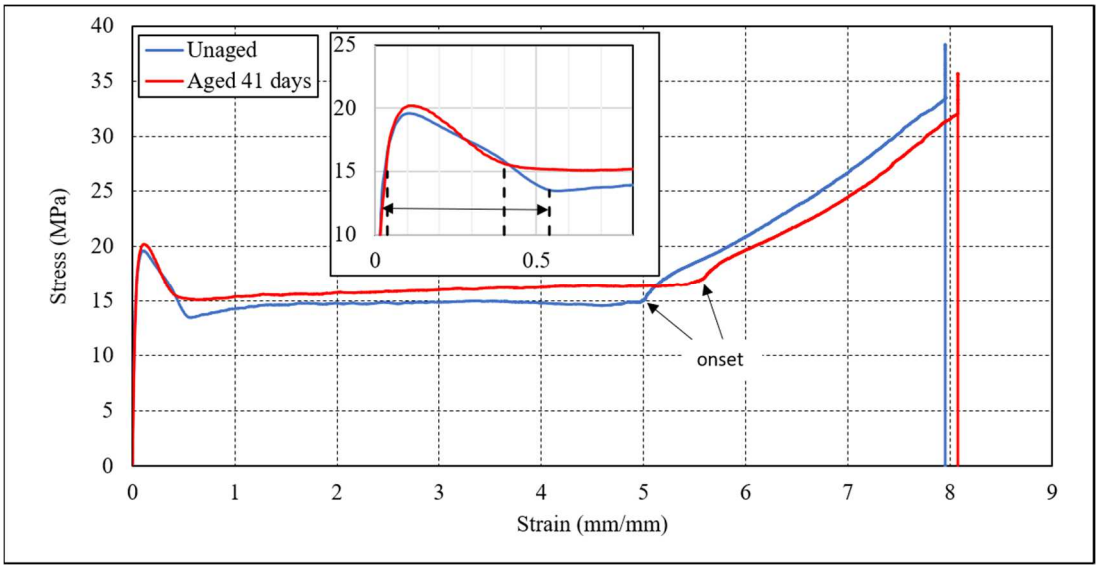

Figure 6.5 Effect of aging on stress-strain behavior tested at10 mm/min. (width of yield zone related to tie molecule. The reduction in width of yield zone mean reduction in tie molecule)

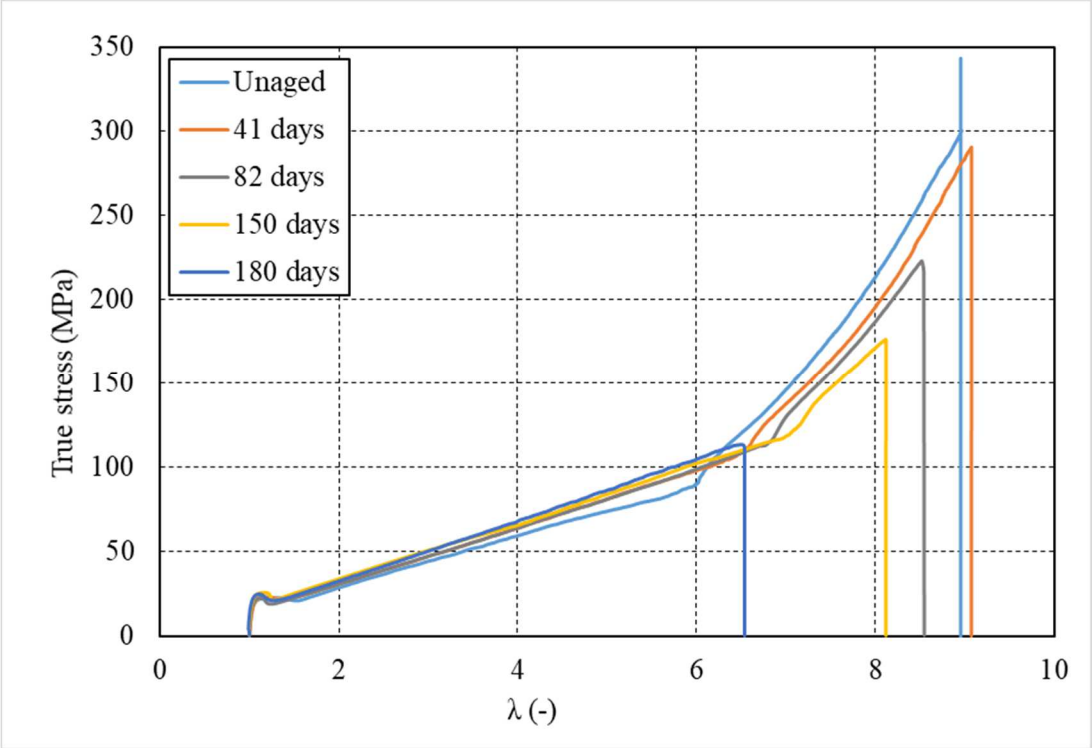

Figure 6.6 Change in tensile curve at 10 mm/min with aging

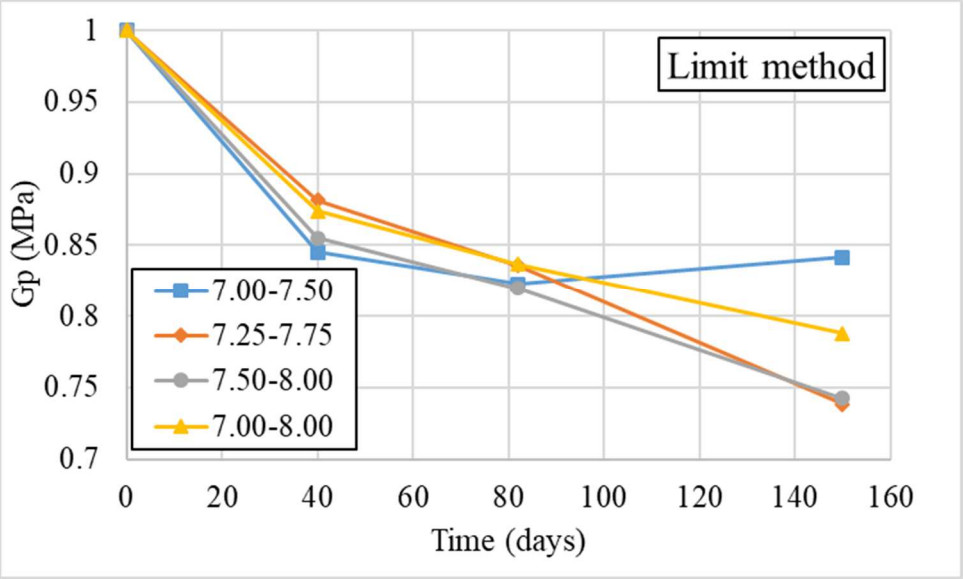

Figure 6.7 Gp with aging time by constant limits method

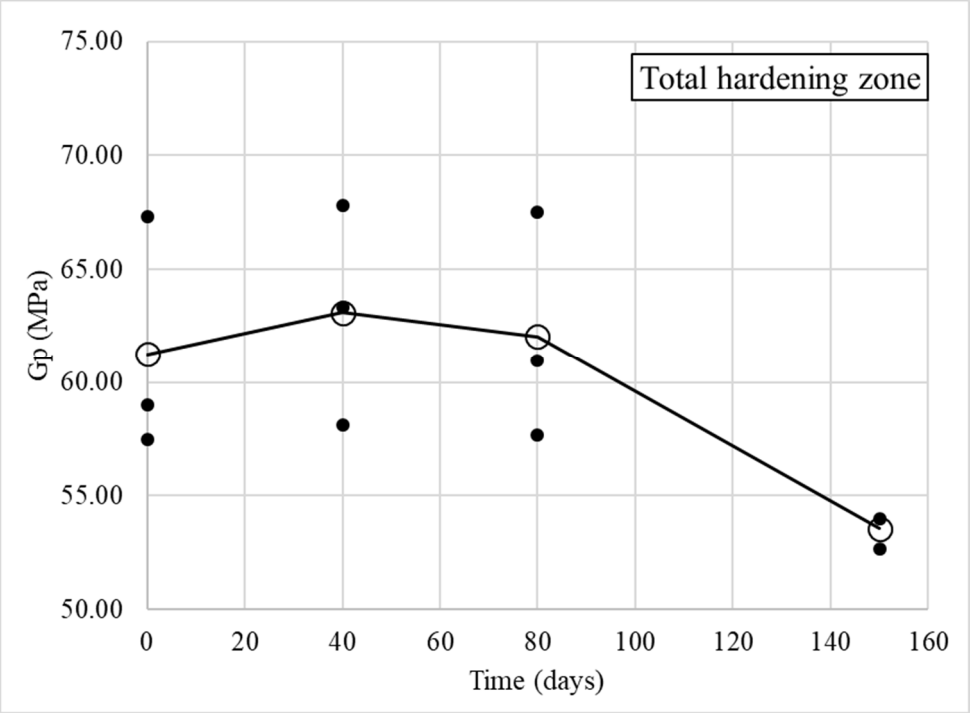

Figure 6.8 Gp with aging time by total hardening region method (solid dot are Gp values, empty circles are average values of Gp)

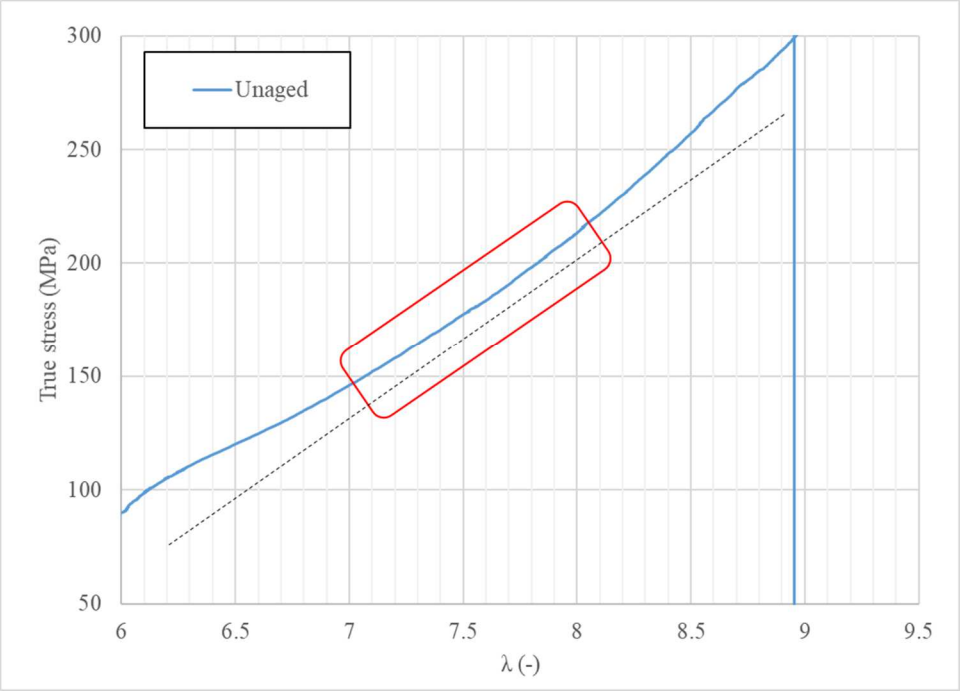

Figure 6.9 Strain hardening zone of unaged specimen

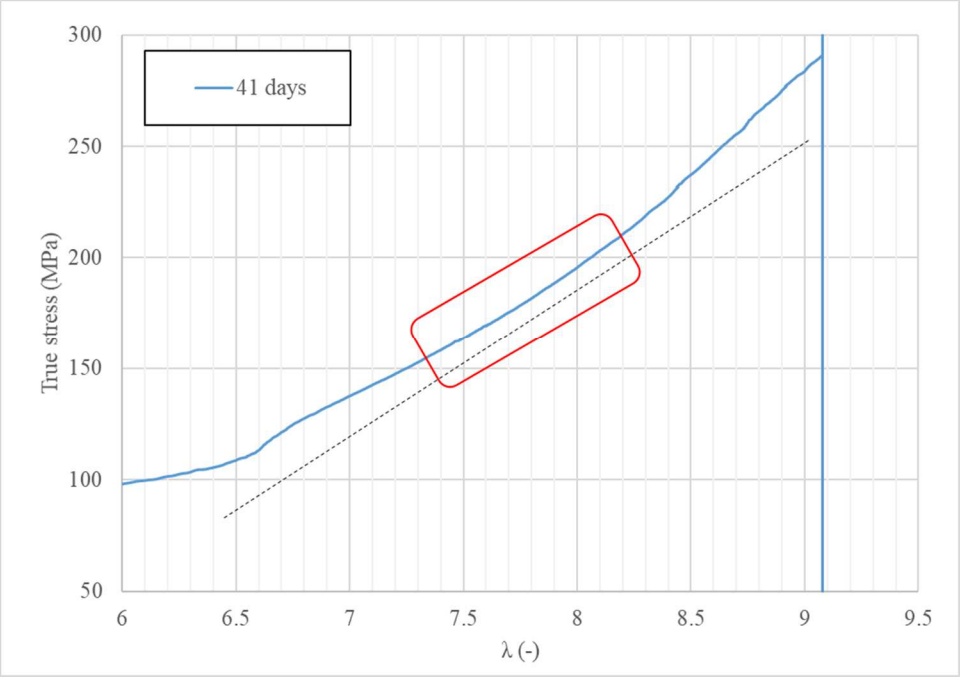

Figure 6.10 Strain hardening zone of 41 days aged specimen

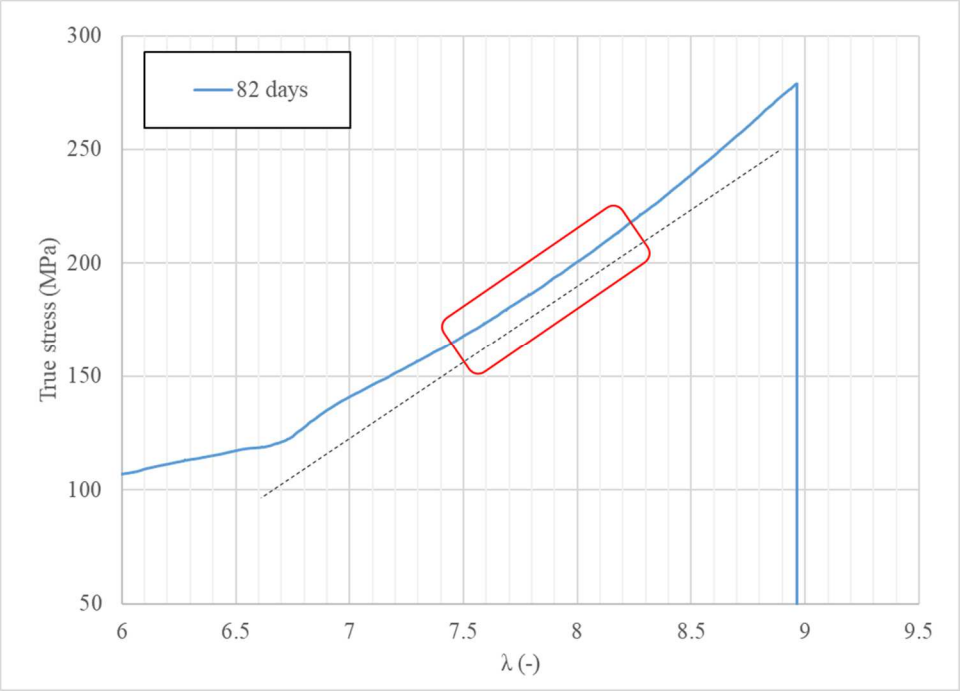

Figure 6.11 Strain hardening zone of 82 aged specimen

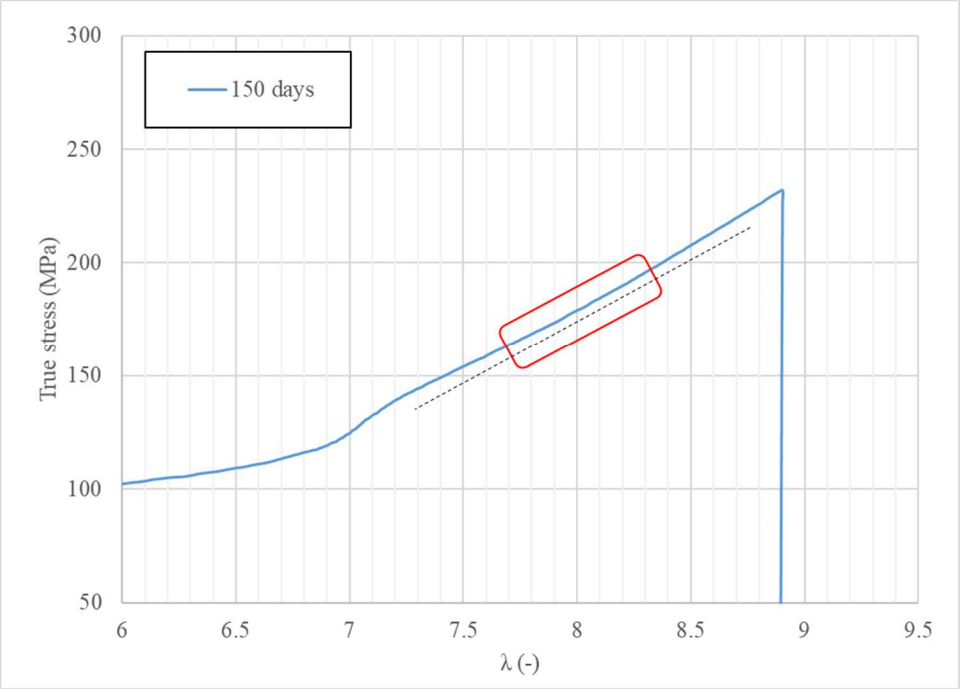

Figure 6.12 Strain hardening zone of 150 days aged specimen

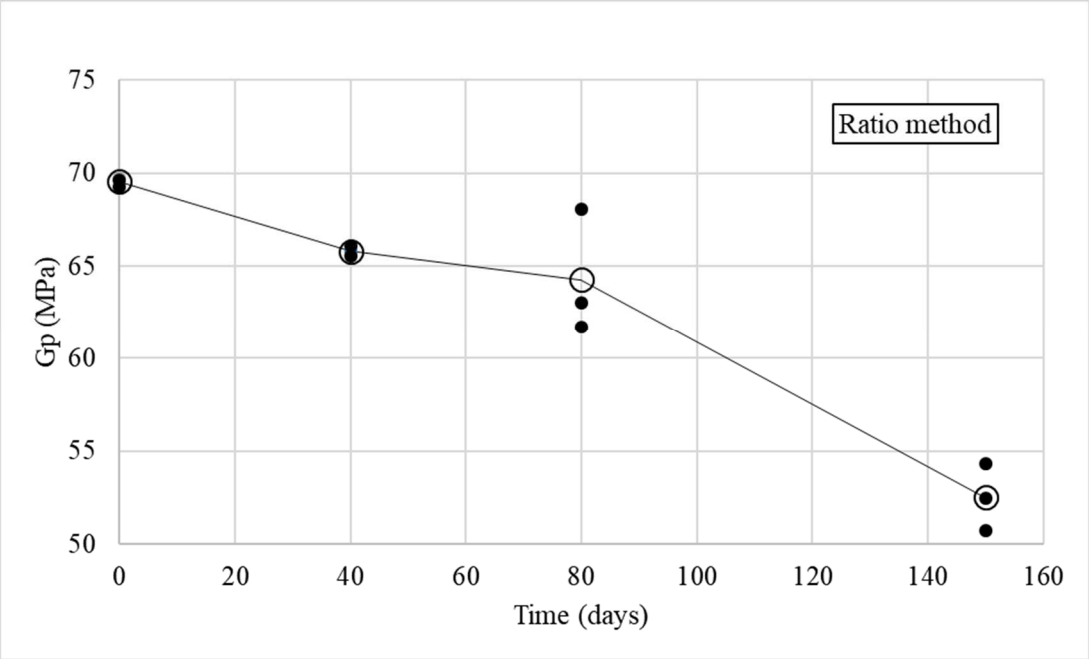

Figure 6.13 Gp with aging time by ratio method (solid dot are Gp values, empty circles are average values of Gp)

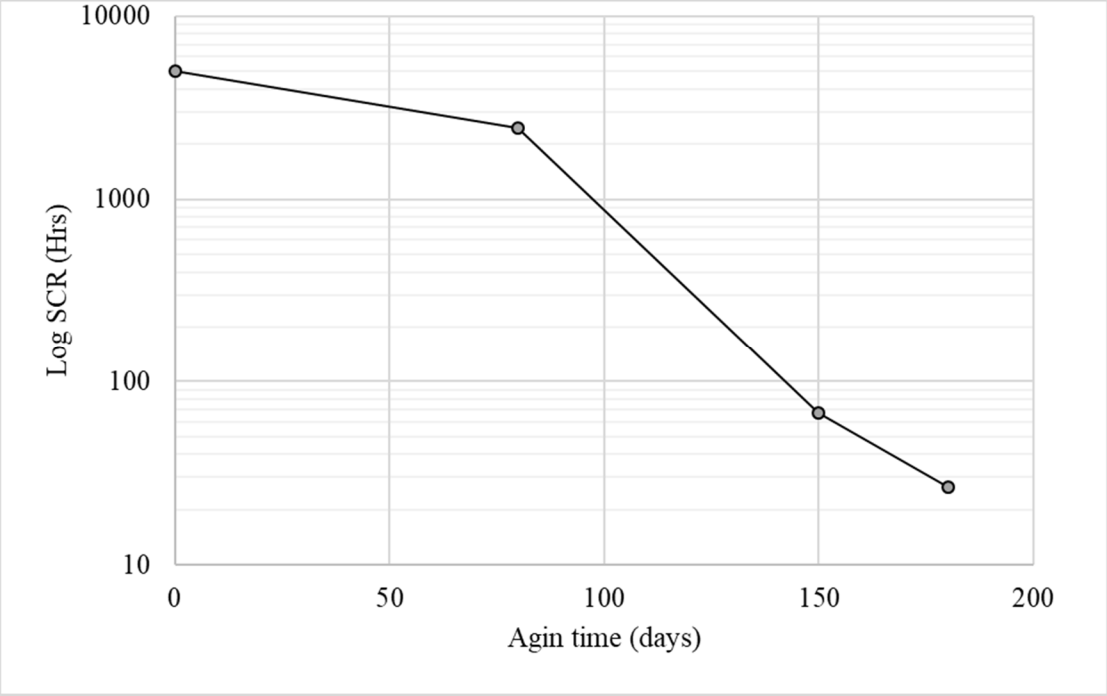

Figure 6.14 SCR with aging time of unaged and aged geomembrane

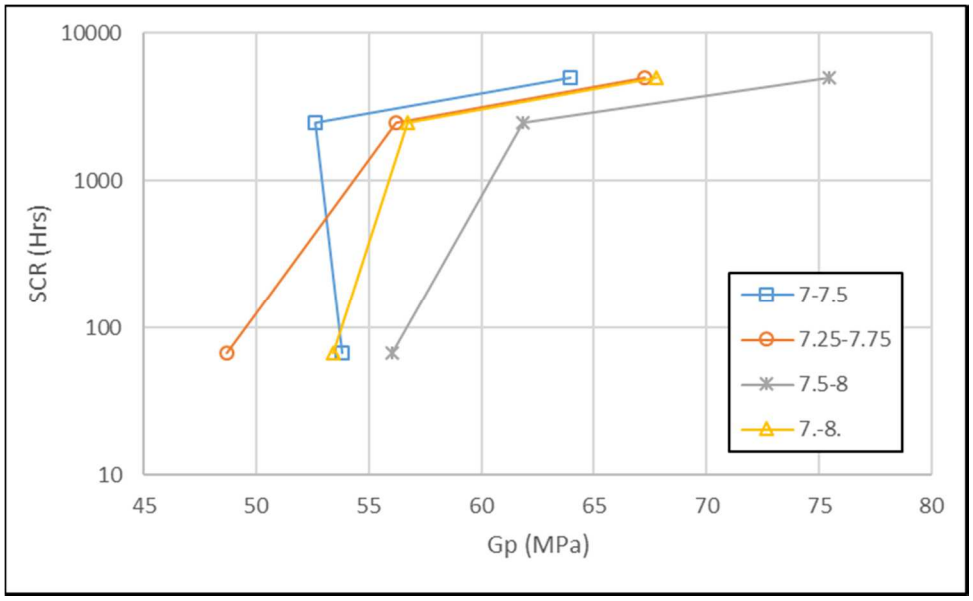

Figure 6.15 Strain hardening modulus (Gp) by constant limits method versus SCR failure time for aging experiment

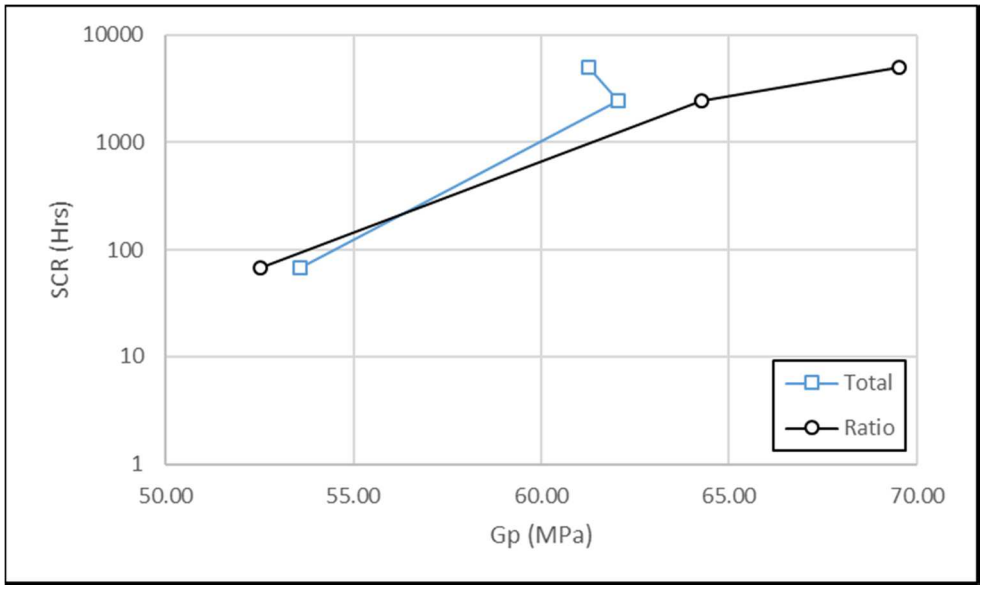

Figure 6.16 Strain hardening modulus (Gp) by total hardening region method and ratio method versus SCR failure time for aging experiment

REFERENCES

[1] ASTM.(2008). "Standard test method for evaluation of stress crack resistance of polyolefin geomembranes using notched constant tensile load test." *ASTM D5397*, ASTM, West Conshohocken, Pa.

[2] "Test method for environmental stress-cracking of ethylene plastics." (1993). *ASTM D 1693,* Vol. 08.02, ASTM, Philadelphia, Pa.

[3] Hsuan, Y.G., Koerner, R.M. and Lord, A.E., Jr., 1993, "Stress Cracking Resistance of HDPE Geomembranes", *Journal of Geotechnical Engineering*, ASCE, Vol. 119,No. 11, pp. 1840-1855.

[4] Kurelec, L., Teeuwen, M., Schoffeleers, H., & Deblieck, R. (2005). Strain hardening modulus as a measure of environmental stress crack resistance of high density polyethylene. *Polymer*, *46*(17), 6369-6379.

[5] SHT test_ISO 18488: Polyethylene (PE)materials for piping systems _ Determination of Strain hardening Modulus in relation to slow crack growth_Test method.

[6] Tisinger, L.G., and Giroud, J.P. 1993. The durability of HDPE geomembranes. Geotechnical Fabrics Report, **11**(6): 4–8.

[7] Haxo, H. E. and Nelson, N.A. (1984). Factors in the durability of polymeric membrane liners. *Proceedings of the International Conference on Geomembranes*, Vol. II, Denver, CO.IFAI Publishers, St. Paul, MN, pp. 287–292.

[8] Koerner, R. M., Halse, Y. H., and Lord Jr., A. E. (1990). Long-term durability and aging of geomembrane. In: Bonaparte, R., Ed., Waste Containment Systems: Construction, Regulation, and Performance. *ASCE Geotechnical Special Publication No.26*, New York, pp. 106–134.

[9] Hsuan, Y. G. and Koerner, R. M. (1998). Antioxidant depletion lifetime in high Density polyethylene geomembranes. ASCE Journal of Geotechnical and Geoenvironmental Engineering, Vol. 124, No. 6, pp. 532-541.

[10] Zanzinger, H., Engelsing, K., & Hausmann, S. (2014). Durability of polyethylene geopipes for landfill applications after several years in service. In *Proceedings of the 10th International Conference on Geosynthetics, Berlin, Germany, 21-25 September 2014*

[11] Peggs, I. D. Liner Performance: Interesting Observations and Test Results. In Geotechnical Frontiers 2017 (pp. 148-159).

[12] Zanzinger, H., Wenzel, M., and Engelsing, K. (2015) Determination of the Stress Cracking Resistance of HDPE Geomembranes by using Accelerates Test Methods

[13] Zanzinger, Helmut & Peggs, Ian. (2013). Stress cracking resistance of HDPE geomembranes with very high densities.

[14] Allison, S. W., Pinnock, P. R. and Ward, I.M. (1966) Polymer, 7(1), 66-69.

[15] Cheng, J. J., Polak, M. A., & Penlidis, A. (2008). A tensile strain hardening test indicator of environmental stress cracking resistance. Journal of Macromolecular Science®, Part A: Pure and Applied Chemistry, 45(8), 599-611.

[16] Bartczak, Z. (2010). Effect of chain entanglements on plastic deformation behavior of ultra□high molecular weight polyethylene. Journal of Polymer Science Part B: Polymer Physics, 48(3), 276-285.

[17] ASTM D638. Standard test method for tensile properties of plastics, Annual Book of Standards, vol. 8.01. (ASTM D638-14, Standard Test Method for Tensile Properties of Plastics, ASTM International, West Conshohocken, PA, 2014).

[18] Robledo, N., Domínguez, C., & García-Muñoz, R. A. (2017). Alternative accelerated and short-term methods for evaluating slow crack growth in polyethylene resins with high crack resistance. Polymer Testing, 62, 366-372.

[19] Engelsing, K. and Zanzinger, H. (2012). A new accelerated test method for stress crack resistance of HDPE geomembranes. Segundo Congreso Panamericano de Géosintéticos, GEOAMERICAS 2012, 01-04 de Mayo, 2012, Lima, Peru, 8p.

[20] Humbert, S., Lame, O., & Vigier, G. (2009). Polyethylene yielding behaviour: What is behind the correlation between yield stress and crystallinity?. *Polymer*, *50*(15), 3755-3761.

[21] Crist, Buckley, and Costas Metaxas. "Neck propagation in polyethylene." *Journal of Polymer Science Part B: Polymer Physics* 42.11 (2004): 2081-2091.

[22] Morais, F. L. D. D., Medeiros, F. D. S., Silva, G. G., Rabello, M. S., & Sousa, A. R. D. (2017). Photodegradation of UHMWPE Filled with Iron Ore Fine. *Materials Research*, *20*(2), 356-364.

[23] Cheng, J. J., Alvarado-Contreras, J. A., Polak, M. A., & Penlidis, A. (2010). Chain entanglements and mechanical behavior of high density polyethylene. *Journal of Engineering Materials and Technology*, *132*(1), 011016.

CHAPTER 7

RECOMMENDATIONS FOR FUTURE WORK

The following summarizes the future work that need to be conducted to further assist in the application of the strain hardening modulus and in the evaluation of stress crack resistance. These are categories in two parts:

7.1 Recommendation for the strain hardening method for geomembrane

1. The evaluation of the strain hardening modulus should be further investigated for other geomembrane resins with different factory initial properties. The experimentations should be conducted at the same set of displacement rates that are applied in our present research. This shall provide sufficient data to carry out further characteristic evaluation of Strain Hardening Modulus. These data shall also provide additional clear interpretation and insight of the roles played by both the geomembrane amorphous phase and the crystalline phase cited in the literature.
2. The measured strain hardening modulus data can be correlated with Stress Crack Resistance data that can be made available for the same HDPE resin. The proposed correlation shall prove useful and less time consuming in determining SCR compared with the method outlined by ASTM 5397.
3. Investigation should be carried out to evaluate the effect of geomembrane manufactured directions (anisotropy) upon the strain hardening modulus through

testing specimens prepared and cut out from the geomembrane sheet in both the parallel process direction and the perpendicular process direction.

4. The strain hardening modulus in this research should be further investigated for geomembrane with same resins but different thickness to study the effect of thickness on results.
5. The methods should be applied to several new geomembrane with similar thicknesses but different SCR results. Correlations between Gp and SCR results should be constructed to select the most represented Gp measurement method.

7.2 Recommendations for evaluating aging of geomembrane including the influence of nanomaterials on strain hardening

1- Strain hardening method and experimentation should be applied for specimens cut out from an aged and degraded geomembrane sheet that had been in use in actual landfill. These experimentations data shall clarify the impact of environmental conditions upon material characteristics and experimental results. Testing results can further be correlated with Stress Crack Resistance data following ASTM 5397 method.

2- Strain hardening method need to be evaluated for geomembrane that degraded in lab and represent aging environments conditions such as water and leachate at high temperature that represent other field conditions.

3- During the installation of the geomembrane sheet in landfill site the sheets are welded together using specialized machine. This installation process is likely to have an impact upon the physical and chemical characteristics of the material

adjacent to the welded edges. Therefore, the selected sampling specimens should cover both nearby and far away locations from the welded edges.

4- Experimentations should be carried out on laboratory aged samples exposed to several parameters that simulate the expected presence of the various nanomaterial such as TiO2, Ag, and carbon nanotube. The surrounding temperature should also be taken into considerations including UV light.

5- Study and compare molecular, morphological and mechanical properties of aged geomembrane that exposed to nanomaterials (such as TiO2, Ag, and carbon nanotube) and how these properties change compare to strain hardening modulus change and SCR.